

Uprising of a Monopile for an Offshore Wind Turbine Foundation

Graduation thesis MSc Offshore and Dredging Engineering

J.B. Crol

December 2015



Upending of a monopile for an offshore wind turbine foundation

by

J.B. Crol

As part of obtaining the degree of

Master of Science

in Offshore and Dredging Engineering

at Delft University of Technology

to be defended publicly on the 10th of December 2015.

Graduation committee

Prof. Dr Ir A.V. Metrikine

Ir J.S. Hoving

Dr Ir K.N. van Dalen

Ir A. Jarquin Laguna

Ir C.J.M. Stam

Delft University of Technology (chairman)

Delft University of Technology

Delft University of Technology

Delft University of Technology

Van Oord Dredging and Marine Contractors bv

Contact details

J.B. Crol (Joris)

MSc Offshore and Dredging Engineering
Student number: 1224328
Noordeinde 91A
2514 GD Den Haag
T: +316 52 06 58 38
E: jbcrol@gmx.com

Delft University of Technology

Faculty of Civil Engineering & Geosciences
Stevinweg 1
2628 CN Delft
T: +31 15 27 89 11 1
<http://www.tudelft.nl>

Van Oord Dredging and Marine Contractors bv

Head Office
Schaardijk 211
3063 NH Rotterdam
T: +31 88 82 60 00 0
<http://www.vanoord.com>

Area Offshore
Jan Blankenweg 2
4207 HN Gorinchem
T: +31 88 82 65 20 0

Abstract

The subject of this report is the upending of a floating monopile for an offshore wind turbine foundation. This is an assignment of Van Oord Dredging and Marine Contractors BV. An analytical model has been developed to simulate the upending of a monopile in Maple™, based on the general theoretical principles and the experience of Van Oord. An experiment was then done to validate the analytical model. The Maple™ script can be used to calculate the forces of the crane for future projects.

The monopile, sealed with two end-caps, is towed by a tugboat from the storage site to the installation site and is then upended by the jack-up vessel of Van Oord, the Aeolus. The end-caps guarantee buoyancy during transport and upending. After upending the end-caps are removed, either internally or externally. A conceptual design has been developed for both removal methods.

With upending the vertical position of the monopile can be reached with a net weight of the pile greater than the safe working load of the crane using the buoyant force. The minimum draught needed for the buoyant force to remain within the safe working load of the crane, determines the minimum hydrostatic pressure needed for the external removal of the bottom-cap. The top-cap can only be removed once the pile has been placed on the seabed, since the buoyant force is the auxiliary of the crane.

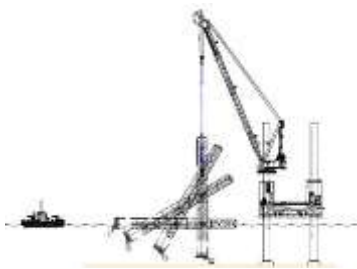


Figure 1: Upending of the monopile

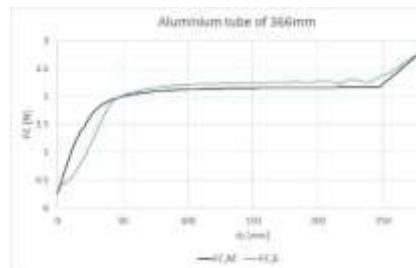


Figure 2: Result experiment and Maple™



Figure 3: Experimental set-up

As shown in figure 1, the upending of the monopile is performed, by vertically displacing the connection point between the pile and the crane. Because the crane hook is attached to the pile with a hinge, the monopile can rotate freely around this point. For the analytical model in Maple™ it is assumed that the upending process is quasi-static because the influence of the inertia is negligible.

The experiment has confirmed that the inertia may indeed be neglected by showing the similarity between two scaled upending tests at different continuous hoisting velocities and the corresponding quasi-static simulation. Therefore the scaled upending correlates to the quasi-static model. It is found that, only when the lifting starts and stops, and respectively the acceleration and deceleration are relatively large, the inertia influences the upending process.

Further research to refine the upending process, as well as the design of the end-caps is recommended. The hoisting speed of the crane can be optimized if the expectations of the experiment and the analytical model are confirmed in practice. The design depends on the airflow when releasing the end-cap and the internal pressure when lowering the pile towards the seabed. The internal pressure can be controlled using a pressure valve. These recommendations will lead to the optimized upending process of monopiles for offshore wind turbine foundations that are transported by towage using end-caps.

Preface

This document has been written as graduation thesis for my Master Offshore and Dredging Engineering at Delft University of Technology. Van Oord Dredging and Marine Contractors BV in Rotterdam offered me an assignment with the opportunity to combine the theory of my Master with projects of the company.

The subject of this assignment is:

“The conceptual design of closing end-caps for an offshore wind turbine foundation monopile facilitating towed transport and upending.”

In order to develop a conceptual design of closing end-caps the monopile wind turbine foundation must be understood. The end-cap has to guarantee buoyancy during the towed transport and upending. Van Oord will use their own installation vessel, the Aeolus, to upend the monopile. The maximum capacity of the Aeolus is the safe working load (F_{SWL}) and this load should not be exceeded.

The goal of this thesis is to make a conceptual design for the top and bottom end-caps, facilitating the towed transport to the site, the upending and installation of the monopiles. The following aspects will be covered in the design process of the end-caps:

1. *Understanding and possibly detailing and/or adjusting the intended monopile towing and upending procedure.*
2. *Analysing the buoyancy requirements needed to bring the monopile weight within the capacity of the crane.*
3. *In addition care should be taken of conditions resulting from necessary testing requirements.*

Acknowledgements

The research reported in this thesis is mainly performed for Van Oord Dredging and Marine Contractors BV, the sponsor company for this work.

First of all, I would like to thank the chairman of my graduation committee Prof. Dr Ir A.V. Metrikine of Civil Engineering at Delft University of Technology and Mr Ir C.J.M. Stam, lead engineer at the department Offshore Engineering of Van Oord as my supervisor during my graduation.

Also I am grateful to the other members of the graduation committee, Ir J.S. Hoving and Ir A. Jarquin Laguna at Delft University of Technology. They helped me during the research, calculations in Maple™ and the execution of the experiment.

Further, I would like to thank my twin-sister, Carlien, my mother, Jorien and my father, Johannes Crol. During my study they proved to be a great support.

Finally, I would like to thank my colleagues at Van Oord, fellow students and all other family and friends for their interest and support.

Table of Content

GRADUATION COMMITTEE	I
CONTACT DETAILS	III
ABSTRACT	V
PREFACE	VII
ACKNOWLEDGEMENTS	IX
TABLE OF CONTENT	X
1 INTRODUCTION	1
1.1 Scope	1
1.2 Objectives	2
1.3 Outline	3
2 MONOPILE FOUNDATION DESIGN	5
2.1 General theory of a support structure	5
2.2 General design of a Monopile	6
2.3 Design of a Monopile Wind Turbine Foundation	9
2.4 Projects of Van Oord	11
2.5 Conditions for the design of a Monopile foundation	13
3 INSTALLATION OF A MONOPILE WIND TURBINE FOUNDATION	15
3.1 Transport of a Monopile for an Offshore Wind Turbine Foundation	15
3.2 Theory of Upending	17
3.3 Removal of the End-caps	19
3.4 Conditions for the Installation of a Monopile	23
4 CONCEPTUAL DESIGN OF THE END-CAPS	25
4.1 Requirements of End-caps	25
4.2 Conceptual designs	30
4.3 Recommendations for the Conceptual design of the End-caps	34
5 ANALYSIS OF THE PROCESS OF UPENDING OF A MONOPILE	35
5.1 Assumptions	35
5.2 Analysis of the Process of Upending of a Monopile	36
5.3 Verification of the analytical model	42
5.4 Results of the analytical model	43
5.5 Assumptions based on the Analytical model	46
6 EXPERIMENTAL UPENDING OF A MONOPILE WIND TURBINE FOUNDATION	47
6.1 Theory of Experimental Upending of Monopile OWTF	47
6.2 Results of the Experimental Upending of the Monopile OWTF	49
6.3 Discussion regarding the Experimental Upending	54
7 COMPARISON OF THE ANALYTICAL MODEL AND THE EXPERIMENT	55
7.1 Comparing the Analytical model and the Experiment	55
7.2 Conclusions based on the Analytical model and the Experiment	56

8	DISCUSSION, CONCLUSIONS AND RECOMMENDATIONS	57
8.1	Discussion	57
8.2	Conclusions of this research	59
8.3	Recommendations for further work	59
APPENDIX A	AEOLUS DATASHEET	61
APPENDIX B	GENERAL ARRANGEMENT BELWIND BY RAMBOLL	61
APPENDIX C	RIGGING ARRANGEMENT FOR MONOPILE BY DHLC	61
APPENDIX D	FLOW STEPS FOR UPENDING MONOPILE	62
APPENDIX E	REQUIREMENTS TO ENVIRONMENTAL CONDITIONS OF AEOLUS	63
APPENDIX F	STANDARD SEAWATER PROPERTIES AT 1°C INCREMENT	64
APPENDIX G	PROPERTIES OF AIR	65
APPENDIX H	MAPLE™ SCRIPT	66
APPENDIX I	EXPERIMENTAL RESULTS	70
APPENDIX J	EXPERIMENT	72
A	LIST OF SYMBOLS AND ABBREVIATIONS	73
B	LIST OF FIGURES	78
C	LIST OF TABLES	79
D	REFERENCES	80

1 Introduction

In Europe, the offshore wind energy industry is rapidly expanding. In the first six months of 2014 the European grid connected 16 wind farms with 224 offshore wind turbines.¹ The largest investment was the 600 MW Gemini project in the Netherlands. The independent power producer Northland Power acquired the majority of the project, along with the contractors Siemens and Van Oord.

In 2015, Van Oord started the installation of the Gemini wind farm, which consists of wind turbines on a monopile foundation. A monopile foundation is a single tube support structure. The steel cylindrical tube is designed to support the total loads of the above-surface structure, to resist the environmental loads imposed on the substructure and the loads induced by the installation method.

There are several ways to transport the pile to its final location. This thesis focusses on towed transport, as a monopile pulled by a tugboat which are connected with a towing arrangement as in figure 4, and upending of monopiles by the “Aeolus”, the installation vessel of Van Oord.

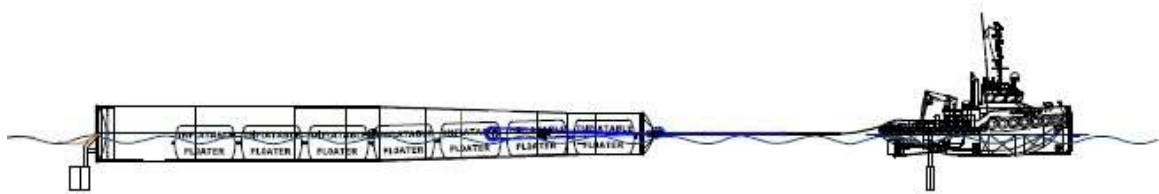


Figure 4: Towed monopile by a tugboat

1.1 Scope

This thesis considers the aspects of a conceptual design of closing end-caps for offshore monopile wind turbine foundation, facilitating towed transport and upending. The subject of this thesis was assigned by Van Oord.

The monopile must be equipped with end-caps to provide buoyancy during the operations of towage and upending. The monopile equipped with the two end-caps during towage is shown in figure 4.

The mass of the anticipated monopile is 1.100 tonnes and the safe working load (F_{SWL}) of the crane vessel is 900t, given in Appendix A. Therefore at least 200t of buoyancy is required to be able to upend the monopile. The end-caps are removed after upending. Removal of the bottom-cap depends on the draft of the monopile needed for buoyancy. The draft causes the hydrostatic pressure on the bottom-cap. The net pressure on the bottom-cap leads to the displacement of the bottom-cap after disconnecting the seal.

1.2 Objectives

The objectives have been formulated in the assignment for this thesis to lead to an optimized conceptual design. First, the procedure of towing and upending the intended monopile must be understood. The transport and the upending determine the maximum loads on the installed end-caps. The end-caps must withstand these loads to guarantee buoyancy of the monopile. The delivery of the monopile by a tug is shown in figure 5.

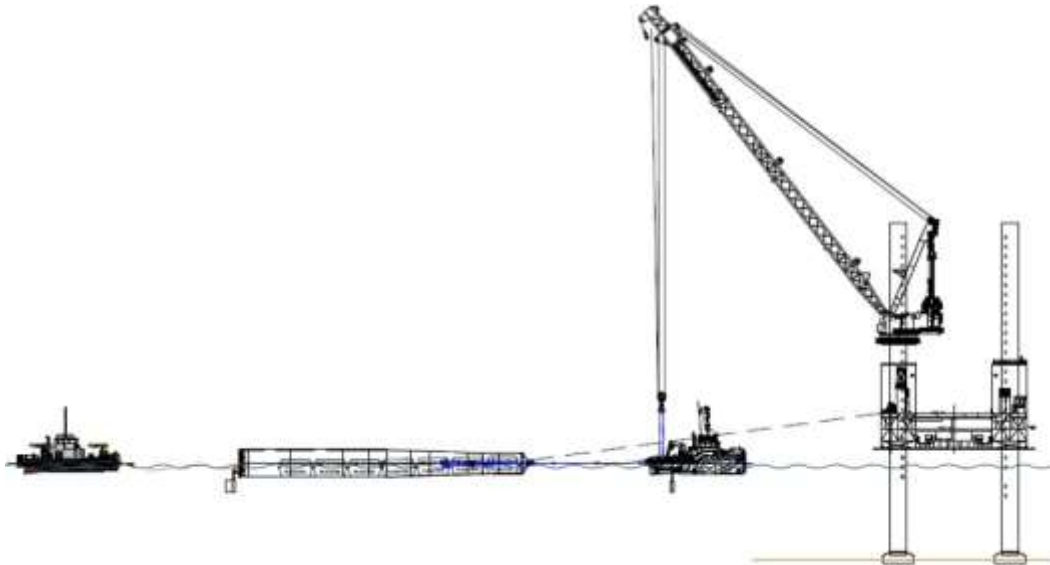


Figure 5: Arrival of the monopile at the installation site

Secondly, the buoyancy requirements to bring the weight of the monopile within the capacity of the crane will result in the initial conditions for disconnecting the end-caps. The draft of the pile and the resulting hydrostatic pressure on the submerged end-cap determine the external load during disconnection. The removal of the submerged end-cap is shown in figure 6.

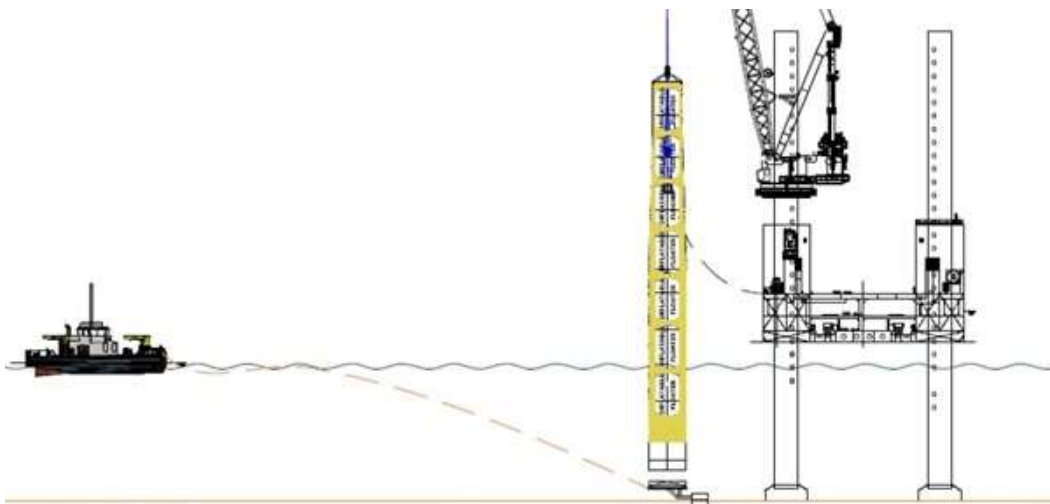


Figure 6: Removal of the bottom-cap

The removal of the bottom-cap depends on the pressure balance on the end-cap and the safe working load of the crane. An internal overpressure is needed to push the bottom-cap out of the monopile. The bottom-cap is connected to the tugboat to control the response of the pile and to pick up the cap.

1.3 Outline

The objectives result the structure of the report. In the next chapter the general theory of the monopile for an offshore wind turbine foundation is explained. The installation of a monopile depends on transport, upending and the removal of the end-caps and is described in chapter 3.

The topic of chapter 4 is the design of the end-caps which is based on the theory of chapter 3. The installation of the monopile, as explained in chapter 3, provides the requirements for the conceptual design of the closing end-caps.

The dominant forces on the pile during the upending are described in chapter 5 to chapter 7. In the chapter 5 the analytical upending is defined. The experimental upending is the topic of chapter 6. The analytical model and the experiment are compared in chapter 7.

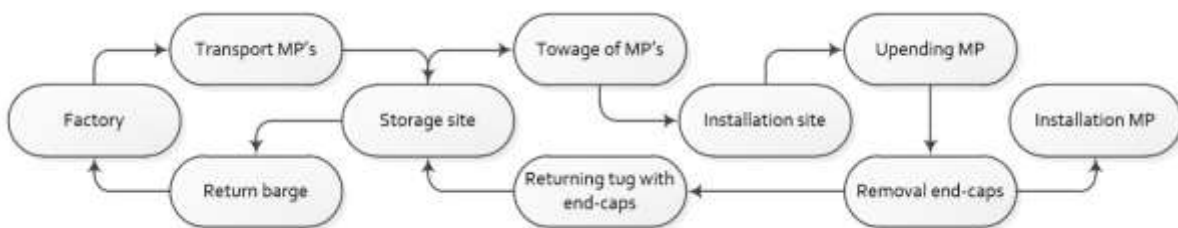


Figure 7: Flowchart of the Installation of a monopile for an offshore wind turbine foundation

Based on the previous chapters the verification and discussion take place in chapter 8. The last chapter with conclusions and recommendations, gives an overview of the steps to refine the installation of a monopile for an offshore wind turbine foundation while using end-caps in the future.



Figure 8: Installed offshore monopile wind turbine foundations with transition pieceⁱⁱ

2 Monopile foundation design

The design of the end-caps is determined by their goal. The end-caps are used to cover both ends of the monopile during transport and upending. The dimensions of the end-caps depend on the dimension of the monopile. The theory and design of a monopile wind turbine foundation is described in the first three sections.

Experience with former projects of Van Oord is taken into account as well. After completion of a project a “Lessons Learned” report is written. This is explained in section 2.4.

2.1 General theory of a support structure

The monopile is a type of support structure that is often used for wind turbines. An overview is given of the most important aspects that have to be taken into account for the foundation design and installation of the monopile. The monopile is a steel hollow cylindrical tube that carries the transition piece, the platform and the wind turbine which exists of the tower, nacelle, rotor and blades, as shown in figure 9. A monopile is a highly efficient type of foundation, which is very popular as shown in figure 10. The monopile is suitable for water depths up to 40 meter.



Figure 9: Wind turbine

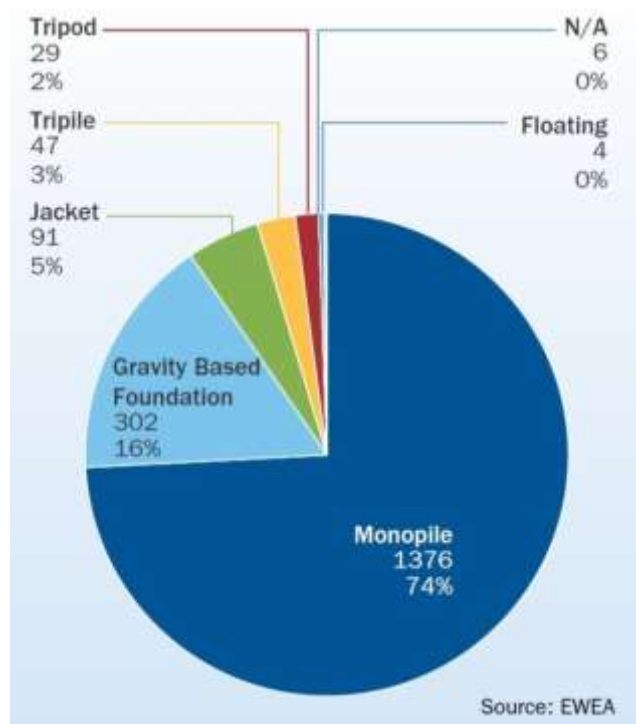


Figure 10: Used foundations of wind farms, end 2012

The design and dimensions of a monopile result from calculations based on the dimensions of the turbine and blades, site-specific data as the environmental conditions (wind, waves and current), seabed topography and the soil conditions. The design of the monopile is explained in the next section.

2.2 General design of a Monopile

The monopile is designed to sustain loads that can occur during installation and operational life of the wind turbine. The requirements for the monopile result from the ultimate (ULS), fatigue (FLS) and serviceability limit state (SLS), which are determined by the static and dynamic forces. The ULS is the maximum load-carrying resistance. The FLS is the possibility of failure due to the cumulative damage effect of cyclic loading. The SLS is the tolerance criteria applicable to normal use without exceeding the load-carrying capacity.

Increase of water depth leads to an increase of bending moment and shear force at seabed level, requiring an increased pile diameter and penetration depth. Increasing the weight of the structure increases the installation loads. The site-specific data for the monopile design have to be known to calculate the right dimensions. The data are briefly described in the next three subsections.

2.2.1 Site-specific conditions

Every location has its site-specific conditions, which influences the design of the wind turbine. The conditions that have to be taken into account are listed below. The normal and extreme climate conditions are used to calculate the SLS, FLS and ULS.

- Water depth
- Wind
- Waves
- Currents
- Morphology
- Soil types
- Earthquakes
- Ice, sea ice and solid ice

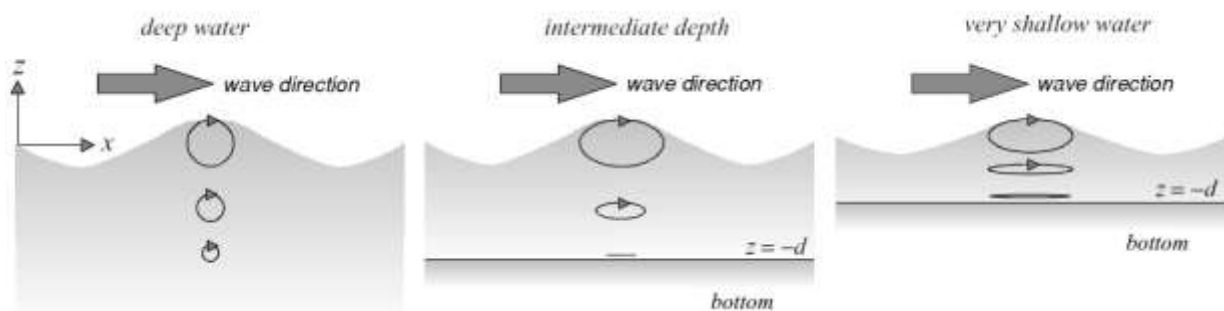


Figure 11: Orbital motion in deep, intermediate-depth and very shallow waterⁱⁱⁱ

On the expected locations there are no earthquakes or exceptional natural circumstances and is no ice, therefore the conditions morphology, earthquakes, ice, sea ice and solid ice are not considered.

The waves in the ocean are generated by the wind. They can break and interact with currents and the sea bottom. Wave induced water particles in the ocean move as shown in figure 11. The type of orbital motion depends on the ratio of water depth (d) divided through the wave length (λ). The waves in shallow water, $d/\lambda < 0.05$ or equation 2.1, are long and have a large influence on the seabed. The waves in deep water, $d/\lambda > 0.5$, do not affect the seabed.

The bottom orbital velocity of the water particles can be expressed with the simple linear wave theory. The orbital path is elliptical becoming flatter towards the bottom^{iv}. The horizontal orbital velocity is defined in equation 2.2 and the bottom orbital velocity in equation 2.3, when $|\cos(kx - \omega t)| = 1$ or $z = -d$.

$$\frac{2\pi \cdot H_s}{g \cdot T^2} \leq \frac{1}{15} \quad 2.1$$

$$u_0 = \frac{H_s \cdot \pi}{T \cdot \sinh(k \cdot d)} \cos(k \cdot x_w - \omega \cdot t) \quad 2.2$$

$$u_b = \frac{H_s \cdot \pi}{T \cdot \sinh(k \cdot d)} = \frac{\omega \cdot a}{\sinh(k \cdot d)} \quad 2.3$$

H_s	Significant wave height	m
g	Gravitational acceleration (≈ 9.81)	m/s ²
T	Wave period	s
u_0	Horizontal component of orbital velocity	m/s
k	Wave number ($= 2\pi/\lambda$)	1/m
d	Water depth	m
x_w	Coordinate of Cartesian reference horizontal in the direction of the wave	m
ω	Wave frequency	rad/s
t	Time	s
u_b	Bottom orbital velocity	m/s
a	Amplitude of the surface fluctuation	m

The significant wave height is defined in equation 2.4. This height can be calculated as the mean of the highest one-third of waves in the wave record. The maximum wave height is needed for the design of the monopile and is defined in equation 2.5. According D. Faulkner this value is the most probable maximum wave height to be expected.^v

$$H_s = \frac{1}{N/3} \sum_{j=1}^{N/3} H_j \quad 2.4$$

$$H_{\max} = H_s \cdot \sqrt{\ln(N)/2} = 1.86 \cdot H_s \quad 2.5$$

$$T = 4.27 \cdot H_s^{0.37} \quad 2.6$$

$$\lambda_s = T \cdot \sqrt{g \cdot d} \quad 2.7$$

N	Number of waves in the wave record	-
j	Rank number of the wave height, j=1 for highest, j=2 for second highest, etc.	-
H_{\max}	Maximum wave height	m
λ_s	Shallow water wave length	m

A wave going into shallow water is influenced by the bottom friction, white capping and depth-induced breaking. The wave becomes steeper and will finally break. The wave height divided by the wave length results in a breaking wave if the value is equal to one-seventh.

The equations are based on a simple linear wave theory, which gives an estimation of the wave characteristics and their effects. The wave period for very shallow water is estimated with equation 2.7. This assumption is rarely needed since the significant wave height and period are very often known at the final location of installation.

2.2.2 Seabed topography

The seabed topography depends on the changing water depth. The continental shelf is from the coast line to the shelf break. At the shelf break the seabed changes from the continental shelf to the continental slope. An angle of the seabed slope larger than one degree results in the shelf break. The continental shelf break can take place at a water depth from 20 to 550 meters with an average of 133 meters.^{vi}

The surface of the seabed for a monopile does not need to be levelled before installation. Before designing a wind farm a site survey has to be done to get an overview of the bathymetry of the seabed. By using this data the total wind farm could need different designs. Besides the depth of the seabed, the type of soil must be known. The soil conditions are explained in the next subsection.

2.2.3 Soil conditions

The soil conditions partially depend on the size of the sediment particles. The particle sizes in millimetre are defined in Table 1^{vii}. The fine, coarse and very coarse soil is split in clay, silt, sand, gravel, cobbles, boulders and large boulders. The difference between the fine and coarse soil comes from the internal resistance, cohesion. Cohesive soil sticks together and non-cohesive soil not. Cohesive soil with undrained shear strength and plasticity, as for example clayey silt, inorganic silt and highly organic soils, is held together by the compressibility, cohesion and adhesion.

Particle sizes [mm]	0.002	0.0063	0.02	0.063	0.2	0.63	2.0	6.3	20	37	63	200	630	>630	
Soil fraction	Fine soil						Coarse soil						Very coarse soil		
Sub-fraction	Clay	Silt			Sand			Gravel			Cobble	Boulder	Large boulder		
		Fine	Medium	Coarse	Fine	Medium	Coarse	Fine	Medium	Coarse					

Table 1: Soil classification after BS EN ISO 14688-1:2002

The pore water pressure influences the shear strength, either drained or undrained. The undrained condition occurs if the internal resistance of the soil particles influences the behaviour of the soil. Coarse and very coarse soil are not influenced by the connectivity and internal resistance. Only if negative pore water pressure results from capillary forces, the water forms bridges between the sand grains.^{viii}

Soil can also be solid, i.e. chalk, which leads to a combination of drilling and pilling. A detailed soil investigation needs to be performed, with at least a borehole taken at every pile location with a laboratory test performed at encountered soil layers. Also seismic survey over the complete field to get an impression of the stratigraphy of the encountered layers.

The soil conditions leads to the dimensions of the monopile which has to be a stable foundation for the wind turbine. The design of a monopile wind turbine foundation is explained in the next section.

2.3 Design of a Monopile Wind Turbine Foundation

The design of a monopile depends on the type of loads that affect the structure and the type of soil at the final location. A flow diagram for the design process is shown in figure 12. The external conditions are the site-specific conditions, as mentioned in subsection 2.2.1.

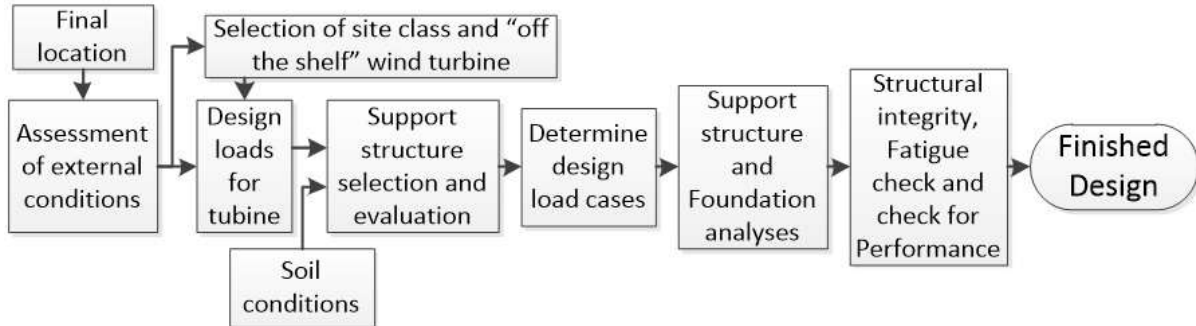


Figure 12: Design process for Offshore wind turbine^{ix}

When the final location and the external conditions are known, the capacity of the turbine must be defined. The turbine capacity results in a rotor size, which needs a certain height above the water level. The selected support structure is the monopile. The design load is location dependent as described in the previous section.

The depth of the monopile into the seabed is indicated by the support structure and the foundation analysis. The last step, “structural integrity, fatigue check and check for performance”, must conclude that the monopile wind turbine functions properly during its expected lifetime. The process concludes on the design of the wind turbine as described in the next subsection.

2.3.1 Design of the wind turbine

The wind turbine consists of different parts as shown in figure 9, figure 13 and in Appendix B. The connection of the monopile to the wind turbine tower is with the transition piece grouted to the monopile. The monopile is the foundation and penetrates into the seabed. The analytical model is in figure 14 as a mass-dashpot system.

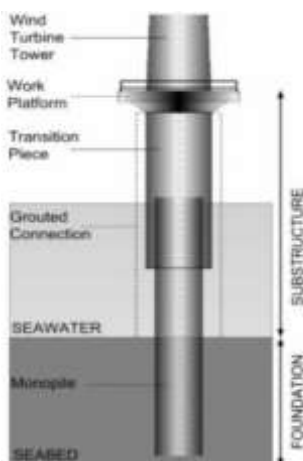


Figure 13: Foundation and substructure of a wind turbine

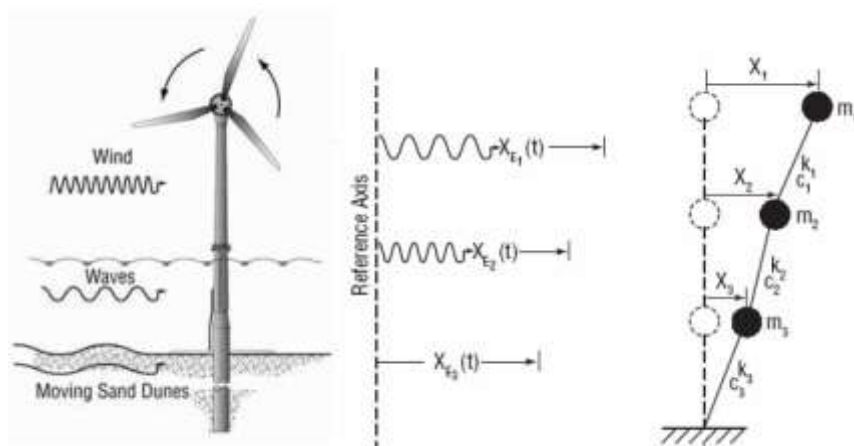


Figure 14: Loads on the wind turbine

The air, water and soil are the different surroundings of the wind turbine which cause the difference between the springs and dampers. The theoretical mass (m), damper (c) and spring (k) system for the forces is given. This defines the nacelle as m_1 , the tower response by k_1 and c_1 , the intermediate platform as m_2 , the transition part response as k_2 and c_2 , the grouted part as m_3 and the monopile response as k_3 and c_3 .

The turbine is in operation at a certain range of wind velocity. Today's wind turbines convert only a fraction of the wind power to electricity and are set to start power regulation for certain wind velocity. Wind turbines are set to start at a 10-min average wind velocity of about 9 to 10 m/s. Full regulation starts at about 14 to 15 m/s and shut-down or idle mode at 25 m/s. Shut-down or idle mode is to prevent structural limitations and resulting wear and tear of the turbine. Idle mode is rotation of the wind turbine 60 to 90 degrees compared to the wind direction or rotating the blades in vane position.

The normal wave conditions in combination with the extreme conditions are used to set the FLS of the foundation. The ULS can be defined with a long-term probability distribution approach. Long-term means at least dozens of years. The peak-over-threshold approach only considers the maximum value of one measurement above the threshold value. The threshold value is depending on the expected local weather conditions.

The wind velocity is height depended and is the most important issue for the durability of the wind turbine. The wind velocity is defined by the local wind conditions.

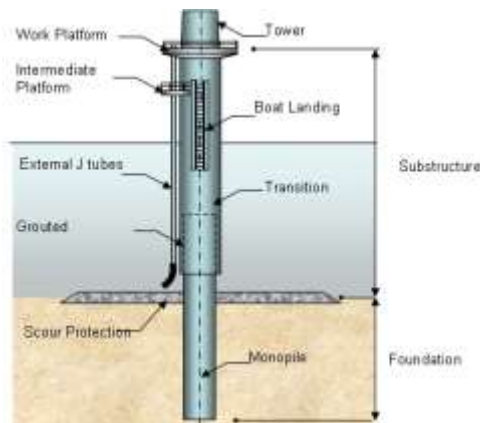


Figure 15: Various components of a monopile foundation (Iuga)*

The additional layer around the monopile, shown in figure 15, is scour protection. Due to the presence of the monopile foundation vortices in the current may be created. These vortices locally increase the current velocity which might be responsible for erosion of seabed material around the foundation. As the erosion around the foundation in fact decrease the penetration depth and increases the bending moment in the monopile, a longer and stronger pile might be required.

As an alternative a scour protection can be installed to prevent scour. It depends on the foundation type and local circumstances which option is the most economical one.

2.4 Projects of Van Oord

Experience with the monopile and the use of end-caps have been gathered during these projects:

- Belwind at the coast of Belgium, completed in December 2010.
- Luchterduinen at the coast of Holland near Noordwijk, completed in May 2015.
- Gemini at the coast of Holland north of Groningen, started in August 2015.

Only the project Belwind has been completed therefore the experience from Belwind is of additional value for this thesis. These three projects are described individually in the next three subsections.

2.4.1 Belwind

Belwind is a project in the Zeebrugge region of the North Sea, about 46 km west off the coast of Oostende. The project consists of 56 wind turbines which provides 165 MW. The wind farm has been completed in 2010 and the “Lessons Learned” report has been written.^{xi}

Learned lessons of the Belwind project are mainly related to two incidents during this project. Monopile A04 and C05 sank because of end-cap failure during towage. In addition to the installation conditions IHC Merwede, the supplier of the end-caps, provided a manual with operating instructions for the Belwind project. Despite the fact that the conditions were met two monopiles have sunk during their transportation. The two monopiles are shown in figure 16 and figure 17. For pile A03 there was a near miss.

The control of the installed end-caps lead to a checklist with preliminary conditions which have to be met before departure of the monopile from the storage site. These conditions are:

- A final check on site and approval of London Offshore Consultancy before tow out.
- 24hrs a day presence on the site of the end-cap engineers of the supplier.
- Full time presence of a site supervisor during preparation and installation of the end-caps.
- All information must be communicated to one single point of contact responsibility for tow-out planning.



Figure 16: Salvage monopile A04



Figure 17: Monopile C05

All monopiles had been checked before departure. The accidents of the two monopiles are very similar. Both accidents were caused by breaking or getting loose of the bolts, which connect the extra protection plate. If the bolts on one side break or get loose, the bolts at the other side will break shortly thereafter. This is caused by the stress of the disconnection at one side.

2.4.1.1 Lessons learned

The accidents were caused by:

- Hydraulic system failure by pressure loss.
- Mechanical system failure by shifting of one complete end-cap of the monopile.
- Leaking seal caused by minor damages to the seal by a hit from an object with sharp corners.

Based on these accidents the learned lessons for hydraulic end-caps during the Belwind project are:

- Every end-cap needs to be equipped with a digital pressure monitoring system with a wireless link so the pressure can be checked on board the tug during towing.
- All monopiles should be checked on the inside diameter. In this case the offshore high voltage system (OHVS) monopile appeared to have a smaller inside diameter due to a large wall thickness of the last steel can. End-caps can more easily adapt to a bigger diameter than to a smaller diameter.
- A counter weight on the bottom end-cap worked well to keep the monopile aligned during towing and it is anticipated to work much better than a rudder.
- The application of foam in the bottom-caps resulted in failure. Due to high pressure under water the foam bubbles started to burst and water could enter the foam. This endangered the floatability of the end-cap and made the end-cap heavier. Also frost damaged the foam.
- The towing arrangement was connected to the end-cap, thus the monopile was towed by the cap. Reason for this was that according the design it was not allowed to weld/attach towing pad eyes or bollards on the monopile. The peak loads acting on the end-cap induced by tide and waves acting on the tug and the monopile can be very high. Therefore they form a risk of movement of the cap. It is preferable to find a design solution with an attached tow arrangement directly to the monopile and not to the cap. This was done on the Walney wind farm in the East Irish Sea in 2012, as shown in figure 18.



Figure 18: Towing monopile on the monopile and not the end-cap

The loose control panel moves around in the waves. Surely it slammed and damaged the hydraulic circuit and the MINIMESS^{®xii} hose, which is the most vulnerable part. Finally both hoses broke loose and the end-cap lost both of its hydraulic circuits. After both hydraulic circuits were leaking monopile C05 sank. After the sinking of C05 an additional protection plate was installed on the end-caps. This has led to the following additional accidents:

- Heavy damaging impact on the control panel.
- Protection plate connected by bolts with insufficient strength.

The additional installed protection should have prevented the accidents. Nevertheless the protection plate resulted in damage of the control panel, caused by the bolts with insufficient strength. Calculations with the safety factor must be used to prevent accidents. This happened for monopile A04. For A03 leakage did only take place in one of the hydraulic circuits, since it lost one protection plate.

The expectation is that most accidents can be prevented during future projects. The end-caps must be designed to have durability and water tightness from the moment of installation at the storage site until the disconnection after upending. The lessons learned from these accidents have defined the conceptual design of the end-caps, which is described in the chapter 4.

2.5 Conditions for the design of a Monopile foundation

Based on the theory for the design of a monopile and previous projects of Van Oord conditions are set. These are used to prevent accidents in future projects. The “lessons learned” give the conditions for the conceptual design in the chapter 4. The conditions are the following:

- The design of the monopile is location dependant. One windfarm can consist of a range of different monopiles when the local conditions vary.
- The end-caps are designed to have a high durability and water tightness from the moment of installation until disconnection after upending. Durability and water tightness are the cause of most accidents.

The general theory of the monopile foundation design and the experience of Van Oord have been explained in this chapter. The combination of these two aspects gives the criteria for the end-caps. The installation of the monopile is described in the next chapter.

3 Installation of a Monopile Wind Turbine Foundation

The installation of a monopile takes place at the wind farm. The monopile is fabricated and transported to the storage site, where the pile is prepared for towage to its final location. At the storage site the end-caps are placed to guarantee water tightness until removal during the installation. After arrival at the installation site the pile is upended and the end-caps are removed. The loads on the monopile during transport, upending and removal provide the requirements of the end-caps.

In this chapter the theory of the installation of a monopile is explained. Transport provides the initial conditions for upending and is explained in the first section. Upending is the last step before the removal of the end-caps and this theory is the topic of the second section. In the third section the removal of the end-caps, the last step before installation of the monopile, is described. The theory is discussed in third section of this chapter.

3.1 Transport of a Monopile for an Offshore Wind Turbine Foundation

The monopiles are transported to the storage site where these are prepared for towage. Transportation from the storage site to the location of the wind farm is shown in figure 19. Before a monopile can float, end-caps or plugs are installed. The towing arrangement makes the connection of the monopile with the tug.

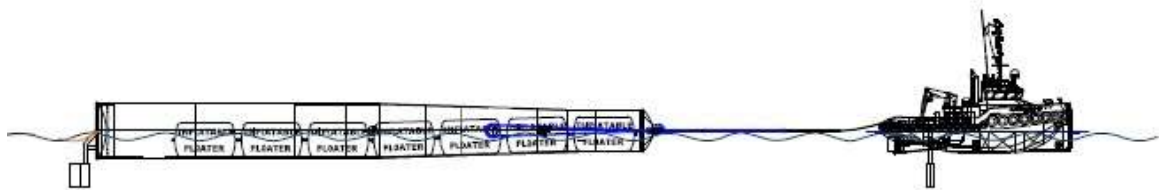


Figure 19: Towage of a monopile

At the storage site the end-caps and the towing arrangement is installed and tests are done. Besides testing the monopiles a weather window to operate is needed. The weather window depends on the requirements for the Aeolus, shown in figure 20, to operate. The requirements of the environmental conditions are given in Appendix E, for jacking, operational, survival and transit. The workable weather window is defined as the period during which the significant wave height, the current and the wind velocity are below the acceptable threshold values. The downtime period is the opposite.



Figure 20: The Aeolus

By using local statistical weather measurements and the threshold values, the expected weather windows are estimated. In case of a tender the period of installation is based on the history of the weather conditions, along the towage route and the installation site. The period of installation is defined before the installation starts.

The weight of a floating monopile causes a submerged part. The submerged part leads to drag and lift forces. The drag force along the submerged monopile are the counter force to the tug. The lift force results from waves and the towage velocity. The lift force acts perpendicular to the undisturbed water flow velocity and the drag force. The lift force causes a decreased submerged volume. Since transportation and upending only take place with gently wave conditions these forces are neglected.

At the installation site the monopile is connected to the local tug, as shown in figure 21. The local tug escorts the monopile to help the jack-up. The needed capacity of the tug is less than the capacity needed to transport the monopile, since the local tug only has to position the monopile which takes place at low velocity.

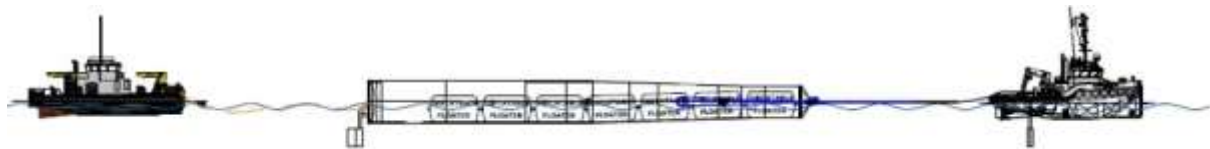


Figure 21: Connection to local tug close to the installation vessel

The rigging arrangement, in Appendix C, makes the connection with the jack-up, shown in figure 22. Positioning the monopile is done after connecting the control lines with the jack-up. The compressors, which seal the end-caps, are controlled from the jack-up during upending. The tug removes the towing gear and returns to the storage site for the next monopile.



Figure 22: Handover from tug to jack-up

Delay during transport is prevented if the end-caps are tested on the storage site and if the threshold value for the Aeolus to operate is not exceeded. The conditions for the transport of a monopile for an offshore wind turbine foundation are the following. First of all the weather window for the period of transport and upending is calculated in advance. The drag and lift force during transport are neglected since this takes place with gently wave conditions. Transport provides the initial conditions for upending.

The next step for the installation of the monopile at the installation site is upending the monopile, topic of the next section.

3.2 Theory of Upending

The tug hands the monopile over to the crane, which installs the pile. The installation starts with upending of the monopile, which is restricted by the safe working load of the crane. Based on the initial conditions shown in figure 23, the crane starts lifting or actually upending the pile, shown in Appendix D.

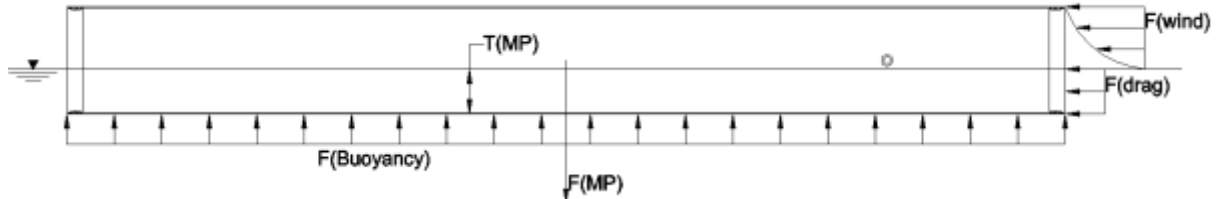


Figure 23: Initial forces on the monopile

The pile starts rotating when the lifting starts, since the trunnions are not aligned with the centre of gravity (CoG). Upending of the monopile depends on multiple independent load factors, which lead to the net force on the pile. Upending is done by hoisting, defined by the hoisting speed and the capacity of the crane, and is determined by the sum of all the forces. The forces results from the hydrostatic and atmospheric pressure, the inertia, the gravity, the viscosity, the elasticity and the surface tension.

During upending of the pile the surroundings of the monopile partial changes. The hydrostatic pressure decreases because the crane puts an upward load on the monopile. This decreases the buoyancy of the pile, equation 3.1. The submerged volume must remain sufficient to keep the load of the crane less than or equivalent to the safe working load, equation 3.2.

$$F_{\nabla} = \rho_{sw} \cdot g \cdot \nabla = \rho_{sw} \cdot g \cdot A_i \cdot L_{MP} = p_h \cdot A_s^{xiii} \tag{3.1}$$

$$F_c = F - F_{\nabla} \leq F_{SWL} \tag{3.2}$$

F_{∇}	Buoyant force	N
ρ_{sw}	Volumetric mass density of seawater	kg/m ³
∇	Submerged volume	m ³
A_s	Submerged cross-sectional area	m ²
L_{MP}	Length of the monopile (≈ 70)	m
F_c	Load lifted by the crane	N
F	Net force	N
F_{SWL}	Safe working load of the crane	N

The inertia of the monopile prevents rotation of the pile. The resistance is based on the changing velocity. The stationary floating monopile resists lifting and the continuous hoisting speed maintains when the lifting stops. The inertia force influences the net force during the changing velocity at the beginning and end of hoisting.

The gravity force on the monopile is unidirectional and constant, unless the mass of the pile changes. During upending the monopile is repositioned and the gravity force remains constant. The removal of the rigging arrangement before upending and the removal of the end-caps after upending reduce the

weight of the pile. The reduction of the weight of the pile decreases the needed buoyant force to remain within the capacity of the crane.

Viscosity is the internal resistance of a fluid to flow.^{xiv} The dynamic viscosity of seawater is in the range of 0.8 until 2 mNs/m. The elasticity is the property of returning to an original form or state following deformation. The elasticity of steel is a constant in the range of 180GPa until 240GPa. Surface tension is the appearance of a film across the surface of a liquid caused by the attraction between its molecules. The surface tension is in the range of 0.18 until 0.37 mN/m^{xv}.

The scalar magnitudes of the forces affects the flow field.^{xvi} The net force on the monopile is defined in equation 3.3 and the forces are defined individually in equation 3.4 to 3.9. The standard seawater properties are shown in Appendix F.

$$F = F_p + F_l + F_G + F_v + F_E + F_T \quad 3.3$$

$$F_p = (\Delta p) \cdot A = (p_0 + p_h) \cdot A = (p_0 + \rho \cdot g \cdot h) \cdot A \quad 3.4$$

$$F_l = m \cdot a = (m + m') \cdot a = \rho \cdot V^2 \cdot l^2 \quad 3.5$$

$$F_G = m \cdot g \quad 3.6$$

$$F_v = \tau \cdot A = (\mu + \varepsilon) \cdot \frac{dV}{d(x,y,z)} \cdot A = (\mu + \varepsilon) \cdot V \cdot l \quad 3.7$$

$$F_E = E \cdot A \quad 3.8$$

$$F_T = \sigma \cdot l \quad 3.9$$

F_p	Pressure force	N
F_l	Inertia force	N
F_G	Gravity force	N
F_v	Viscous force	N
F_E	Elasticity force	N
F_T	Surface tension force	N
p	Pressure	N/m ²
A	Cross-sectional area	m ²
p_0	Atmospheric pressure (≈ 101325 N/m ²)	N/m ²
p_h	Hydrostatic pressure	N/m ²
h	Distance below seawater level	m
m	Mass	kg
a	Acceleration	m/s ²
m'	Hydrodynamic mass	kg
V	Velocity vector (u, v, w)	m/s
l	Length	m
τ	Shear stress	N/m ²
μ	Dynamic viscosity	N s/m ²
ε	Eddy viscosity	N s/m ²
$dV/d(x, y, z)$	Velocity gradient	s ⁻¹
E	Elasticity	N/m ²
σ	Surface tension	N/m

3.3.1.2 Hydrodynamic pressure

Hydrodynamic pressure is the resulting force by a fluid or gas in motion. External loads do not only depend on gravity, density and the water depth, but also on the flow velocity. The relation of the motion leads to the kinetics, which can be calculated by using the Bernoulli equation, equation 3.11^{xvii}. The simplified equation, equation 3.12, is valid for an irrotational flow ($\nabla \times V=0$) and a perfect fluid ($\mu_w=0$) with a steady flow ($\delta\Phi/\delta t=0$).

$$\rho_{sw} \cdot \frac{\delta V}{\delta t} + \rho_{sw} \cdot (\nabla \cdot V) \cdot V - \mu_w \cdot \nabla^2 \cdot V + \nabla \cdot \left(p_0 + \rho_{sw} \cdot g \cdot h + \frac{1}{2} \cdot \rho_{sw} \cdot V^2 \right) = 0 \quad 3.11$$

$$p_0 + \rho_{sw} \cdot g \cdot T_{MP,max} + \frac{1}{2} \cdot \rho_{sw} \cdot V^2 = constant = p_0 + \frac{n \cdot R \cdot T_{mp}}{V_a} + \frac{1}{2} \cdot \rho_a \cdot (u^2 + v^2 + w^2) \quad 3.12$$

Φ	Velocity potential	m/s
∇	Operator (of 3D Cartesian system)	m
μ_w	Dynamic viscosity of the wave	N s/m ²
$T_{MP,max}$	Maximum draft of the monopile	m
n	Amount of substance of air	mol
R	Gas constant (≈ 8.314472)	J K ⁻¹ mol ⁻¹
T_{mp}	Temperature inside the monopile	K
V_a	Volume of air	m ³
ρ_a	Volumetric mass density of air (≈ 1.25)	kg/m ³

The flow causes dynamic pressure and kinetics, the motion of the air. The overpressure inside the monopile is needed for the flow of air out of the pile. The flow of air in motion is the hydrokinetics.

3.3.1.3 Hydrokinetics

The hydrokinetics are the behaviour of fluid in motion. This behaviour leads to the dynamic pressure, as explained in the previous subsection. This results from the flow of air out of the monopile. The flow of air causes an additional pressure decrease. The flow velocity of air can be calculated with equation 3.13.

$$V = \sqrt{\frac{\rho_{sw} \cdot g \cdot T_{MP,max} + \frac{1}{2} \cdot \rho_{sw} \cdot V^2 - \frac{n \cdot R \cdot T_{mp}}{V_a}}{\frac{1}{2} \cdot \rho_a}} \quad 3.13$$

$$\tau(x, y, z) = \mu \cdot \frac{dV}{d(x, y, z)} \quad 3.14$$

$$\nu = \frac{\mu}{\rho} \quad 3.15$$

ν	Kinematic viscosity	m ² /s
-------	---------------------	-------------------

The air, which flows out of the monopile, causes friction along the wall of the bottom-cap and the monopile. The friction decreases the amount of air that escapes. The resulting shear stress is defined in equation 3.14. The velocity vector is a three-dimensional flow velocity. The u-, v-, w-axes are related to the x-, y-, z-axes.

The outflow of air relative to the displacement of the bottom-cap must be calculated. This is used to define the total internal overpressure to fully disconnect the bottom-cap. The relation of the kinematic viscosity and the dynamic viscosity is shown in equation 3.15. This depends on the density of the fluid or gas.

The hydromechanics explain the reason why the internal overpressure is preferred for the removal of the bottom-cap. The process of removal is based on the static, dynamic and kinetic hydromechanics.

3.3.1.4 Process of removal

The process of removal of the bottom-cap is done with internal overpressure. The overpressure pushes the bottom-cap out of the monopile. The initial conditions are shown in figure 24. The hydrostatic (P(h)) and internal (P(i)) pressure are shown in figure 25.

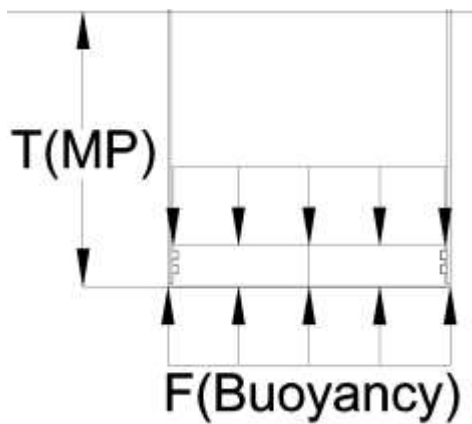


Figure 24: Initial pressure on the bottom-cap

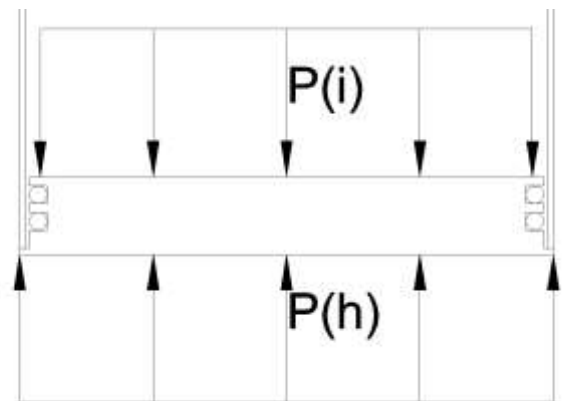


Figure 25: Pressure on the bottom-cap

During the disconnection of the seal the bottom-cap starts moving when the friction of the seal with the monopile is less than the pressure difference. Friction can damage the seal, so the seals must be checked when returned at the installation site. Hydrostatic response of the bottom-cap takes place until the seal is (partially) disconnected from the monopile.

The hydrodynamic response starts when either the seawater, the case with an internal under pressure, or the air, the case with an internal overpressure, can flow. The size of the gap and the pressure difference influence the hydrodynamic response. The flow velocity, the hydrokinetic response, is part of this response. The flow velocity, in equation 3.16, the needed internal pressure, in equation 3.17, and the needed volume of air, in equation 3.18, can be calculated.

$$\Delta p = \frac{1}{2} \cdot \rho_a \cdot V^2 = p_i - (p_0 + p_h) \tag{3.16}$$

$$p_i = p_0 + \rho_{sw} \cdot g \cdot T_{MP,max} \tag{3.17}$$

$$V_a = \frac{n \cdot R \cdot T_{mp}}{p_i} \tag{3.18}$$

$$F = (m + m') \cdot g + c_v \frac{\delta w}{\delta t} \tag{3.19}$$

Δp	Pressure difference	N/m ²
p_i	Internal pressure	N/m ²
c_v	Fluid viscosity	Pa s

The flow of air out of the monopile decreases the internal pressure, which leads to the displacement of the bottom-cap. The total load on the bottom-cap pushes the cap out of the pile. The displacement, velocity and acceleration of the bottom-cap decreases the internal pressure. The pressure inside the pile must be sufficient before disconnecting the seals and lead to a fully removed bottom-cap.

There are two types of bottom-caps either a cap which floats or one which sinks. A floating cap needs a calculated internal overpressure to fully remove the bottom-cap. A sinking cap needs a small overpressure to guarantee the initial displacement of the bottom-cap.

Based on previous experience, end-caps do not have to float. A floating bottom-cap increases the risk of damage during removal from the monopile. A connection point for a cable to the winch at the tugboat or the jack-up is needed. The internal overpressure gives the initial acceleration of the bottom-cap out of the monopile.

The total load is calculated with equation 3.19. This equation result the total load by the mass, the hydrodynamic mass and the fluid which sticks to the mass, the combination of the previous three subsections. The next step after removal of the bottom cap is the removal of the top-cap. This is explained in the next section.

3.3.2 Removal top-cap

After removal of the bottom-cap, the top-cap is removed. The goal of the top-cap is to retain air inside the monopile for buoyancy. The top-cap is removed when the crane does not need the buoyant force to lift the monopile. The F_{SWL} of the crane must not be exceeded.

3.3.2.1 Buoyancy restrictions

The buoyancy restrictions depend on the safe working load of the crane. The relative density of the submerged steel based on the density of seawater leads to the minimal submerged volume of the monopile to remove the top-cap. The relative density is used to calculate the load lifted by the crane, using equation 3.21.

$$A_{MP} \cdot T_b \cdot (\rho_s - \rho_{sw}) + A_{MP} \cdot (L_{MP} - T_b) \cdot \rho_s = F_c \leq F_{SWL} \quad 3.20$$

$$\frac{F_{MP}}{\rho_s} \cdot (\rho_s - \rho_{sw}) = \frac{1100t}{7850kg/m^3} \cdot (7850kg/m^3 - 1025kg/m^3) = 956t = F_c \geq F_{SWL} \quad 3.21$$

A_{MP}	Cross-sectional area of the monopile	m^2
T_b	Draft of the bottom-cap	m
ρ_s	Volumetric mass density of steel ($\approx 7850 \text{ kg/m}^3$)	kg/m^3
F_{MP}	Weight of the monopile	N

The relative density for a monopile of 1100t is calculated with equation 3.21. The total load of the fully submerged monopile is more than the F_{SWL} . The top-cap can only be removed when the monopile is placed on the seabed. Lowering the monopile increases the hydrostatic pressure and the buoyant force of the monopile. The increasing internal pressure leads to the maximum load on the top-cap. The top-cap must be designed to withstand this force.

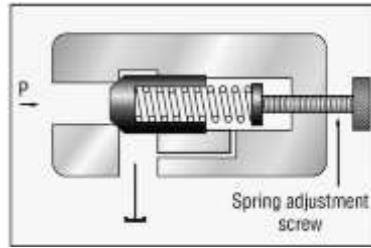


Figure 26: Spring controlled pressure valve

A pressure valve must be installed on the top-cap to define the maximum internal pressure. By opening the valve, air is released and the internal pressure of the monopile will decrease. The buoyant force must remain sufficient for the crane. An example of a controlled pressure valve is shown in figure 26.

The screw of the valve defines the pressure needed to open the valve. The spring stiffness with the initial displacement sets the needed pressure. If the pressure exceeds the spring force, as defined in equation 3.22, the valve will open. With an open valve the pressure is reduced until the defined maximum pressure.

$$F_k = k \cdot (x_k + x_{k,0}) \tag{3.22}$$

F_k	Spring force	N
k	Spring stiffness	N/m
x_k	Displacement of the spring	m
$x_{k,0}$	Initial displacement of the spring	m

The needed internal pressure must be calculated and adjusted on the valve before the monopile leaves the storage site. This is based on the dimensions of the monopile and the final installed location.

3.4 Conditions for the Installation of a Monopile

The conditions that influence the installation of a monopile offshore from the storage site until the final installation are mentioned in this chapter. Based on the theory the recommendations and assumptions for the installation of a monopile for an offshore wind turbine foundation are combined to define the conditions to install a monopile offshore. The conditions are:

- A weather window for the installation of a monopile has to be calculated in advance.
- Drag and lift force during towage can be neglected since this takes place with gently wave conditions.
- Transport provides the initial conditions for upending.
- Removal of the bottom-caps is a dynamic process.
- The top-cap are removed when the pile is placed on the seabed.
- The crane only lifts the vertical load when the vertical pile is clamped by the gripper.

The monopile is analysed theoretically until installation. The dominant forces must be determined to simplify upending of a monopile. Based on the theory the recommendations and assumptions are either confirmed or rejected in the next chapters.

4 Conceptual design of the End-caps

The conditions based on the theory and the “Lessons learned” from projects of Van Oord together form the requirements for an optimized conceptual design of the end-caps. Since the monopile is designed for loads much bigger than possible during transport or installation, the end-caps are the weakest points. The loads which the end-caps have to encounter determine the prerequisites.

With the theory in chapter 3 these loads are calculated. The maximum loads are horizontal, vertical or a combination of both from the storage site until disconnection at the installation site. The prerequisites for the design of the end-caps are the following:

- End-caps have to be designed with a high durability. The end-caps should always be checked at the storage site.
- End-caps have to be equipped with manometers.
- End-caps used as a top-cap must have a pressure valve which is set after installation on the monopile for the installation conditions of that specific pile.
- End-caps have to be equipped with a digital pressure monitoring system.
- The rigging arrangement must be installed on the pile and not on the end-caps.
- Two installed end-caps need to have a weight balance for safe transport of the monopile.
- The control panel of the end-cap must be well protected.

The most important aspects to optimize the concept are discussed in the next section. In the second section these aspects lead to two designs of the end-caps. Finally the best conceptual design is defined in the last section of this chapter.

4.1 Requirements of End-caps

The requirements of the end-caps have been mentioned above. Important aspects are the dimensions of the pile, the conditions of the end-caps and the force balance. These issues will be described in the next three subsections.

4.1.1 Dimensions of the Monopile

The dimensions of the monopile, as explained in chapter 2, depend on the dimensions of the wind turbine, the soil properties and the weather conditions at the final location. The dimensions of the monopile are defined and given by the client. The end-caps must fit inside the ends of the monopile. Generally the internal diameter and wall thickness varies both within a single project and also relative to other projects, as shown in table 2 on the next page.

The difference between the inner diameter of the monopile and the outer diameter of the end-cap is filled with a piston seal. The piston seal must guarantee water tightness when it is clamped. When the seal is released, or unclamped, the end-cap has to move freely. Using two individual seals on each end-cap increases the safety.

Two parallel independent seals for every single end-cap result the highest probability of water tightness. The distance between the seals must be sufficient to prevent interaction, but not too big to prevent counterforces between the seals. The distance between the installed seals must be at least the wall thickness of the monopile. This leads to the penetration depth of the end-cap into the monopile.

Details Project	Outer diameter [mm]	Wall thickness [mm]	Inner diameter [mm]
Belwind	5000	70	4860
	5000	60	4880
	4072	60	3952
	4072	55	3962
Gemini	6000	70	5860
	5800	70	5660
	5600	65	5470
	4522/4243	75	4372/4093
Luchterduinen	5000	60	4880
	4500	70	4360

Table 2: Properties of monopiles of projects of Van Oord

The pressure of the seals should be monitored continuously to check the water tightness. The seals must satisfy the buoyancy requirements, described in the next subsection.

4.1.2 Conditions of the End-caps

The end-caps are used repeatedly and must not fail. The conditions for the end-caps to be used properly depends on the type of sealing system. The types of sealing system are described in the next subsection. In the second subsection the dimensions of the end-cap are described. Finally the position of the sealing system is mentioned in the last subsection.

4.1.2.1 Type of the sealing system

The type of sealing system depends on the specific details of such a system. The three types of systems that can be used are: mechanical, hydraulic and pneumatic. Every type has its own advantages.

A mechanical system consists of elements that interact on mechanical principles. The mechanical system has the advantage that it can be used more often, but this depends on the sealing material. The hydraulic system can be applied as the sealing material for a mechanical system.

The hydraulic system consists of a non-metallic material captured in a groove such as rubber, polytetrafluoroethylene (PTFE) or thermoplastic elastomers. The system seals after deformation by a controllable external force. The material is incompressible and can withstand high forces.

The pneumatic system is also based on deformation, but by a gaseous medium. Gas is compressible and absorbs excessive forces. Such compressible substance is less controllable than the material of a hydraulic system.

The mechanical and hydraulic system are combined for the seal of the conceptual design. The dimensions needed for the sealing system influence the dimensions of the end-cap. This is described in the next subsection.

4.1.2.2 Dimensions of the End-cap

The difference between the inner diameter of the monopile and the outer diameter of the end-cap is filled with the piston seal. The piston seal must guarantee water tightness when it is clamped. When the seal releases, or unclamps, the end-cap has to be able to move freely. Using two individual seals on each end-cap increases the safety.

The seal must fill the space between the inner diameter of the monopile and the outer diameter of the end-cap. The increasing size of the outer diameter of the seal, to fill the increasing difference between the internal diameter of the pile and the outer diameter of the cap, will lead to an increasing penetration depth of the end-cap into the monopile. The penetration depth is needed to keep a gap between the two seals and prevent interaction. The pressure on the seals must be monitored.

The minimum width of the end-cap is directly related to the size of the seal. The seal is positioned in a groove. The groove for the seal must have a depth equal to or larger than the diameter of the seal without pressure. The seal is protected during removal and transport back to the storage site.

The shape of the end-caps influences the transport of the monopile. During transportation of the monopile the friction depends on the drag coefficient (C_d). The shape of the end-cap influences the drag coefficient, as shown in figure 27. The shape of the top-cap is best to be spherical and the shape of the bottom-cap is best to be flat.

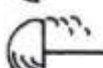
Shape	C_d	Shape	C_d
	1.17		0.38
	1.42		0.42
	1.42		0.59
	1.38		0.8
	1.05		0.5

Figure 27: Some common shapes and their drag coefficients

After the type and dimensions of the sealing system, the position of the hydraulic pressure system is described in the next subsection.

4.1.2.3 Position of the pressure system

The hydraulic pressure system is positioned close to the seal. The system must withstand the harsh offshore environment and has to be protected against collision with the monopile. Combining the mechanical and hydraulic system leads to the following advantages:

- Solid and long lasting end-caps
- The controllable hydrostatic pressure system can (dis-) connect the end-cap to the monopile.
- The system controls the hydraulic pressure of both seals individually.

The seal is the most important element of the end-caps. When the seal fails there will be a delay in the installation of the wind farm. Testing the seal before departure at the storage site can prevent failure of the seal. Replacement of the seal should be an easy and quick process. Disconnection of the end-cap is related to the force balance. This is explained in the next subsection.

4.1.3 Force balance

The end-cap have to maintain a monopile floating during transport. Water can only flow into the monopile when the end-caps are disconnected. For disconnection of the end-caps the forces resulting from upending have to be known, section 3.2. The forces depend on the hydrostatic pressure, wind and waves. Hydrostatic pressure is the dominant force.

Pressure difference on the end-cap leads to suction or pumping when the seals are released from the monopile. With a pressure balance neither suction nor pumping will take place. The pressure balance and the dynamic pressure are described in the next two subsections.

4.1.3.1 Hydrostatic pressure

The last important aspect of the end-caps is the pressure balance, as described in chapter 2 and 3. A slight overpressure inside the monopile is preferred, to guarantee the flow of air out of the monopile. The air pushes the end-cap out of the monopile, based on the simplified Bernoulli equation in section 3.3. With an external overpressure the bottom-cap must be designed to be lifted into the pile. To control the internal pressure a valve must be installed on the end-cap.

The hydrostatic pressure on a monopile is on the immersed part of the pile. The pressure depends on the water depth, as defined in equation 4.1. The hydrostatic pressure is fluctuating caused by waves. Monopiles are installed at water depths up to 35 meters, with a pressure up to 4.5bar, 453kN/m².

$$p = p_0 + \rho_{sw} \cdot g \cdot h = 101315 \frac{N}{m^2} + 1025 \frac{kg}{m^3} \cdot 9.81 \frac{m}{s^2} \cdot 35m = 1bar + 3.5bar = 453 \frac{kN}{m^2} \quad 4.1$$

Monopiles with internal overpressure and connected end-cap are risky and can endanger the crew and the environment. The pressure increase is at the installation site to prevent these risks. The capacity of the compressor is restricted and this leads to additional time at the installation site. A good example of a compressor is the Rotary Screw Compressor HSD 831 SFC^{xviii} of KAESER Kompressoren GmbH. The compressor is used for the further calculations. To increase or decrease the internal pressure a compressor must be available on the Aeolus.

Manometers have to be installed before the end-cap is disconnected to observe the expected behaviour of the end-caps after disconnecting the seals. The manometers must be placed at a protected location to prevent damage during installation and disconnection of the end-caps. A digital pressure monitoring system in combination with the wireless connection gives the best control for the removal of the end-caps.

Increasing the pressure will depend on the flow rate of the compressor, a screw blower^{xix}, and the needed pressure increase. To combine all conditions, two conceptual designs will be explained in the next section. The properties of the end-caps have to be used to create an optimized conceptual design. A pressure difference will lead to either a flow of air or seawater. This is the dynamic pressure as mentioned in section 3.3. The influence on the design is described in the next subsection.

4.1.3.2 Dynamic pressure

The pressure difference will lead to a dynamic response of the end-cap. The flow of air or seawater will be the response after disconnection of the seals. The pressure difference and the density of the flowing substance result the expected flow velocity. Rewriting equation 3.12 results equation 4.2.

$$p_0 + \rho_{sw} \cdot g \cdot h + \frac{1}{2} \rho_{sw} \cdot V^2 = \text{constant} = p_0 + \rho_a \cdot g \cdot h + \frac{1}{2} \rho_a \cdot V^2 \quad 4.2$$

$$\rho_{sw} \cdot g \cdot T_{MP} + \frac{1}{2} \rho_{sw} \cdot V^2 = \rho_a \cdot g \cdot h + \frac{1}{2} \rho_a \cdot V^2 \quad 4.3$$

$$\frac{v_{sw} \cdot \rho_{sw}}{2} + p_e = \frac{v_a^2 \cdot \rho_a}{2} + p_i \quad 4.4$$

$$A_{ext} \cdot v_{sw} = A_{int} \cdot v_a \quad 4.5$$

T_{MP}	Draft of the monopile	m
v_a	Flow velocity of air	m/s
v_{sw}	Flow velocity of seawater	m/s
p_e	External pressure against the end-cap (hydrostatic pressure)	N/m ²
A_{int}	Internal cross-sectional area	m ²
A_{ext}	External cross-sectional area	m ²

As mentioned before the dimensions of the bottom-cap can lead to either a needed internal overpressure to push the end-cap out of or external overpressure to push the end-cap into the pile. In both cases the end-cap is repositioned until there is a pressure balance. Internal overpressure takes additional installation time because of the needed increase of the pressure. External overpressure can result projection of the bottom-cap into the pile.

The gripper of the Aeolus, which holds the monopile, is assumed to be inelastic. The position of the end-cap is directly related to the pile. The velocity vector of the pressure difference gives the conditions for the end-cap. The displacement of the end-cap and the air that flows out of the monopile will decrease the pressure difference.

With the dimensions, conditions and force balance all requirements for the conceptual designs are mentioned. The conceptual designs combine these and are defined in the next section.

4.2 Conceptual designs

The conceptual designs of the end-cap based on the theory are developed. Every design depends on the dimensions, the sealing system and the pressure balance as mentioned in the previous section. These are combined with the use of the end-caps as described in chapter 3. The most important aspects are:

- End-caps must result in a waterproof monopile.
- End-caps must have a valve to control the internal and external pressure.
- End-caps need to cause the least friction during towage.
- End-caps must be able to be used at both ends of the monopile for transport and upending.

All recently used end-caps have the same concept of disconnection: the bottom-cap is pushed out of the monopile and the top-cap is lifted by the crane when the monopile is placed on the seabed. The advantage of the bottom-cap with a protection plate is that the plate can be used as an additional contact point with the monopile, as protection of penetration of the end-cap into the pile. The protection plate increases the safety of instruments inside the cap. As a part of this study an alternative concept the bottom-cap, which floats and is lifted through the pile has been investigated. Both concepts are described in this section.

The first concept is similar to the commonly used end-caps. For this concept the mechanical and hydraulic sealing system will be combined for the seal of the end-caps. There will be several contact points between the monopile and the end-cap to position the cap. The bottom- and top-cap of the first conceptual design are shown below. The protection plate protects the pressure system. For the right overlay of the end-caps with the pile, the diameter of the protection plate ($D(op)$) must be smaller than the outer diameter ($D(o)$) and greater than the inner diameter ($D(i)$) of the monopile. Preferred is exact the same as the outer diameter of the pile minus the standard deviation of the outer diameter. This results a floating pile without a changing outer diameter.

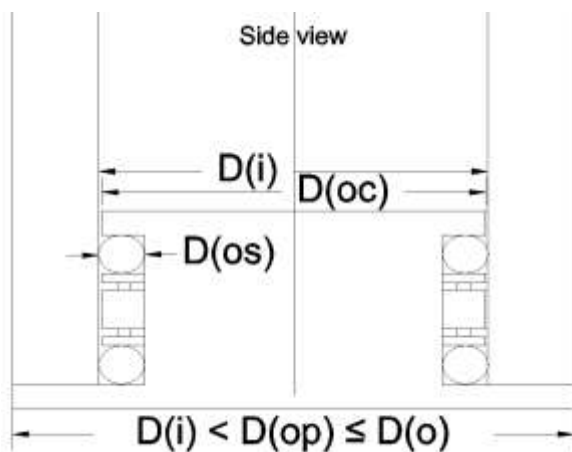


Figure 28: Conceptual design 1, bottom-cap

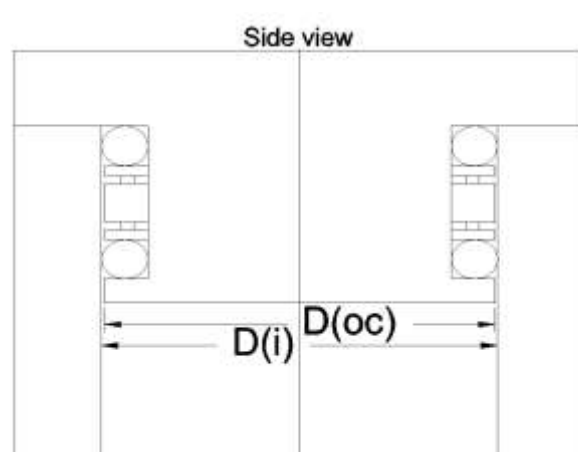


Figure 29: Conceptual design 1, top-cap

The second concept of the end-cap has a smaller diameter than the inner diameter at the top of the monopile, $D(i,t)$. A bottom-cap that floats meets this condition can be lifted up through the monopile at the installation site.

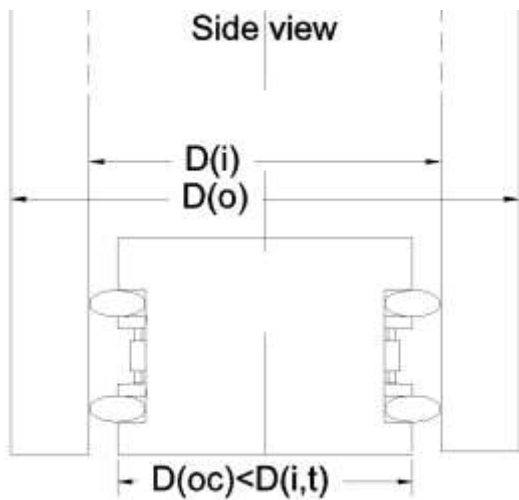


Figure 30: Conceptual design 2, bottom-cap

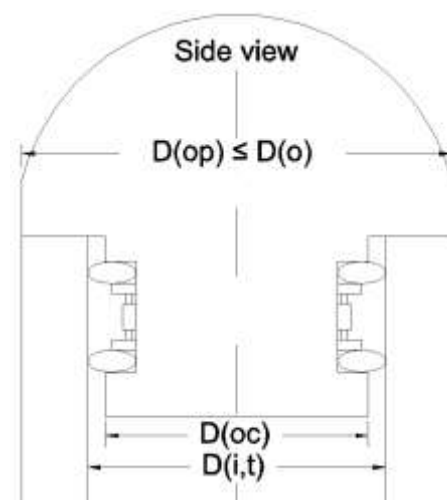


Figure 31: Conceptual design 2, top-cap

The top-cap of the second conceptual design has a spherical top, which decreases the drag coefficient c.q. the friction coefficient during towing. The additional space in the top-cap can be used for a winch to lift the bottom-cap. Both concepts of the top-cap can be combined with one of the other two bottom-caps. For a combination with the bottom-cap of the second design it must be possible to lift the cap through the monopile. For such a case the top-cap of the first conceptual design can be adjusted. This concept is shown in figure 32. The additional space with the spherical top is used for the winch.

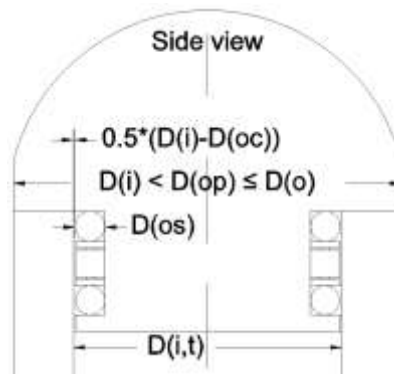


Figure 32: Conceptual design 1, top-cap with spherical protection plate

The two concepts use cylinders which deforms the sealing material. The difference between the concepts is the restricted outer diameter of the cap, $D(oc)$. In the two conceptual designs the installation of the seal, the minimum width and the possible position of the hydraulic pressure system of the seals at the end-caps are different. The two types of seal are a rubber tube deformed from a different direction. All combinations of the sealing system and the different shapes of the protection plate are possible.

The outer diameter of the seal without pressure will lead to the maximum possible extension under pressure. The difference is shown in the two top-views in figure 33 and figure 34. The outer diameter

of the seal and the outer diameter of the protection plate is shown in the figures. Only the visible part of the seal is yellow.

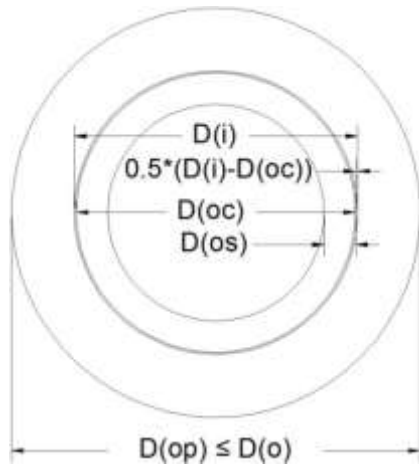


Figure 33: Dimensions monopile and end-cap

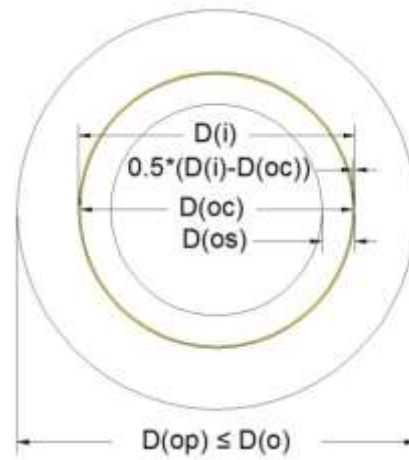


Figure 34: Dimensions sealed (yellow) end-cap

Either by pushing the end-cap out of or pulling-up the end-cap through the monopile. In the next two subsections the two concepts are described individually.

4.2.1 First conceptual design

In case of the first conceptual design external disconnection is the only way to remove the cap. The plate on the end-cap, which protects the hydraulic pressure system and prevents the end-cap to penetrate into the monopile, must be pulled or pushed out of the monopile because the diameter of the protection plate is larger than the inner diameter of the monopile. This design is shown in figure 35.

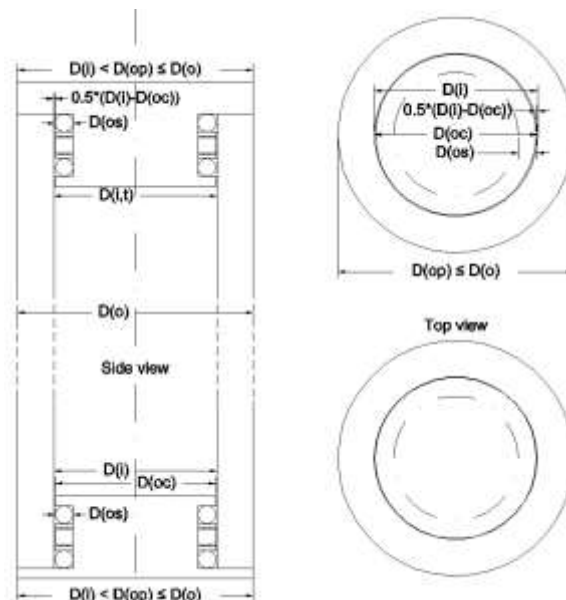


Figure 35: Conceptual design 1

The needed pressure balance for the removal of the bottom-cap depends on the hydrostatic and dynamic pressure as explained in subsection 4.1.3.2. Equation 4.2 give the value for the pressure balance.

A pressure difference results a flow velocity. The velocity vector is three dimensional and can go in any direction. An estimation of the flow velocity can be made with equations 4.6 or 4.7. The velocity depends on the difference in pressure and the size of the gap between the monopile and the cap.

$$v_a = \sqrt{2 \cdot (p_e - p_i) / \rho_a \left(1 - [A_{int} / A_{ext}]^2\right)} \quad 4.6$$

$$v_{sw} = \sqrt{2 \cdot (p_i - p_e) / \rho_{sw} \left(1 - [A_{ext} / A_{int}]^2\right)} \quad 4.7$$

The flow velocity depends also on the density of the flowing substance either air or seawater. The density difference between these substances is a factor thousand. The density of seawater is given in Appendix F and the density of air can be calculated with equation 4.8 or result from Appendix G.

$$\rho_a = \frac{P_i}{R \cdot T_{mp}} \quad 4.8$$

The pressure or the temperature inside the monopile must be measured to know the internal pressure. The pressure difference can be used to estimate the flow velocity. The external pressure is not constant, because of the changing water level caused by waves. The maximum and minimum external pressures are caused by the crest and the trough of the waves.

Since the bottom-cap must be pushed out of the monopile, the internal pressure must be higher than the external pressure. The internal pressure can be increased by a pump on the monopile through a valve in the end-cap. The flow rate of the pump on the monopile and the draft needed for the acquired buoyant force results in the additional time of installation.

The free air delivery (FAD) of the HSD 831 SFC, named in subsection 4.1.3.1, is 5160 m³/hour. This compressor is used to calculate the time to increase the pressure inside the monopile. This is shown in equation 4.9 to 4.12.

$$p_i \geq p_e = p_0 + \rho_{sw} \cdot g \cdot T_{MP} \quad 4.9$$

$$n = \frac{R \cdot T_{mp}}{p_0 \cdot V_a} \quad 4.10$$

$$V_{ad} = \frac{n \cdot R \cdot T_{mp}}{p_i - p_0} \quad 4.11$$

$$t = \frac{V_{ad}}{Q} \quad 4.12$$

V_{ad}	Added volume of air	m ³
Q	Flow rate (≈5160 m ³ /h)	m ³ /s

For Boyle's law, the amount of mole of air must be known. The internal pressure of the monopile is assumed to be atmospheric. The mole of air is used in equation 4.12 to calculate the added volume of air. The time needed to increase the volume of air for an internal overpressure is related to the flow rate.

4.2.2 Second conceptual design

The second conceptual design has no protection plate because it must be possible to pull the end-cap up to the top-cap. The internal diameter of the monopile gives the maximum diameter of the end-cap if it cannot split. The second conceptual design cannot split and is shown in figure 36.

The disadvantage of lifting the bottom-cap through the pile is launching the cap. The external overpressure gives the initial acceleration of the bottom-cap when the seal is disconnected. A controlled internal pressure in the monopile leads to a gently moving bottom-cap. The cap moves up when lowering the monopile into the water after disconnecting the seal. Finally the top- and bottom-cap can be lifted out of the monopile when the pile is positioned on the seabed.

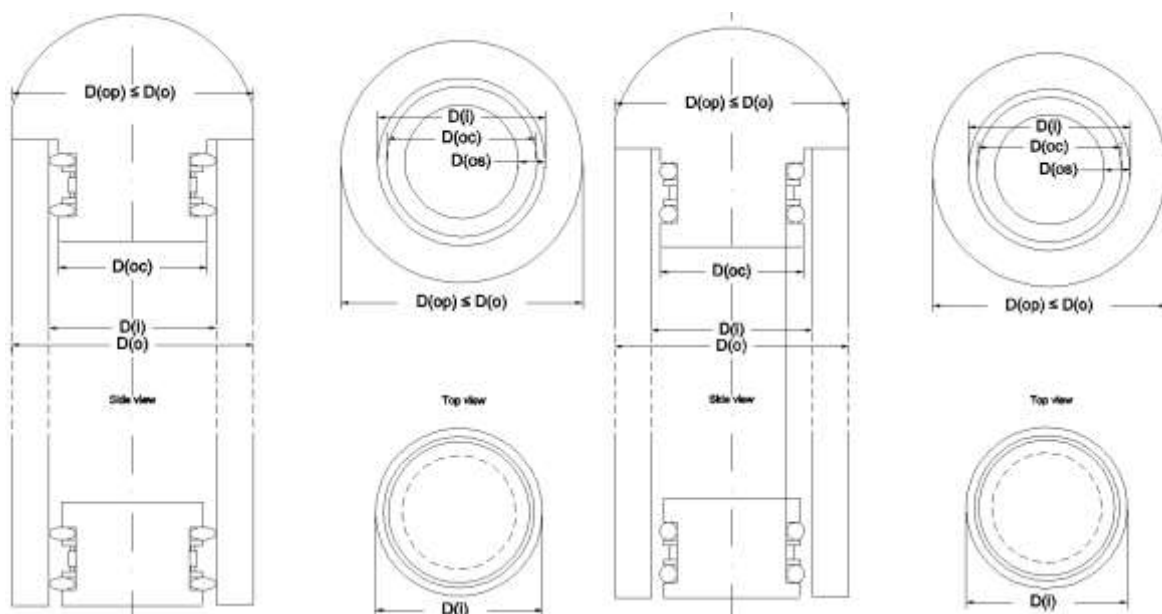


Figure 36: Conceptual design 2, sealed and unsealed

The conditions to prevent a launched bottom-cap can be calculated with the equations mentioned in the previous subsection. The controlled internal pressure of the monopile gives controlled behaviour of the bottom-cap. Lowering the pile into the water must be with a controlled internal pressure. The controlled pressure valve must be installed on every top-cap for controlled behaviour of the caps.

4.3 Recommendations for the Conceptual design of the End-caps

The recommendations for the design of an end-cap depend on the properties as the dimensions of the pile, the quality of the cap, the sealing system of the end-caps and the pressure balance. The recommendations are:

- Two parallel independent seals for every single end-cap which are continuously monitored to obtain a high quality.
- The seals have to be tested and replaced if necessary at the storage site.
- The pressure balance has to be calculated or measured before disconnecting the seals.
- The end-caps need to have a valve to control the internal pressure.
- The end-caps can be used at both ends of the monopile for transport and upending.

With the two conceptual designs the final design of the end-caps must be consider with the quality based on the financial perspective. For every project a new design of the end-caps is used.

5 Analysis of the Process of Upending of a Monopile

In this chapter, the analytical model for upending of a monopile for an offshore wind turbine foundation is explained using the theory from chapter 3. The theory is used for a quasi-static model. Assumptions needed for the quasi-static model are made in the first section. In the second section the analytical model is explained. The result of the model is the topic of the third section. In the last section conclusions based on the analytical upending of a monopile are drawn.

5.1 Assumptions

To make an analytical model the reality is simplified by applying assumptions. The forces defined in section 3.2 are applied. The six forces result from the pressure, the inertia, the gravity, the viscosity, the elasticity and the surface tension, are compared and assumptions are made.

The inertia force depends on the acceleration of the pile. The acceleration is only dominant at the beginning and the end of a realistic model. The velocity is constant during the analytical model and the inertia is neglected. The influence of inertia becomes clear in the comparison of the analytical and experimental results in chapter 7.

The external forces do not deform the monopile because of the elasticity of steel. The elastic force is neglected. The viscosity and surface tension are neglected since the pressure and the gravity are dominant. The analytical and experimental results are compared for confirmation. The assumptions for the analytical model of upending are:

- Lifting is purely the vertical force since the crane is connected to the pile with a hinge.
- The steel pile is assumed to be rigid because the elasticity of steel is high.
- The viscosity and the surface tension are neglected because the pressure and gravity force are dominant.
- The inertia may be neglected and therefor the process can be considered to be quasi-static.

Based on the assumptions of the elasticity, the inertia, the viscosity and the surface tension the model is assumed to be quasi-static. The net force on the pile during upending depends only on the pressure and gravity forces, equation 5.1.

$$F = F_p + F_G \quad 5.1$$

The quasi-static model is applied as a model for upending of an offshore wind turbine monopile, topic of the next section.

5.2 Analysis of the Process of Upending of a Monopile

In this section the analytical model for upending of a monopile for an offshore wind turbine foundation is explained. The analytical model is written in Maple™, a math software that combines the world's most powerful math engine with an interface to analyse, explore, visualise and solve mathematical problems^{xx}.

In the analytical model the local axis are aligned with the pile and the initial reference point is where the crane lifts the pile. Lifting the pile is the vertical displacement perpendicular to the seawater level. The vertical displacement of the crane hook is the numerical input of the analytical model with step size (d_z).

The initial reference point is the centre of rotation (CoR) since the crane applies the force on the system with a hinge. The other forces are the gravity and the buoyance force. Based on the three forces the angle of the pile is calculated. The calculation is done with an iteration in Maple™, explained in the next subsection.

5.2.1 Applied Iteration in the Model for Upending of the Monopile

The analytical model for upending is using an iteration in Maple™ to calculate the angle of the monopile. The iteration is done after each step of vertical displacement by the crane hook. The angle causes a resulting moment at the centre of rotation. The moment at the centre of rotation should be zero.

The iteration depends on the resulting moment in the centre of rotation with the defined angle. Whether the resulting moment is positive or negative the angle increases or decreases. If the sign changes between two consecutive points the step size of the angle (d_α) is halved. The iteration is stopped when the resulting moment is almost zero ($1E-10$ Newton metre, the predefined tolerance).

The iteration gives the angle of the pile which leads to the submerged volume of the monopile. The equation of the submerged volume depends on the phase which is related to that position. The phases are explained in the next subsection.

5.2.2 Phases during Upending of the Monopile

Upending of the monopile for the offshore wind turbine foundation depends on the different phases. The model has an initial and final situation. To get from the initial to the final situation there are four phases related to α_i , the angle of the monopile with the horizon, shown in figure 37.

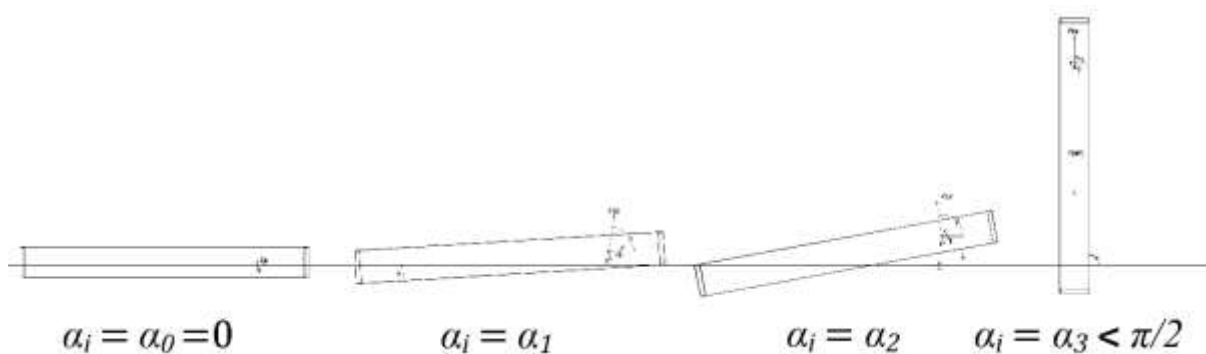


Figure 37: Phases during Upending of the Monopile

For every phase the equations needed for the iteration change. The phases are defined as:

1. Hoisting until the top-cap emerges, phase 1 is when α_i is: $0 < \alpha_i \leq \alpha_1$. The angle α_1 is when the top-cap emerges. The angle depends on the dimensions of the monopile.
2. Hoisting until the bottom-cap submerges, phase 2 is when α_i is: $\alpha_1 < \alpha_i \leq \alpha_2$. The angle α_2 is when the bottom-cap submerges and depends on the dimensions of the monopile.
3. Hoisting until the monopile is vertical, phase 3 is till α_i is a half Pi: $\alpha_2 < \alpha_i < \pi/2$. The angle α_3 is till the monopile reaches the absolute vertical position.
4. Hoisting until the crane force is equal to the safe working load: $F_{SWL} = 8.829E6$ N. With $\alpha_i = \alpha_4 = \pi/2$.

The initial conditions, the four phases and the final conditions are described separately in the subsequent sub-subsections.

5.2.2.1 Initial conditions

The initial situation is the vertical force balance between buoyancy and gravity. The monopile is at rest, $\alpha_i = \alpha_0$ and the forces result a submerged volume, defined in equation 5.2. The monopile is with the dimensions as a length of 70 meters and an outer diameter of 7 meter and with a mass of 1100t and a weight of 10791kN. The initial conditions of the monopile are shown in figure 38.

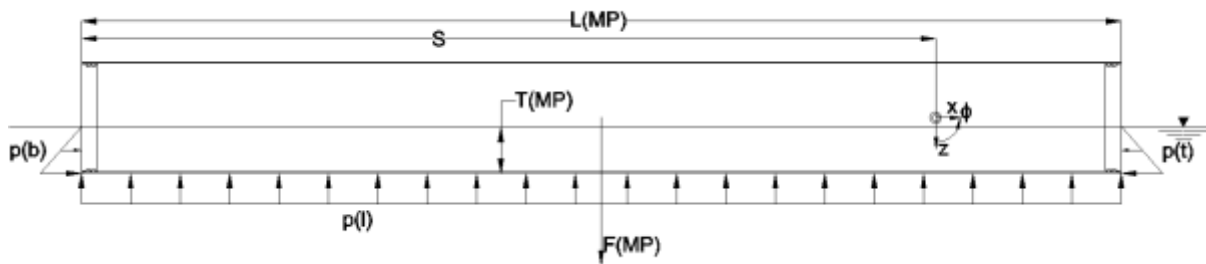


Figure 38: Initial conditions of the monopile

$$F_G = F_\nabla = \rho_{sw} \cdot g \cdot \nabla = \rho_{sw} \cdot g \cdot A_s \cdot L_{MP} = p_h \cdot A_s \tag{5.2}$$

$$h_0 \rightarrow \frac{\nabla}{L_{MP}} = A_s(x) = \frac{D_o^2}{4} \cos^{-1} \left(\frac{D_o - 2 \cdot h_0}{D_o} \right) - \left(\frac{1}{2} D_o - h_0 \right) \cdot \sqrt{(D_o - h_0) \cdot h_0} \tag{5.3}$$

h_0	Initial draft	m
D_o	Outer diameter of the monopile	m

The initial draft for the initial conditions is calculated with equation 5.3. The initial draft of the monopile is h_0 , about 2.98 meter. In figure 38 this is indicated as the draft of the monopile with T(MP). The dimensions of the monopile related to the centre of the crane (CoC), also the CoR, are given. The top-cap is at $x = L_{MP} - S$ and the bottom-cap is at $x = -S$. When the crane starts lifting the first phase starts.

5.2.2.2 Phase 1

Phase 1 starts when the pile is hoisted by the crane. The first phase is until the top-cap emerges with $\alpha_i = \alpha_i$, shown in figure 39. During phase 1 the submerged length is the total length of the monopile. The crane changes the vertical load balance. The load lifted decreases the total submerged volume of the pile.

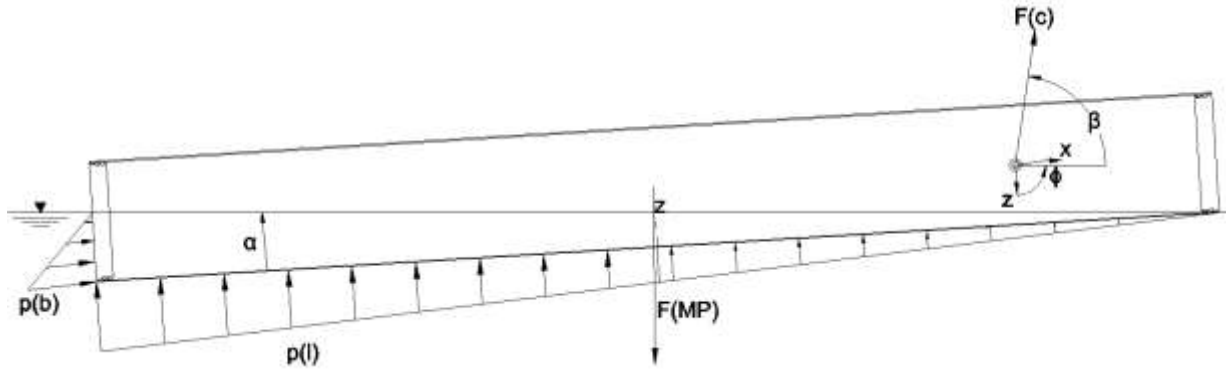


Figure 39: End of Phase 1

The submerged volume is calculated with equation 5.4. Rewriting and simplifying with equation 5.5 leads to equation 5.6. The angle α is changed until the resulting moment, equation 5.7, is less than the predefined tolerance. Changing the angle influences the draft along the pile, the submerged volume and the coordinates of the centre of buoyance (CoB), defined on the x-axis in equation 5.8 and on the z-axis in equation 5.9.

$$\nabla = (F_{MP} - F_C) / (g \cdot \rho_{sw}) = \int_{-S}^{L_{MP}-S} A_s(x) dx = \quad 5.4$$

$$\int_{-S}^{L_{MP}-S} \frac{1}{4} D_0^2 \cdot \cos^{-1} \left[\frac{D_0 - 2 \cdot T_{MP}(x)}{D_0} \right] - \left(\frac{1}{2} D_0 - T(x) \right) \cdot \sqrt{[D_0 - T(x)] T_{MP}(x)} dx$$

$$T_{MP}(x) = h_0 - z - x \cdot \sin(\alpha) = h_0 - z - x \cdot [z/L] \quad 5.5$$

$$\nabla = A_{Tt} \cdot L_{MP} + \frac{1}{2} \cdot (A_{Tb} - A_{Tt}) \cdot L_{MP} = \frac{1}{2} \cdot (A_{Tb} + A_{Tt}) \cdot L_{MP} \quad 5.6$$

$$\sum M_{CoR} = F_G \cdot \sin(\alpha) \cdot x_{MP} + F_V \cdot \sin(\alpha) \cdot x_V \quad 5.7$$

$$CoB_x = \frac{A_{Tt} \cdot L \cdot (\frac{1}{2} L - S) + (A_{Tb} - A_{Tt}) \cdot \frac{1}{2} L \cdot (\frac{1}{3} L - S)}{A_{Tt} \cdot \frac{1}{2} L + A_{Tb} \cdot \frac{1}{2} L} \quad 5.8$$

$$CoB_z = \frac{A_{Tt} \cdot L \cdot (r_o - \frac{1}{2} T_t) + (A_{Tb} - A_{Tt}) \cdot \frac{1}{2} L \cdot (r_o - [T_t + \frac{1}{3} (T_b - T_t)])}{A_{Tt} \cdot \frac{1}{2} L + A_{Tb} \cdot \frac{1}{2} L} \quad 5.9$$

$T_{MP}(x)$	Draft of the monopile at coordinate x	m
z	Vertical displacement by the crane	m
α	Angle of the monopile with the horizon	rad
L	Submerged length of the monopile	m
S	Distance between bottom-cap and trunnions (≈ 59.8)	m
A_{Tt}	Submerged cross-sectional area at the top-cap, $A_{Tt} = A_s(L_{MP}-S)$	m ²
A_{Tb}	Submerged cross-sectional area at the bottom-cap, $A_{Tb} = A_s(-S)$	m ²

CoB	Centre of buoyancy at Cartesian coordinates (x, y, z)	m
r_o	Outer radius of the monopile	m
M_{CoR}	Moment at the centre of the rotation	Nm
x_{MP}	Coordinate of the centre of gravity along the monopile (≈ -24.8)	m
x_V	Coordinate of the centre of buoyance along the monopile (CoB_x)	m
T_t	Draft of the top-cap, $T_t = T_{MP}(L_{MP}-S)$	m

When the top-cap emerges the submerged length decreases. This is the beginning of phase 2.

5.2.2.3 Phase 2

Phase 2 starts when the top-cap emerges. The phase is until the bottom-cap is submerged with $\alpha_1 = \alpha_2$, shown in figure 40. The figure shows that the submerged length of the monopile decreases. The submerged length is calculated with equation 5.10. The equations for the submerged volume and the coordinates of CoB change and are given in equations 5.11 to 5.13.

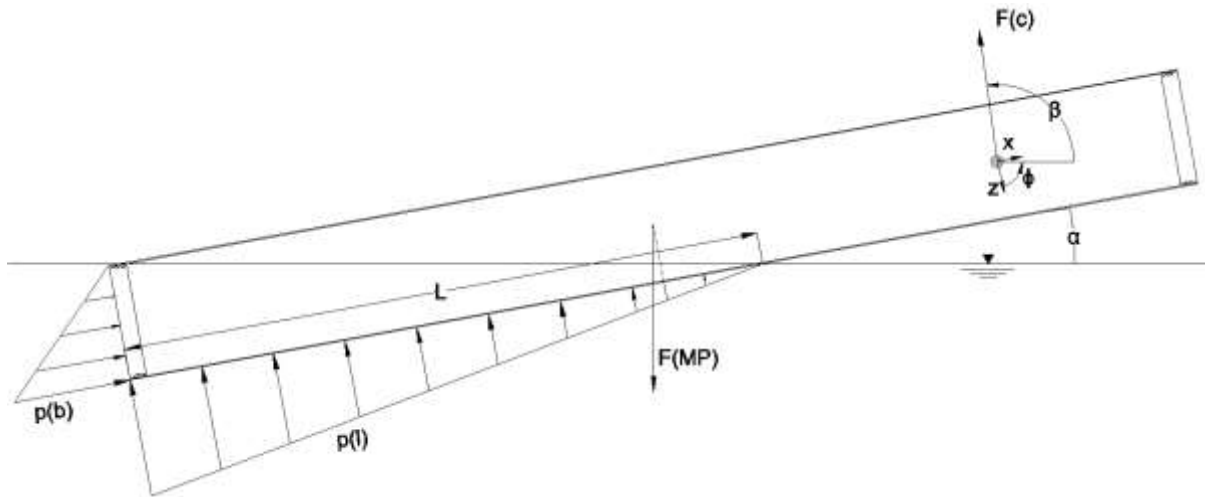


Figure 40: End of phase 2

$$L = T_b / \sin(\alpha) \tag{5.10}$$

$$\nabla = A_{Tb} \cdot \frac{1}{2} L \tag{5.11}$$

$$x_V = CoB_x = \frac{A_{Tb} \cdot \frac{1}{2} L \cdot (\frac{1}{3} L - S)}{A_{Tb} \cdot \frac{1}{2} L} = \frac{1}{3} L - S \tag{5.12}$$

$$CoB_z = \frac{A_{Tb} \cdot \frac{1}{2} L \cdot (r_o - \frac{1}{3} T_b)}{A_{Tb} \cdot \frac{1}{2} L} = r_o - \frac{1}{3} T_b \tag{5.13}$$

After submerging of the bottom-cap the submerged volume of the monopile exist of a fully submerged, a partially submerged and an emerged part. To define these volumes other equations have to be used and phase 3 starts.

5.2.2.4 Phase 3

Phase 3 starts when the bottom-cap is fully submerged and is till the pile is absolutely vertical, till α_i is a half Pi radians as $\alpha_i = \alpha_3 < \pi/2$. In phase 3 equation 5.14 defines the emerged, partially submerged (∇_2) and the fully submerged (∇_1) parts of the monopile. The submerged length is split into a completely submerged length (λ_i) and a partially submerged length ($L - \lambda_i$). The symbols of the different parts are shown in figure 41.

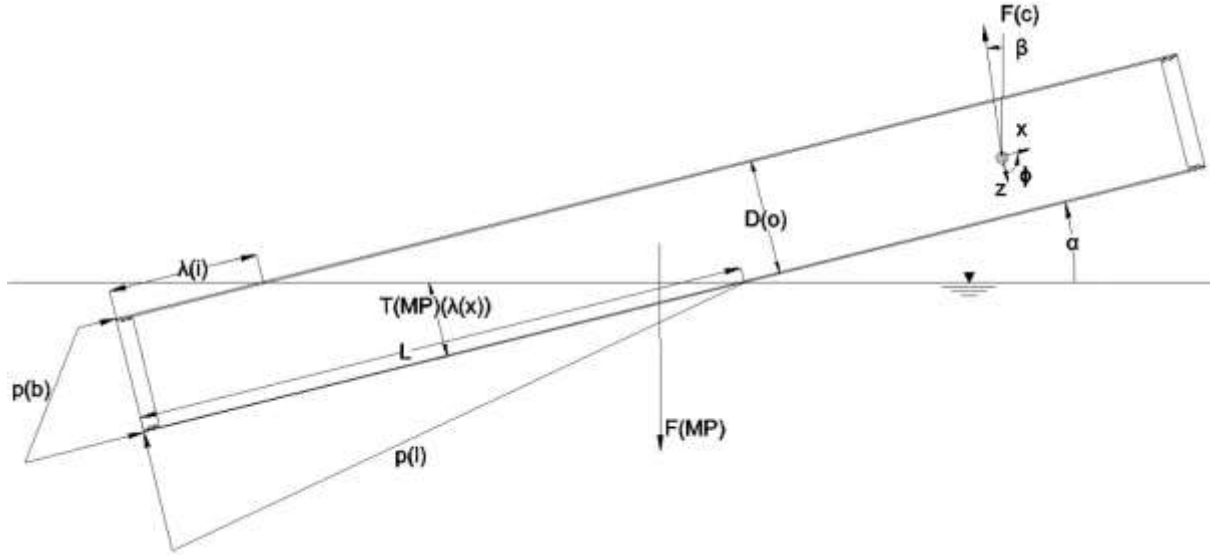


Figure 41: Position of the monopile during phase 3

$$\nabla = \nabla_1 + \nabla_2 = A_{MP} \cdot \lambda_i + A_{MP} \cdot \frac{1}{2} \cdot (L - \lambda_i) = \frac{\pi}{4} \cdot D_o^2 \cdot \frac{1}{2} \cdot (L + \lambda_i) \quad 5.14$$

$$\lambda_i = T_b / \sin(\alpha) - D_o / \tan(\alpha) = (T_b - D_o \cdot \cos(\alpha)) / \sin(\alpha) \quad 5.15$$

$$CoB_x = \frac{\nabla_1 \cdot [\frac{1}{2} \cdot \lambda_i - S] + \nabla_2 \cdot [\frac{1}{3} \cdot L + \frac{2}{3} \cdot \lambda_i - S]}{\nabla_1 + \nabla_2} \quad 5.16$$

$$CoB_z = \frac{\nabla_1 \cdot [r_o - \frac{1}{2} \cdot D_o] + \nabla_2 \cdot [r_o - \frac{1}{3} \cdot D_o]}{\nabla_1 + \nabla_2} = \frac{\nabla_2 \cdot [r_o - \frac{1}{3} \cdot D_o]}{\nabla_1 + \nabla_2} \quad 5.17$$

∇_1	Fully submerged volume of the monopile	m^3
∇_2	Partially submerged volume of the monopile	m^3
λ_i	Partially submerged length of the pile, $0 < T(x) < D_o$	m

The submerged volume in phase 3 depends on the angle of the pile. This defines the total submerged length, defined in the previous phase, and the partially submerged length in equation 5.15. The CoB coordinates are redefined with these two lengths.

The centre of buoyance on the z-axis of the fully submerged volume is aligned with the initial reference point and the centre of rotation. This simplifies equation 5.17. When the pile is in the absolute vertical position, as in figure 42, phase 4 starts.

5.2.2.5 Phase 4

In phase 4 the pile is absolutely vertical. The lifted height and the rotation of the monopile are likely to be less than the safe working load of the crane. This can be confirmed with the result of the experiment in chapter 6. Further lifting increases the crane load linear and the decreases the draft linear. The equations are the same as used in phase 3 since $L = \lambda_f = T_b$.

The submerged volume is directly related to the vertical displacement by the crane. The centre of the submerged volume is the centre of buoyance. The coordinates are related to the initial reference point and the calculated angle of the pile. The final position is in figure 43 and is the end of phase 4.

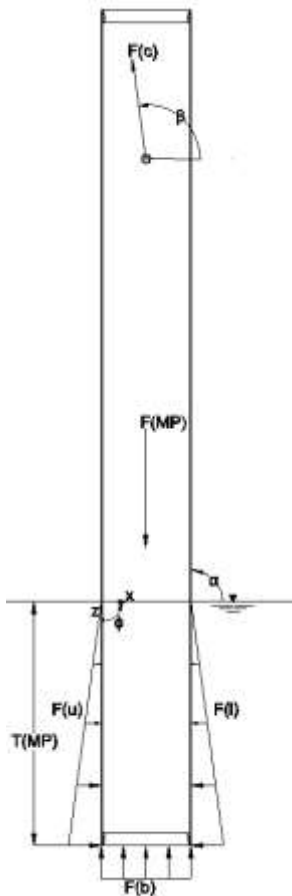


Figure 42: End of phase 3

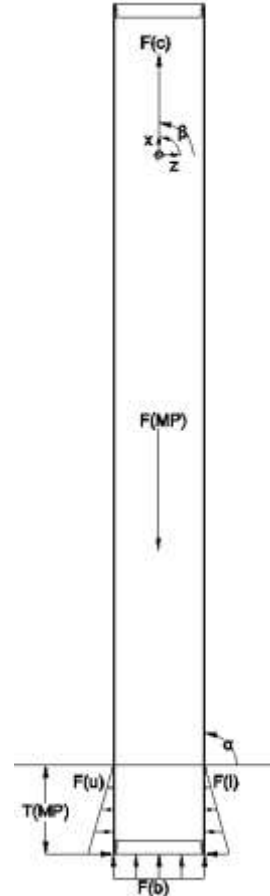


Figure 43: End of phase 4

$$F_c = F - F_{\nabla} \leq F_{SWL} \tag{5.18}$$

The final position is reached when the crane reaches the safe working load, equation 5.18. The minimum submerged length related to the dimensions of the monopile, d_z and the safe working load results in the boundary condition. The used code in Maple™, the condition when hoisting stops, is:

```
> if vSub <= 200 then phase:=2 end if;
```

The verification and the results of the analytical model is the topic of the next two sections.

5.3 Verification of the analytical model

To use the result of the analytical model, the results must be verified. The input is the lifted height which results the forces, the angle of the pile and the resulting moment at the centre of rotation. The coordinates of the centre of rotation is known at [0, 0, 0], the centre of the crane.

The first point which is checked is when the pile is lifted 2.43 meter, when the top-cap emerges. The angle is calculated and checked if the resulting draft, submerged length and volume are correct.

$$T_b = h_0 - z + S \cdot \sin(\alpha) =$$

$$2.979887604 - 2.43 + 59.8 \cdot \sin(0.0540465982) = 3.780300948 \quad 5.19$$

$$T_t = h_0 - z - (L_{MP} - S) \cdot \sin(\alpha) =$$

$$2.979887604 - 2.43 - 10.2 \cdot \sin(0.0540465982) = -0.0011193548 \quad 5.20$$

$$L_{MP} = T_b / \sin(\alpha) = 69.97927899 \quad 5.21$$

$$\nabla = \frac{1}{2} \cdot A_{Tb} \cdot L_{MP} = 743.2090155 \quad 5.22$$

The result in the table is compared with the result according Maple™.

Data	Manual	Maple™
T_b	3.780300948	3.7803009469
T_t	-0.0011193548	-0.0011193547
L_{MP}	69.97927899	69.9792789953
∇	743.2090155	743.2090155757

The differences are only compared at one point, to confirm the Maple™ result this must also be checked at another point. The second point which is checked is when the pile is lifted 11.63 meter, the point the bottom-cap submerges.

$$2.979887604 - 11.63 + 59.8 \cdot \sin(0.2648266175) = 7.002055261 \quad 5.23$$

$$2.979887604 - 11.63 - 10.2 \cdot \sin(0.2648266175) = -11.31988012 \quad 5.24$$

$$L_{MP} = T_b / \sin(\alpha) = 26.75175182 \quad 5.25$$

$$\lambda_i = T_b / \sin(\alpha) - D_o / \tan(\alpha) = 0.9402008275 \quad 5.26$$

$$\nabla = A_{MP} \cdot \frac{1}{2} \cdot (L_{MP} + \lambda_i) = 532.8556144 \quad 5.27$$

The result in the table is compared with the result according Maple™.

Data	Manual	Maple™
T_b	7.002055261	7.0020552608
T_t	-11.31988012	-11.3198801239
L_{MP}	26.75175182	26.7517518190
λ_i	0.9402008275	0.9402008268
∇	532.8556144	532.8556143490

The difference between the Maple and the manual calculated values are less than 1E-7. The Maple™ script is validated and the results can be used for a comparison with the experiment.

5.4 Results of the analytical model

The results of the analytical model are based on the given equations in section 5.2. The hoisting of the pile is calculated with the Maple™ script in Appendix H. An overview of the whole process of a monopile is shown in figure 44. The graph gives a clear overview of the ratio between the load and the vertical displacement. The individual result of every single phase is in figure 45 to figure 47.

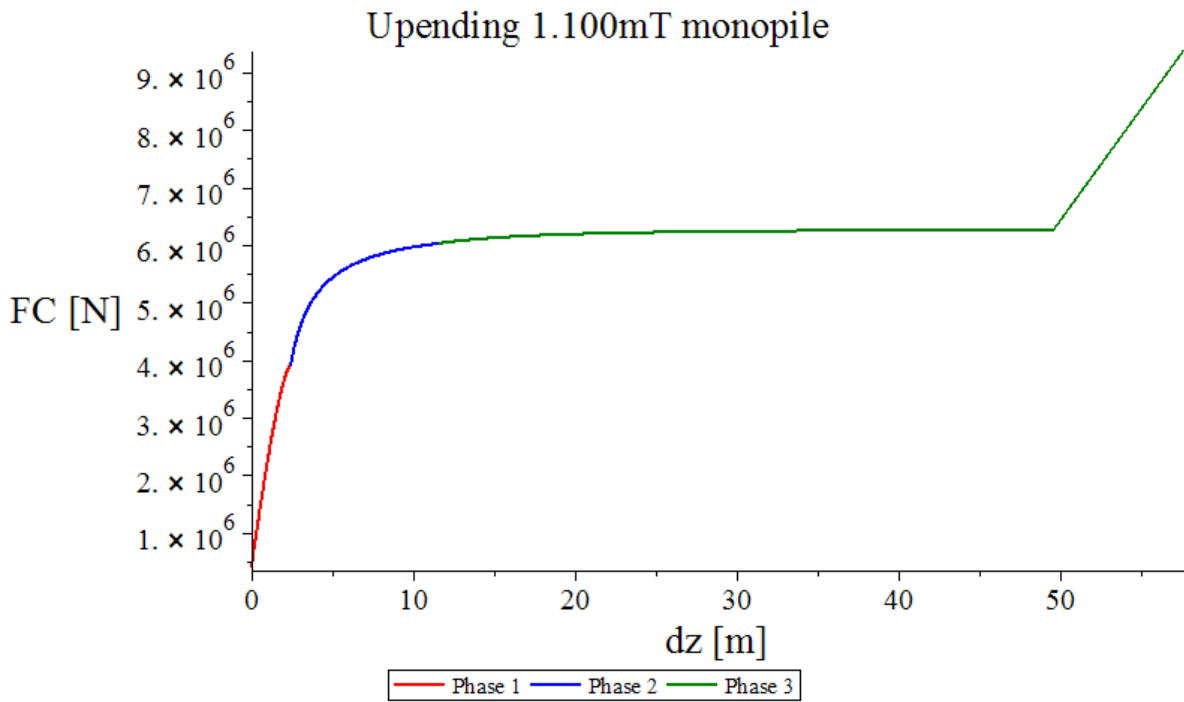


Figure 44: Upending according Maple™

The initial load lifted by the crane, FC, is the hook and the cables of the rigging arrangement. During the experiment the equipment is a higher percentage of the total load than during upending a monopile offshore. For the calculations in Maple™ the initial load is set on the weight of the crane hook. The weight of the crane hook is an initial conditions for upending of a monopile.

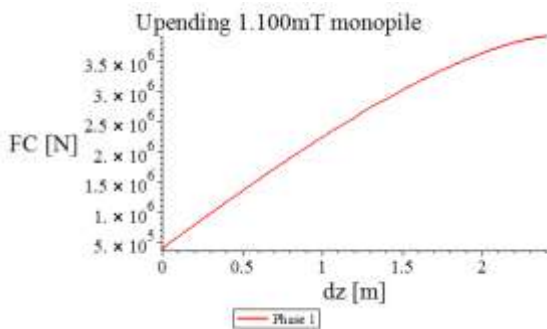


Figure 45: Upending monopile phase 1 according Maple™

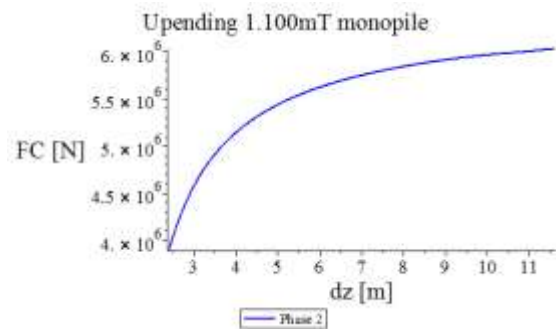


Figure 46: Upending monopile phase 2 according Maple™

During phase 1 the load increases almost linear due to the displacement by the crane, figure 45. The graph is not linear, the gradient of the line decreases during phase 1. Phase 2 starts when the top-cap is emerged, figure 46. Phase 2 indicates that the pile rotates and the crane load approaches a constant value.

There is a discontinuity between phase 1 and phase 2. This is expected at every phase change based on the assumptions and the changing equations. The gradient change from phase 1 to 2 is visible in figure 44. The phase-gradient is also the result of the changing equations. The data in table 3 are from the last two steps in phase 1 and the first two steps in phase 2 to explain the phase change.

Phase	Z [m]	VSub	alpha [rad]	L [m]
1	2.41	743.6156596632	0.0536971779	70.0000000000
1	2.42	743.4370036594	0.0538709384	70.0000000000
2	2.43	743.2090155757	0.0540465982	69.9792789953
2	2.44	741.6717324786	0.0542731819	69.7524797019

Table 3: Phase change from phase 1 to 2

After submerging of the bottom-cap, the submerged length and the submerged volume of the pile slowly decrease. As a result the load lifted by the crane increases gently. Phase 3 is shown in figure 47.

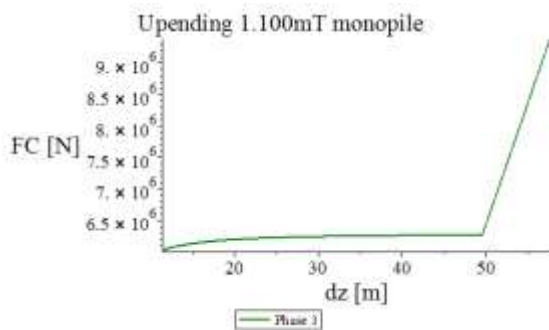


Figure 47: Upending monopile phase 3 according Maple™

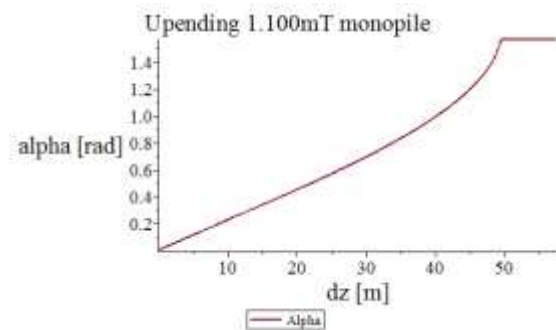


Figure 48: Angle α during upending according Maple™

The submerged volume in phase 3 exists of two individual submerged volumes, ∇_1 and ∇_2 as in equation 5.14. In phase 3 the volume remains gently decreasing until the angle reaches a half Pi. The gradient becomes linear with d_z when the pile is vertical. There is no phase change since the same equations are used as explained in section 5.2.2.5.

The vertical position is reached with a rotational acceleration, shown in figure 48. The angle increases ten degrees with a vertical displacement of one meter. The boundary conditions in Maple™ is the absolute vertical position. The equations do not have a limitation at the angle of half a Pi. The boundary is set as:

```
if alpha >= evalf(Pi/2) then alpha := evalf(Pi/2) end if;
```

The analytical model of the monopile was adjusted to calculate the behaviour of the piles used during the experiment. The results for the scaled monopiles used during the experiment in the next chapter are calculated with the analytical model. The scaling factor, δ , used to calculate the dimensions of the different experimental model is explained in the next chapter.

The three models used during the experiment are the on mass scaled and the on the outer-diameter scaled aluminium monopiles, in figure 49 and figure 50, and the on the mass scaled steel monopile in figure 51.

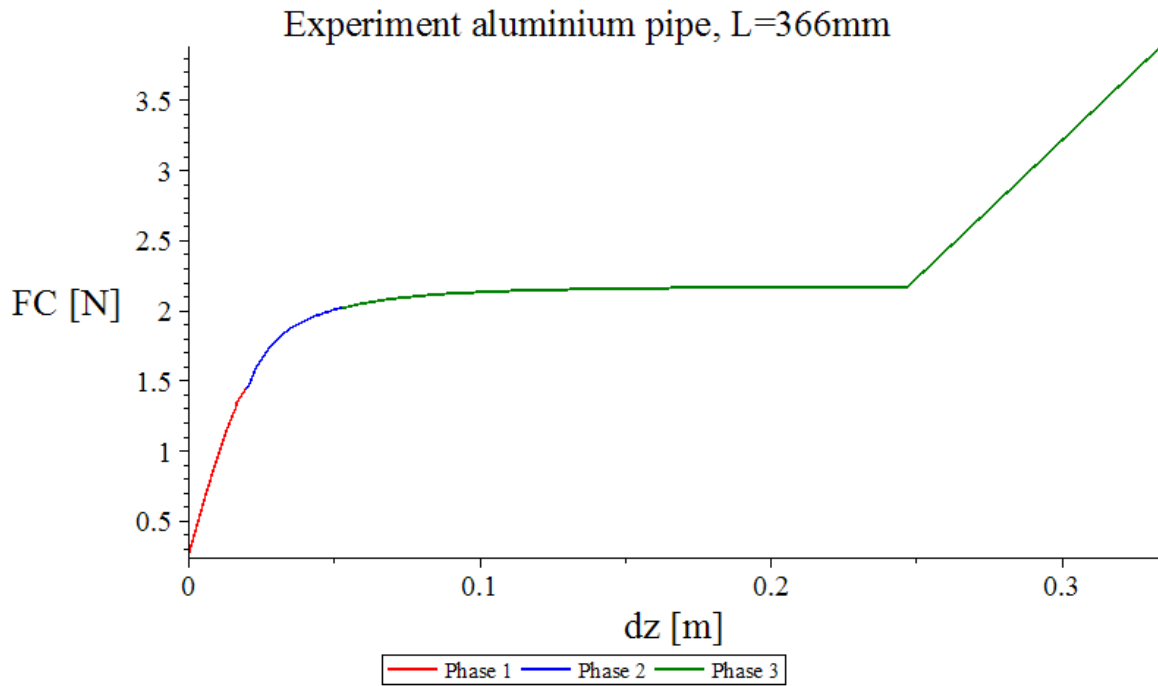


Figure 49: Analytical results of the mass scaled aluminium monopile

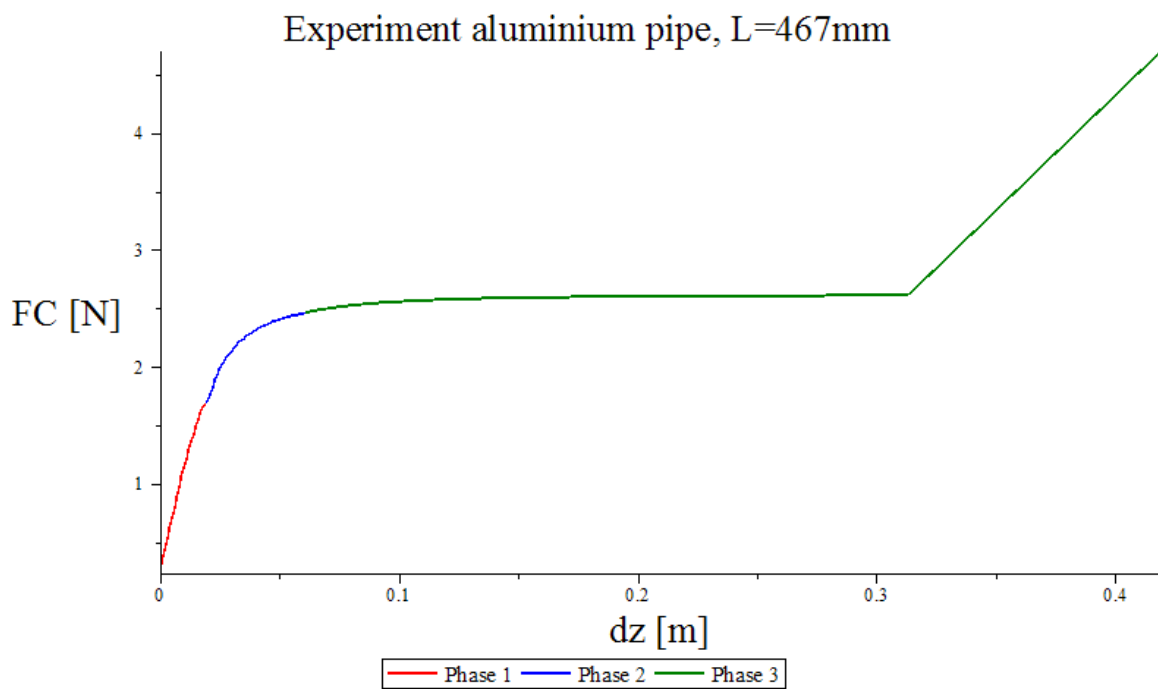


Figure 50: Analytical results of the with the outer-diameter scaled aluminium monopile

The analytical results of the both scaled aluminium piles are similar to the results of the monopile.

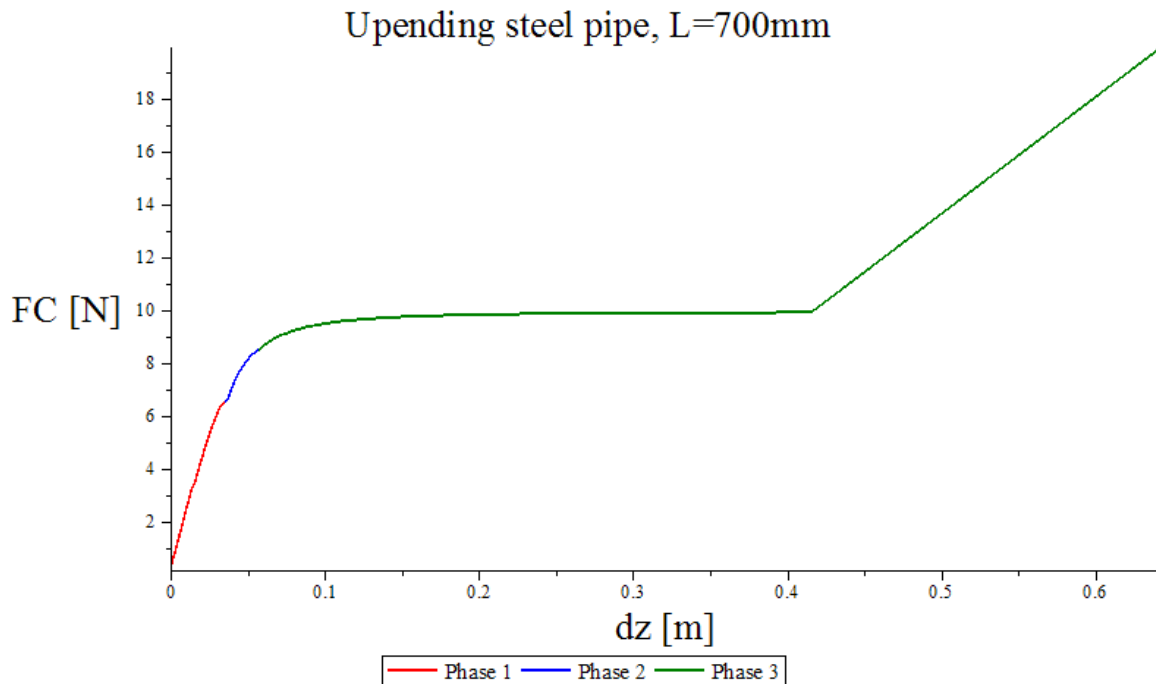


Figure 51: Analytical results of the mass scaled steel monopile

5.5 Assumptions based on the Analytical model

The assumptions based on the analytical model for the behavior of upending of the monopile for an offshore wind turbine foundation are:

- Lifting is purely the vertical force since the crane is connected to the pile with a hinge.
- Dynamic loads are not dominant and can be neglected.
- All variable external loads, as the wind, the waves and the currents, can be neglected.
- With the help of the gripper only vertical loads are lifted after upending and clamping the pile. The gripper will not decrease the load lifted by the crane.

In chapter 6 an experiment to validate the theory, the assumptions and the analytical model is described. The analytical model is compared with the results of the experiment in chapter 7.

6 Experimental Upending of a Monopile Wind Turbine Foundation

The experiment has been executed to define the accuracy of the analytical model. The experiment evaluates the response of the monopile with the crane. The experimental model is scaled and is described in the first section. In the second section the different used models are defined. The result of the experiment is the topic of the third section. In the last section of this chapter the experimental results are discussed.

6.1 Theory of Experimental Upending of Monopile OWTF

The experiment at model scale is easier, faster and cheaper than testing a monopile. The dimensions of the models are derived from the scale factor as defined in equation 6.1.

$$\text{monopile} = \delta \cdot \text{model} \tag{6.1}$$

δ	Scaling factor	-
----------	----------------	---

Some properties cannot be scaled. The gravity, the density, the fluid kinematics and the dynamic viscosity scaling factors are close to one. The model is based on a pile with a weight of 1100t, an outer diameter of 7000mm and a length of 70 meter.

The results of the experiment depend on the weight, the material, the pressure, the response of the water and of the pile. The six forces as defined in equation 3.3 are compared to scale the models.

The six forces are either static or dynamic. Dynamic forces are the inertia and the viscosity, since the forces depend on the acceleration. The acceleration is only dominant at the beginning and the end of the run. At least two runs at a different velocities with the same pile have been executed. The influence of inertia is shown in chapter 7 by comparing the analytical and experimental results.

The experimental model depends on the scaling factor, topic of the next subsection. Based on the scaling factor the models are defined in the second subsection.

6.1.1 Scaling factor of the Experimental Model

The scaling factor influences the dimensions and the response of the pile. The scaling factor depends on the dimensions of the installed monopile and the dimensions of the model (m) used during the experiment. The density of the fluid and the hoisting speed influence the experiment. The scaling factors are given in equation 6.2 to 6.7.

$$\delta_D = D_{MP} / D_m = \delta_l \tag{6.2}$$

$$\delta_V = V_{MP} / V_m = \delta_l^3 \tag{6.3}$$

$$\delta_\rho = \rho_{MP} / \rho_m \tag{6.4}$$

$$\delta_m = m_{MP} / m_m = \delta_v \cdot \delta_\rho \tag{6.5}$$

$$\delta_v = v_{MP} / v_m \tag{6.6}$$

$$\delta_I = \delta_\rho \cdot \delta_v^2 \cdot \delta_l^2 = \delta_p \tag{6.7}$$

δ_D	Diameter scale	-
D_{MP}	Diameter of the monopile	m^3

D_m	Diameter of the model	m^3
δ_l	Length scale	-
δ_V	Volume scale	-
V_{MP}	Volume of the monopile	m^3
V_m	Volume of the model	m^3
δ_ρ	Density scale	-
ρ_{MP}	Density of the monopile	kg/m^3
ρ_m	Density of the model	kg/m^3
δ_m	Mass scale	-
m_{MP}	Mass of the monopile	kg
m_m	Mass of the model	kg
δ_v	Velocity scale	-
v_{MP}	Velocity of the monopile	m/s
v_m	Velocity of the model	m/s
δ_I	Inertia scale	-
δ_p	Scale factor of the pressure	-

All given scaling factors depend on either the dimensions, the density or the velocity. A three-dimensional scaled model of the monopile is not available in steel, since the wall should be too thin. The models are of a different material, aluminium and PVC, to observe the properties of a monopile during upending. The properly scaled models of steel, aluminium and PVC are given in table 4.

	Steel	Aluminium	PVC
$\delta(D_o)$	100.000	150.000	150.000
$\delta(V)$	17.946	99.854	87.845
$\delta(\rho)$	1.000	2.907	5.709
L (V) [mm]	67.763	125.747	105.998
L (m) [mm]	67.763	365.597	605.152
L (D _o) [mm]	700.000	466.667	466.667

Table 4: Scaling factors and calculated length for the models

The calculated lengths for the models are based on the scaling factor of either volume (V), mass (m) or outer diameter (D_o) of that material. The calculated models are evaluated in the next subsection.

6.1.2 Experimental Models of the Monopile Wind Turbine Foundation

The scaling factor is used to calculate the different models, given in Table 4. The calculated lengths of the three materials lead to incorrect conclusions if differently scaled models are compared. The models with a length to width ratio and the length to mass ratio have been used. The calculated steel models will either behave as a floating cube or as a pile with a deep draught.

The dimensions of the steel pile are determined by the outer diameter of 52mm and a wall thickness of 1.8mm. The long steel model is used to check the assumption about the viscosity and the surface tension. The behaviour of the long steel pile can be compared with the aluminium pile of 467mm.

The aluminium piles scaled with both the mass and the diameter are used. The models are more comparable with a real monopile. Aluminium has a natural oxide coating which is similar to the coating

used on a monopile. The draft of the aluminium model is about 40% of the total diameter, close to the initial draft of the monopile.

A PVC pile is longer according to the scale based on the low density. The response of PVC with water is different than the response of steel. Because the lack of compatibility there is no PVC model used. The model of the piles are scaled and compared individually. The results is the topic of the next section.

6.2 Results of the Experimental Upending of the Monopile OWTF

The experimental upending of a monopile for an offshore wind turbine foundation has been done using a digital measurement system and with a video observation. The digital measurement system has received the measurement data. The video observation are used to analyse unexpected results.

The experiment consists of at least three individual runs with every model. The first type of run has been done stepwise, the second type has been done at a low velocity and the third type has been done at a high velocity. The result of the stepwise run has been compared with the stepwise calculations in Maple™. After each step the data have been measured when the pile is in equilibrium. This run has been done twice with an equivalent step size.

The runs at a continuous velocity have been executed three times with the same velocity to compare the results of the individual runs. The two different velocities are compared to check the assumed quasi-static behaviour of the monopile. The rotation of the axis has been measured with a tachometer to obtain data of the runs from the different models with the same velocity.

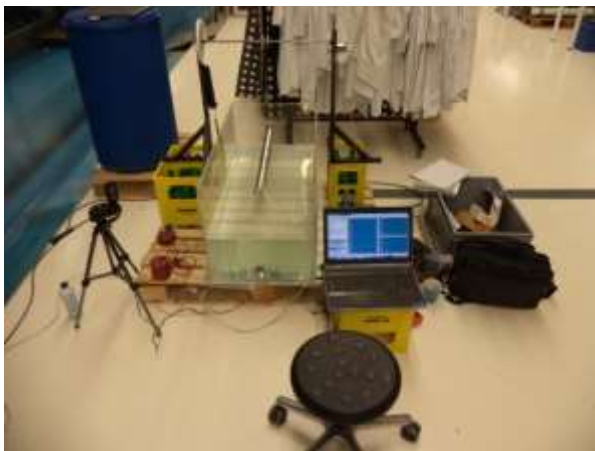


Figure 52: Overview of the experimental setup

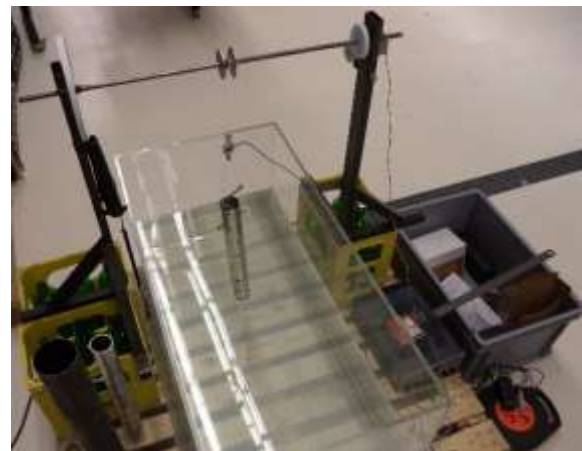


Figure 53: Experimental setup

The experimental setup is shown in figure 52 and figure 53. The used equipment is an S-Type load cell, the NI data acquisition USB-6002, MP3, a DC geared motor, the tachometer and a HP DC power supply.

The crane loads have been measured with an S-Type load cell, which gives an analogue signal. The signal is converted with the data acquisition USB converter to give input for the MP3 measurement program. MP3 is a measurement program to measure, display and store the digitized analogue voltage device signals. The DC geared motor is powered with the HP DC power supply. The HP DC power supply is stable, regulated and insensitive to ambient temperature variations.

In every experiment there are inaccuracies due to the setup which is not completely comparable with an offshore installation site.

The expected inaccuracies are:

- The rotation of the rigging axis and the measurement of the rotation.
 - Caused by the lack of accuracy of the distance between the reflection points and the circle with the drilled centre hole.
- Measured loads on the pile.
 - Caused by the elasticity of the line and the additional weight on the crane hook.
- Natural frequency of the line.

The data of the mentioned runs are listed below in table 5. Three runs have been executed at every velocity. Run 10 and 13 are neglected due to inaccuracies and mistakes during the runs.

Run	Material	Length [mm]	Hoisting speed [rpm]
1	Aluminium	366	Step-wise
2	Aluminium	366	Step-wise
3	Aluminium	366	12
4	Aluminium	366	12
5	Aluminium	366	12
6	Aluminium	366	20
7	Aluminium	366	20
8	Aluminium	366	20
9	Aluminium	366	4
10	Aluminium	467	21
11	Aluminium	467	21
12	Aluminium	467	21
13	Aluminium	366	4
14	Aluminium	366	4
15	Steel	700	18
16	Steel	700	18
17	Steel	700	18

Table 5: List of all experimental runs

The natural frequency, equation 6.8, of the pile did not influence the behaviour of the pile during the experiment. The frequencies of external loads do not have the same frequency.

$$\omega_n = \sqrt{k/m} \rightarrow k = (3 \cdot E \cdot I) / L^3; \quad I = (\pi \cdot [D_o^4 - D_i^4]) / 64 \rightarrow \omega_n \approx 5.8 \cdot 10^{-3} s^{-1} \quad 6.8$$

ω_n	Natural frequency	rad/s
I	Mass moment of inertia	m ⁴
D_i	Inner diameter of the monopile	m

The experimental runs are described in the next subsections. The first subsection is about the stepwise experimental runs. The runs with a continuous velocity are topic of the second subsection.

6.2.1 Stepwise run of Experimental Upending a Monopile OWTF

The stepwise experimental upending has been done with the aluminium pile of 366mm. Run 1 to 9, 13 and 14, have been executed with this pile. The first two runs are stepwise and quasi-static, since the velocity cannot influence the loads. The results of the stepwise runs are shown in figure 54.

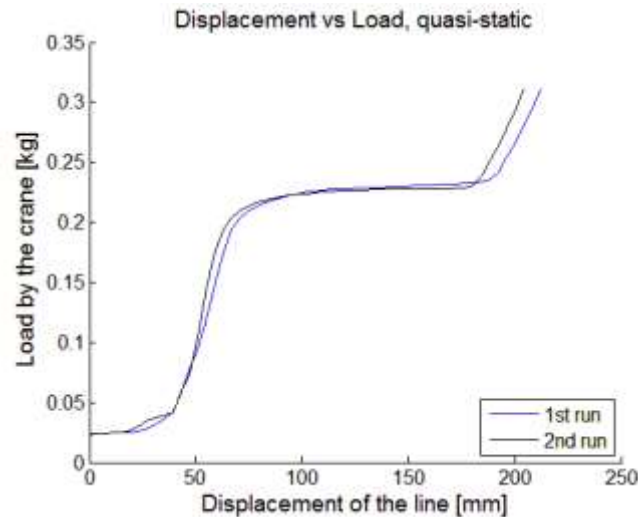


Figure 54: Displacement versus load, quasi-static runs

The difference between the two runs, run 1 shown in blue and run 2 in black, is caused by the experiment runs. Run 1 represents upending the pile out of the water and run 2 was lowering the pile into the water. The difference is caused by the behaviour and response of the water and the accuracy of the equipment.

The range of the measurements confirms the multiple runs with the same pile at the same velocity to get a general behaviour of the run. The runs with a continuous velocity are topic of the next subsection.

6.2.2 Continuous Experimental Upending of a Monopile OWTF

The experimental runs 3 to 17 have been executed with a continuous velocity with the three different models. The results of the three models have been compared. The aluminium pile of 366mm has been lifted with three different velocities to check the assumptions. The aluminium pile of 467mm and the steel pile have been lifted at a high velocity to check the influence of the scaling factor and the type of material.

Run 3, 4 and 5 have been done with a velocity of 12 revolutions per minute (rpm), run 6, 7 and 8 have been done at 20rpm and run 9 and 14 have been done at 4rpm. Only hoisting speeds faster than 10rpm can be measured by the tachometer. The velocity of the runs at 4 rpm has been measured manually. The results of all three different velocities are relevant because the pile is scaled with the mass scale of a real monopile. The graphs with the displacement versus the load are in Appendix I.

The graphs in figure 75 and figure 76 look different because the line was tensioned before the run started. The response of the pile is similar for all three different velocities. Run 3 to 8 have been compared with the step-wise runs to check the inaccuracies and the resulting data. The data are shown in figure 55 to figure 60 on the next page. In the graphs the step-wise run is shown in blue, the run at 12rpm is shown in red and the run at 20rpm is shown in black.

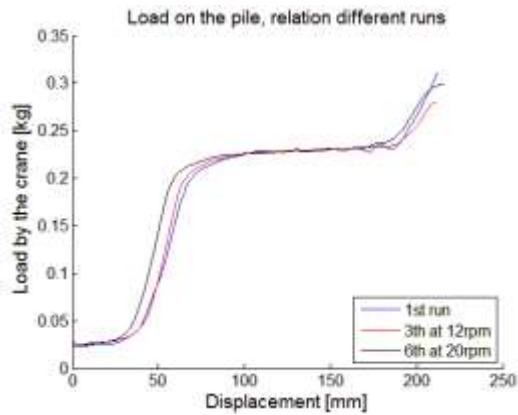


Figure 55: Run 1, 3, 6

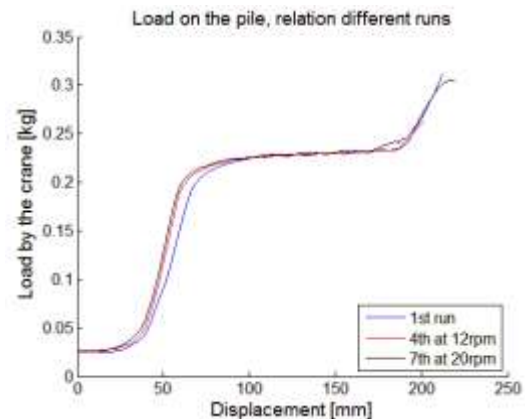


Figure 56: Run 1, 4, 7

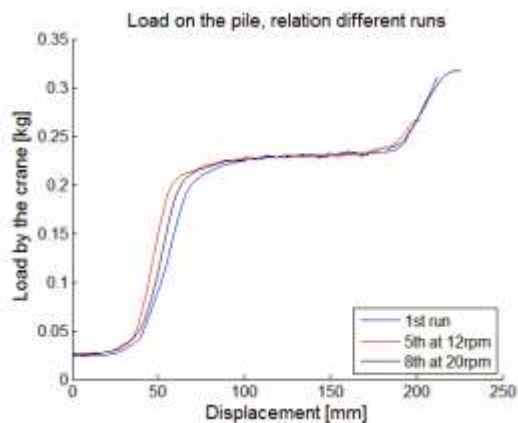


Figure 57: Run 1, 5, 8

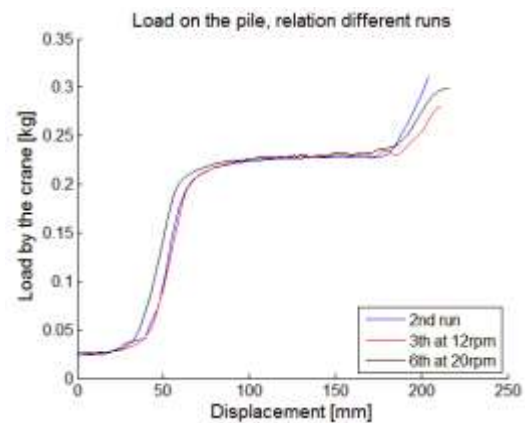


Figure 58: Run 2, 3, 6

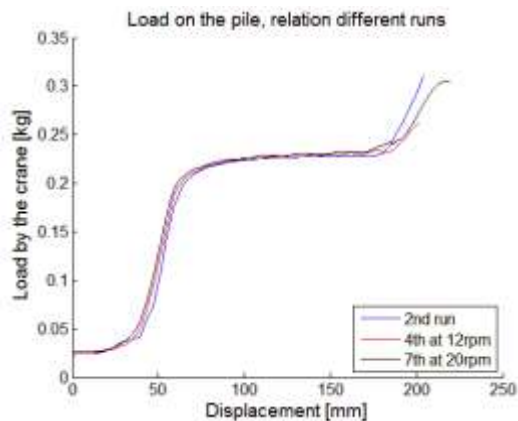


Figure 59: Run 2, 4, 7

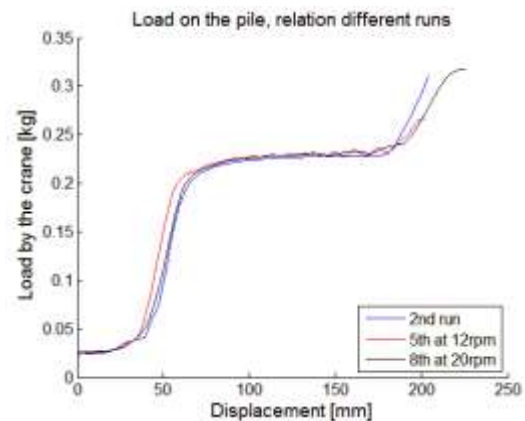


Figure 60: Run 2, 5, 8

The graphs of the quasi-static run with two runs at a different continuous hoisting velocity shows similarities and differences. The range of all eight runs with the steep gradient both at the beginning of the run and in the vertical position of the pile are the same. The differences of the gradient are either in the beginning of the run or in the vertical position.

In figure 56 the results indicate a different initial gradient and end up in the same vertical position. In figure 59 the three lines are aligned until the pile is vertical, when the results become independent. The differences are caused since at the beginning the pile is floating with a variable tension in the line. Also the dynamic forces could have an influence on the behaviour of the pile since these are velocity dependent.

The difference between the step-wise and continuous run is the response of the pile. The response is not caused by the natural frequencies of the piles, but by the waves created by lifting and the rotational velocity of the pile. The waves are reflected by the wall of the tank and cause the response of the pile. The hoisting speed of the pile causes the frequency of the waves and the time to reflect.

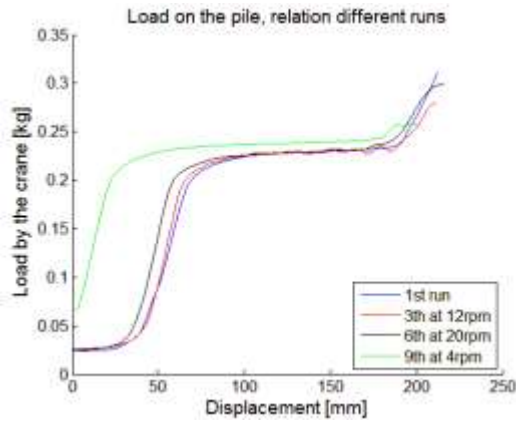


Figure 61: 3 runs at different hoisting speed

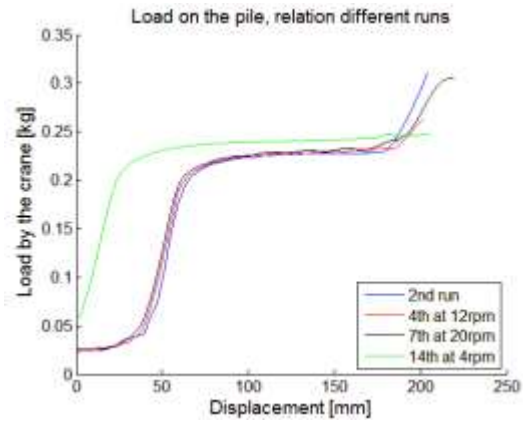


Figure 62: 3 runs at different hoisting speed

The three different velocities are compared in figure 61 and figure 62. The phase velocity of longer waves is faster than the velocity of shorter waves. This confirms the waves in the run at 12rpm shown in red and 20rpm shown in black. The run at 4rpm, shown in green, causes waves which are too long to be observed.

The initial difference in the run at 4rpm takes place because the line was pre-tensioned. The run shows that the external forces have less influence on the behaviour of the lifted pile. The difference between the initial steep gradient and the second steep gradient changes. The difference can be caused by the hydrodynamic mass of the moment of inertia. The difference should also be the case between the other two runs, but these are aligned with the numerical outcome of the experimental run.

The response of the aluminium pile of 366mm, based on the scaling factor of the mass, has been compared with the response of the longer aluminium and the steel pile, both based on the scaling factor of the outer diameter. The aluminium pile of 467mm was used in run 11 and 12. The runs with a hoisting speed of 21rpm are shown in figure 63. The steel pile of 700mm was used in run 15 to 17. The runs with a hoisting speed of 18rpm are shown in figure 64. The difference between the first 9 runs is caused by the total load lifted.

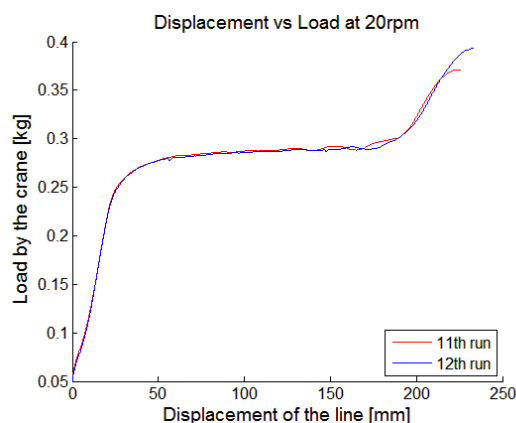


Figure 63: Displacement versus load of a long pile

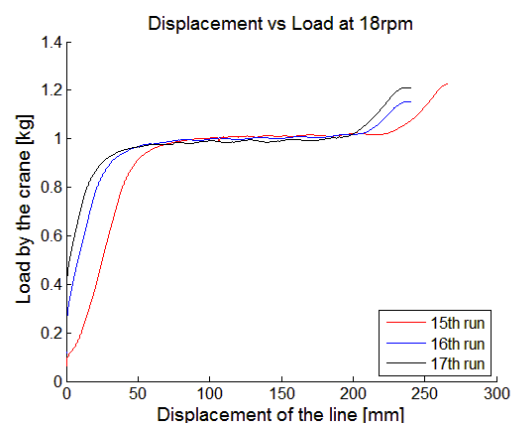


Figure 64: Displacement versus load of a steel pile

The results are similar to the result of the mass scaled aluminium pile. The different positions of the pile in the tank shows the different waves which are caused by the pile and reflected by the walls of the tank. The line was pre-tensioned before the crane started lifting the pile.

The runs with the long aluminium pile were aligned based on the numerical outcome of the runs. The runs with the steel pile show that the moment the run in monopile3 was started was not synchronized with starting the DC geared motor. This causes the spread of the initial value in figure 64.

During the experiment the pile was photographed. The phase changes of the analytical model in Maple™ during the experiment are shown in figure 65 to figure 68 and Appendix I. The gradient of the load decreases continuously and the rotation and the submerged volume during the phase changes clarifies the gradient. The different results of the experiment are discussed in the next section.



Figure 65: Initial conditions



Figure 66: End of phase 1



Figure 67: End of phase 2



Figure 68: Vertical

6.3 Discussion regarding the Experimental Upending

The results of the experiment are used to discuss the general behaviour of a monopile during upending.

Upending of the monopiles of different materials with varying velocities showed the same response. Initially, when lifting the pile, the crane load increased rapidly. The gradient decreased until the pile was vertical for all different piles with the different velocities. The crane force almost remains constant when the bottom-cap is submerged, in phase 3. The similarity is shown in figure 55 to figure 62.

Only the waves caused by the lifted pile and reflected by the walls of the tank are different in these figures. The reflected waves influence the behaviour of the pile and the load on the crane during experimental upending. The waves are different since the length, the mass and the velocity of the piles are different. The response depends on the influence of inertia of the pile during upending.

Upending of the monopile can be considered as a quasi-static process since a comparison of the experimental tests, executed with different hoisting velocities and therefore with different accelerations, shows that the influence of inertia of the pile is negligible.

In the scale model tests the monopile reaches a vertical position without exceeding the safe working load of the crane. This shows that a monopile with a weight larger than the crane capacity may be upended completely using its buoyance to the crane its advantage.

The inaccuracies during the experimental upending are negligible. The result of the experiment, with the different scaled monopiles of different materials, shows the general response of a model scaled monopile during upending. The response must be confirmed with full-scale upending of a monopile. The analytical model of the previous chapter and the experimental results in this chapter are compared in chapter 7.

7 Comparison of the Analytical model and the Experiment

In this chapter the analytical model is compared with the results of the experiment. The theory has been simplified with the assumptions of the analytical model in chapter 5. The experiment has confirmed the analytical model.

First, in section 7.1, the analytical model and the experimental results are compared. In the second section the comparison and the assumptions from the previous chapters are combined to draw conclusions.

7.1 Comparing the Analytical model and the Experiment

In this section the analytical model and the experiment are compared. The model depends on the theory and the assumption of the net force. The experiment gives the gradient of the crane load. The runs with the aluminium pile of 366mm are shown in figure 69 and with the pile of 467mm in figure 70. The results of the analytical model are marked in black and of the experiment in blue.

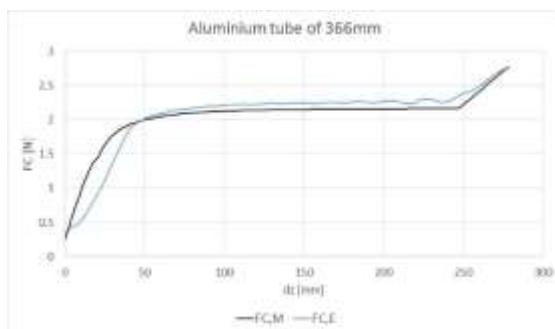


Figure 69: Aluminium pile of 366mm

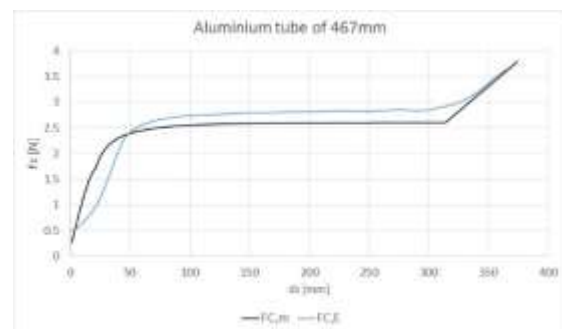


Figure 70: Aluminium pile of 467mm

The similarity of the models is the rapid increasing load, the gradient of the crane load. The gradient decreases during lifting until the pile is vertical. Since the rigging arrangement has already been lifted, both models do not begin at zero. The analytical model has an initial lifted load to end up with the same result as the experimental run.

The differences of the models take place at the beginning of phase 1, and from the end of phase 2 to phase 4, topic of next two subsections.

7.1.1 Initial difference of Upending of a Monopile for an OWTF

The initial difference during upending is caused by an assumption in the analytical model. The inertia is neglected since it is only dominant at the beginning and at the end of upending. When the crane starts lifting the pile is accelerated until it reaches the hoisting speed of the crane.

The results of the aluminium pile of 366mm are more similar to the analytical model than the results of the aluminium pile of 467mm. The pile of 366mm is scaled with the mass scale and the pile of 467mm with the diameter scale. The numerical input is based on the pile used in the experiment.

The initial difference for upending is caused by the inertia of the monopile. The influence decreases when the velocity, or actually the acceleration of the monopile, is minimized.

7.1.2 Difference from phase 2 to 4 of Upending a Monopile for an OWTF

The force difference from the end of phase 2 to phase 4 can be explained with the hydrostatic pressure. The pile is pushed out of the water, which decreases the submerged volume and increases the crane load. The length difference of the two piles shows the influence of the hydrostatic pressure.

In the analytical model the pile rotates and determines the new centre of buoyance and the resulting moment at the centre of rotation. The buoyant force is calculated with the hydrostatic pressure and the position of the pile is independent of the velocity of the pile.

The water molecules are individually attracted and cause the continuously decreasing of the submerged volume. The hydrodynamic mass leads to an additional mass of the pile. The equations of the analytical model change based on the boundary conditions. The analytical model is not a continuous process and the hydrodynamic mass is neglected.

The sea surface tension can be confirmed with a full-scale experiment. The phase change in the analytical model is overestimated. These two aspects explain the difference between the analytical model and the experiment.

7.2 Conclusions based on the Analytical model and the Experiment

The comparison of the results of the analytical model and the results of the experiment is described in this section. The assumptions made for the external forces and the operation of the Aeolus have to be confirmed with a full-scale experiment. The remaining conclusions and assumptions are:

- The upending of a monopile is quasi-static since experimental runs with different velocities and piles of different materials give similar results. The inertia is not dominant and may therefore be neglected.
- The analytical model confirms that the monopile with a larger weight than the crane capacity can be lifted and reaches the vertical position by using the buoyant force of the monopile.

The dynamic loads are dominant when the crane starts lifting and when the pile is vertical. The differences between the mass-scaled and the real operation can be neglected. Scaling the operation partially confirms the conclusion based on the quasi-static behaviour. This assumption is based on the hoisting speed.

The natural frequency of the pile has been neglected. Confirmation with a full-scale experiment is necessary. The gradient of the crane load is based on the tension in the hoisting line. The Aeolus is equipped to operate with a controlled tensioned hoisting line which will operate similar.

The inaccuracy of the measurements is caused by the experimental setup. An experiment with an improved setup should be done to verify this assumption. The experiment is done on scale since a full-scale experiment is more expensive and with a high risk.

The comparison in this chapter is used for the discussion, the conclusions and the recommendations in chapter 8.

8 Discussion, Conclusions and Recommendations

This report analyses the transport and upending of the offshore monopile wind turbine foundations. In this chapter the research, the assumptions and the assignment are discussed, the conclusions are drawn and the recommendations are mentioned. In the first section the two processes of installation, the end-caps and the objectives of Van Oord are discussed. The most relevant conclusions are given in the second section and in the third section the recommendations for further research are given.

8.1 Discussion

The discussion of this report is split into four sections because each process has its own impact on the design of the end-caps. The first two subsections are about the process of the transport and the upending of the monopile. In the third subsection the design of the end-caps is discussed. In the last subsection the covered objectives of Van Oord are mentioned with the results in this report.

8.1.1 Transport

The transport of the monopile from the storage site to the Aeolus is done with a tugboat. The assumptions for the transport are mentioned in section 2.2.1 and 3.1. The first assumption is about the weather conditions and the second assumption is about the initial conditions for upending.

The weather conditions can restrict the Aeolus to operate. The period between the connection and the removal of the end-cap is variable and therefore this is an additional requirement for the quality of the end-cap. The test at the storage site is needed to check the quality of the end-caps. The weather conditions do not affect the load of the pile during transport.

The initial conditions for upending of the pile are based on the floating pile. The centre of gravity and the centre of rotation depend on the design of the pile, the design of the end-caps and the position of the rigging arrangement. The centre of rotation is the position where the rigging arrangement is placed on the monopile since the crane hook is attached to the pile with a hinge.

The first assumption can be confirmed with a full-scale experiment. The second assumption has been confirmed by the similarity of the analytical model and the experiment. The loads on the end-caps during transport are less dominant than during upending. The assumptions for upending are described in the next subsection.

8.1.2 Upending

The initial conditions for upending at the installation site are determined by the transported monopile. The initial conditions can be optimized by refining the design of the monopile. The assumptions during upending of the monopile are based on the loads on the pile.

The forces on the pile are caused by the pressure, the inertia, the gravity, the viscosity, the elasticity and the sea surface tension as given in section 3.2. In section 5.1 it is assumed that the behaviour of the pile is quasi-static and only depends on the pressure and the gravity, as confirmed in section 7.2. The inertia is not dominant and may therefore be neglected.

The rotation of the pile and the waves caused by the pile and reflected by the walls of the tank has influenced the results of the experiment. The assumptions for the external forces have not been confirmed.

8.1.3 End-caps

The design of the end-caps affects the transport, the upending and the removal of the end-caps. The conceptual designs of the end-caps must be optimized after further research. The design and the influence on the installation of the monopile wind turbine foundation are described. Two important design details are:

- The shape of the end-cap influences the transport of the pile. This has been assumed for the conceptual designs but it has not been confirmed by the experiment.
- Either internal or external removal of the end-caps gives the minimum draft of the pile after upending. The internal pressure and the maximum expected wave height influence the draft needed for removal of the bottom-cap.

Further research on the design and the way of removal of the end-caps should be done. The conclusions and recommendations are given later in this chapter.

8.1.4 Discussion of the Objectives of Van Oord

The objectives mentioned in the assignment of Van Oord, shown in section 1.2, are mentioned in this section.

1. *Understanding and possibly detailing and/or adjusting the intended monopile towing and upending procedure.*

The transport and upending procedure is discussed in detail in this report. Both processes are described and upending is the dominant procedure. The upending has been confirmed by the theory, calculations and the experiment. A future installation can be calculated with the Maple™ script. The experiment has confirmed the calculations.

2. *Analysing the buoyancy requirements needed to bring the monopile weight within the capacity of the crane.*

During the experiment the lifted load did not exceed the capacity of the crane. The scaled monopile reaches the vertical position by upending without exceeding the safe working load. The buoyancy requirements lead to the hydrostatic pressure on the submerged volume. The required internal pressure increases when the bottom-cap is removed externally. This leads to an increase of the total mass of the pile and the additional draft needed for buoyance.

3. *In addition care should be taken of conditions resulting from necessary testing requirements.*

The equipment used for the experiment has influenced the results. The dissimilarity of the analytical model and the experiment has confirmed this partially. A full-scale experiment is needed to verify this in practice.

The last step of this research is defining the conclusions and recommendations for further research of the end-caps of a monopile for an offshore wind turbine foundation. The conclusions and recommendations are the topic of the next two sections.

8.2 Conclusions of this research

The final conclusions are drawn as a combination of all validated assumptions and the conclusions, mentioned individually in the previous chapters. The conclusions for the upending of a monopile for an offshore wind turbine foundation are:

- The upending of a monopile is quasi-static since experimental runs with different velocities give similar results, therefore upending only depends on the buoyance and gravity forces. The inertia is not dominant and may therefore be neglected.
- The inertia influences the response of the pile due to the acceleration when lifting starts and when the pile reaches the vertical position, since the hydrodynamic mass causes a rotational acceleration when the monopile is almost vertical.
- The analytical model confirms that the monopile with a larger weight than the crane capacity can be lifted and reaches the vertical position by using the buoyant force of the monopile.
- The Maple™ script can be used to calculate the forces of the crane on the monopile during upending for future projects.

The conclusions lead to recommendations for further research. The recommendations are named in the next subsection.

8.3 Recommendations for further work

Based on this report recommendations for further research are given in this section. During the research assumptions have been made and these are partially validated in this chapter. The recommendations for upending of a monopile for an offshore wind turbine foundation are:

- Testing at the storage site is recommended to maintain high-quality end-caps.
- A weather window for the period of installation should be calculated in advance.
- The theoretical, analytical and experimental research should be verified in practice.
- The forces that influence transport and upending of the monopile have to be confirmed.
- The scaling factor used for the experiment must be validated in practice.
- Analysing the pressure which determines the boundary conditions for the conceptual design of the end-caps. A pressure valve in the top-cap should be used to set the maximum internal pressure.
- The dimensions of the end-cap related to the pile influence the force on the bottom-cap and the air gap for the airflow for external removal of the end-cap. Further research to analyse the airflow when releasing the bottom-cap and the consequences on the design is recommended.

The assumptions based on the external forces and the operation of the Aeolus must be verified in practice. An experiment should be done either full-scale or in a towing tank with a wave generator. Further research and experiments will lead to optimized upending of a monopile for an offshore wind turbine foundation.

Appendix A Aeolus datasheet

Name	Aeolus
Type	Offshore wind farm transport and installation vessel
Classification	Det Norske Veritas: X 1A1 - Self-elevating Wind Turbine Unit, CD-Crane DYNPOS AUT-R-EO-OPP-F-NAUT-OSV(A)
Trading area	Unrestricted
Year of construction	2014
Dimensions	Length overall 139.40 m
Breadth overall	38.06 m
Depth (to main deck)	9.12 m
Draft (design)	5.70 m
Tonnage	14,800 GT - 4,440 NT
Deadweight	6,500 tons
Velocity (at 5.40 m draught)	12.00 kn
NMF offshore installation crane	
SWL main hoist:	900 tons / 18.00 - 30.00 m
SWL auxiliary hoist:	100 tons / 19.50 - 86.00 m
Auxiliary cranes	2 x 20 tons / 24.00 m
Main engines	4 x 4,320 kW
Propulsion	10,000 kW
Bow thrusters	2 x 2,500 kW
Stern thrusters	2 x 2,500 kW
Total power installed	17,715 kW
Accommodation	74 persons
Bunkers	Fuel oil 1,000 m ³ , Fresh water 900 m ³
Jack-up system	4 legs - length 81.00 m - diameter 4.50 m
Clear deck area	3,300 m ²
Dynamic Positioning System	DP Class 2

The weight of the rigging and the hook increases the load and is used in equation 3.5 and 3.6. From the safe working load of 900tons only 850tons is used for upending of the monopile by the additional weight of the hook and rigging arrangement.

Outreach [m]	Safe working load [t]	Hoisting speed [m/min], [m/s]	
< 18	0	0	0
18 ≤ 30	900	5.0	0.0833
30 ≤ 40	650	6.9	0.115
40 ≤ 54	500	7.5	0.125
54 ≤ 60	450	9.6	0.16
60 ≤ 80	300	12.3	0.205
< 80	0	0	0

Appendix B General Arrangement Belwind by RAMBOLL

Appendix C Rigging arrangement for monopile by DHL

Appendix D FLOW steps for upending monopile

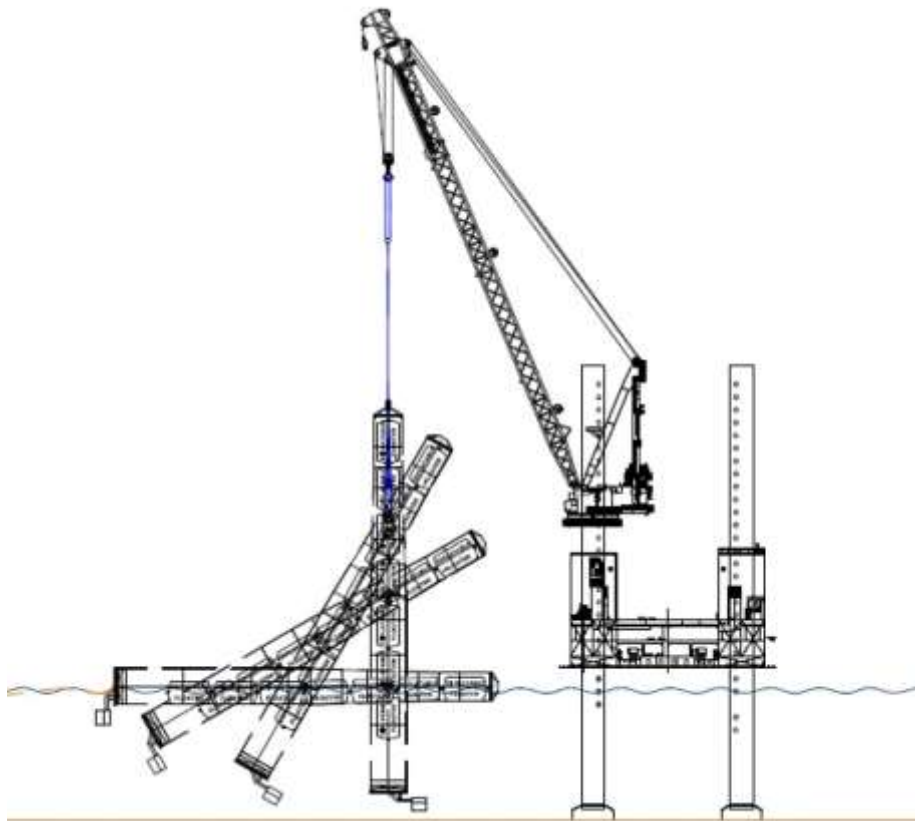


Figure 71: FLOW upending monopile

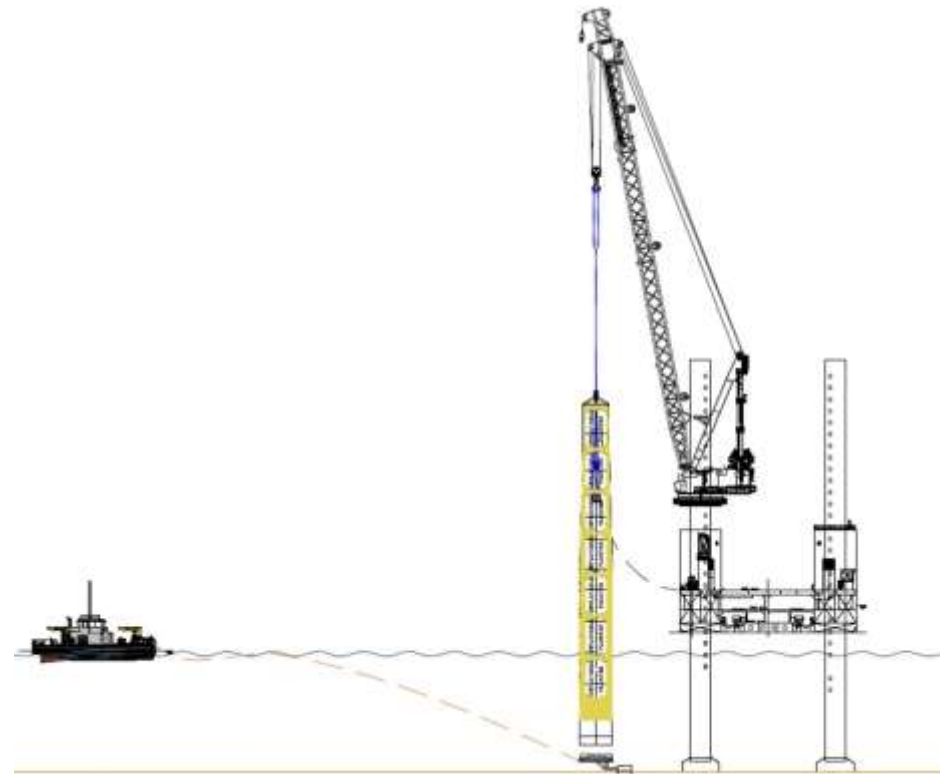


Figure 72: FLOW Controlled pressurize and released bottom cap

Appendix E Requirements to environmental conditions of Aeolus

The requirements to environmental conditions of the Aeolus are defined by J.J.Sietas KG, Schiffswerf GmbH u.Co. The conditions are for several conditions for jacking, operational, survival and transit. These conditions are mentioned below.

Operational mode conditions	Jacking	Jacked up operational	Jacked up survival	Transit
Local conditions				
Significant wave height [m]	1.80	3.60	8.50	8.50
Maximum wave height [m]	3.35	6.65	15.70	
Wave period [s]	3.0-15.00	5.0-15.00	15.00	3.0-18.00
Wind velocity (1 min mean) [m/s]	15.00	20.00	40.00	53.00
Current [m/s]	1.03	1.54	1.03	
Leg penetration [m]		5.00	5.00	
Airgaps [m]		7.00	14.00	
Crane operations	no	yes	no	

Date: 2010-12-03

Page 5 of 87

J.J.SIETAS KG
Schiffswerf GmbH u.Co.
Project 0-1690-00

REQUIREMENTS TO ENVIRONMENTAL CONDITIONS

AMBIENT CONDITIONS

If not otherwise stated, the ship's systems are dimensioned for the following ambient conditions:

- Sea water: -0°C / +32°C
- Air outside (except of structural parts): -20°C / +35°C
- Air outside structural parts: -10°C / +35°C
- Air inside (winter/summer): 22°C / +27°C
- Humidity summer: outside: 70 %, inside: 50-70%
- Humidity winter: outside: 100 %, inside: 50 %
- Engine room temperature: +0°C / +45°C

OPERATIONAL MODE

The jack-up vessel to be designed for the following five operational modes:

- Transit
 - Flooding mode
 - Jacking mode (up and down)
 - Semi-jacked mode
 - Semi-jacked mode means, that all the legs will be lowered and have the full impact of the jacked up weight, but the vessel is not yet out of the water
 - Jacked mode
 - Jacked mode means, all the legs will be lowered and have the full impact of the jacked up weight and the vessel is fully out of water
- The requirements are based on semi jacked or full jacked out operation on 45 m water depth and 5,00 m sea tied penetration (incl. top on spud can) and air gap up to 14,00 m.

The semi-jacked condition in general to comply with environmental conditions equal to the jacking conditions for current and wind speed, the permissible wave height in semi jacked condition to be determined by means of reverse engineering. Additionally limited crane operations can be performed. The exact allowable semi-jacked sea state and crane operations to be determined.

Appendix F Standard seawater properties at 1°C increment^{xxi}

Temperature. (T_{sw})	Density ρ_{sw}	$\partial\rho_{sw}/\partial T_{sw}$	Viscos μ	$\partial\mu/\partial T_{sw}$	$\nu = \mu/\rho$	$\partial\nu/\partial T_{sw}$	Pressure p_v	$\partial p_v/\partial T_{sw}$
(°C)	(kg/m ³)	(kg/m ³ ·°C)	(Pa·s)	(Pa·s/°C)	(m ² /s)	(m ² /s·°C)	(MPa)	(MPa/°C)
1	1028.094	-0.0680	0.00184	-6.186E-	1.7926E-	-6.005E-	6.4363E-	4.639E-
2	1028.019	-0.0810	0.00178	-5.862E-	1.7341E-	-5.689E-	6.9153E-	4.944E-
3	1027.932	-0.0930	0.00172	-5.561E-	1.6787E-	-5.395E-	7.4256E-	5.265E-
4	1027.833	-0.1050	0.00167	-5.282E-	1.6262E-	-5.122E-	7.9689E-	5.604E-
5	1027.722	-0.1170	0.00162	-5.021E-	1.5762E-	-4.867E-	8.5471E-	5.962E-
6	1027.600	-0.1280	0.00157	-4.777E-	1.5288E-	-4.630E-	9.1620E-	6.340E-
7	1027.466	-0.1390	0.00152	-4.549E-	1.4836E-	-4.408E-	9.8157E-	6.738E-
8	1027.321	-0.1500	0.00148	-4.337E-	1.4406E-	-4.200E-	1.0510E-	7.156E-
9	1027.165	-0.1605	0.00143	-4.137E-	1.3995E-	-4.006E-	1.1248E-	7.597E-
10	1027.000	-0.1710	0.00139	-3.950E-	1.3604E-	-3.823E-	1.2030E-	8.061E-
11	1026.823	-0.1815	0.00135	-3.774E-	1.3230E-	-3.652E-	1.2861E-	8.550E-
12	1026.637	-0.1915	0.00132	-3.609E-	1.2873E-	-3.492E-	1.3741E-	9.063E-
13	1026.441	-0.2010	0.00128	-3.454E-	1.2532E-	-3.341E-	1.4674E-	9.601E-
14	1026.236	-0.2105	0.00125	-3.308E-	1.2205E-	-3.198E-	1.5662E-	1.017E-
15	1026.021	-0.2195	0.00122	-3.170E-	1.1892E-	-3.064E-	1.6709E-	1.076E-
16	1025.796	-0.2290	0.00118	-3.040E-	1.1592E-	-2.938E-	1.7816E-	1.139E-
17	1025.563	-0.2380	0.00115	-2.918E-	1.1304E-	-2.819E-	1.8987E-	1.204E-
18	1025.321	-0.2470	0.00113	-2.801E-	1.1028E-	-2.706E-	2.0225E-	1.272E-
19	1025.070	-0.2555	0.00110	-2.692E-	1.0763E-	-2.599E-	2.1533E-	1.344E-
20	1024.810	-0.2640	0.00107	-2.588E-	1.0508E-	-2.498E-	2.2914E-	1.419E-
21	1024.542	-0.2725	0.00105	-2.489E-	1.0263E-	-2.402E-	2.4373E-	1.498E-
22	1024.265	-0.2805	0.00102	-2.396E-	1.0027E-	-2.312E-	2.5912E-	1.581E-
23	1023.980	-0.2890	0.00100	-2.307E-	9.8002E-	-2.226E-	2.7535E-	1.667E-
24	1023.688	-0.2970	0.00098	-2.223E-	9.5818E-	-2.144E-	2.9247E-	1.757E-
25	1023.387	-0.3050	0.00095	-2.143E-	9.3713E-	-2.066E-	3.1050E-	1.851E-
26	1023.078	-0.3125	0.00093	-2.067E-	9.1683E-	-1.993E-	3.2950E-	1.949E-
27	1022.762	-0.3200	0.00091	-1.995E-	8.9726E-	-1.922E-	3.4950E-	2.052E-
28	1022.438	-0.3275	0.00089	-1.926E-	8.7837E-	-1.856E-	3.7056E-	2.159E-
29	1022.107	-0.3345	0.00087	-1.860E-	8.6014E-	-1.792E-	3.9271E-	2.271E-
30	1021.769	-0.3420	0.00086	-1.798E-	8.4253E-	-1.731E-	4.1600E-	2.388E-

Appendix G Properties of Air^{xxii}

Temperature (T_{air})	Density (ρ_{air})	Viscosity (μ_{air})	$\nu_{air} = \mu_{air}/\rho_{air}$	Thermal diffusivity
(°C)	(kg/m ³)	(Pa·s)	(m ² /s)	(m ² /s·°C)
1	1.2885	1.7280E-5	1.3411E-5	1.8638E-5
2	1.2838	1.7330E-5	1.3499E-5	1.8766E-5
3	1.2792	1.7379E-5	1.3586E-5	1.8894E-5
4	1.2745	1.7428E-5	1.3674E-5	1.9022E-5
5	1.2699	1.7478E-5	1.3763E-5	1.9151E-5
6	1.2654	1.7527E-5	1.3851E-5	1.9279E-5
7	1.2608	1.7576E-5	1.3940E-5	1.9409E-5
8	1.2563	1.7625E-5	1.4029E-5	1.9538E-5
9	1.2519	1.7673E-5	1.4118E-5	1.9668E-5
10	1.2474	1.7722E-5	1.4207E-5	1.9798E-5
11	1.2430	1.7771E-5	1.4297E-5	1.9929E-5
12	1.2386	1.7819E-5	1.4386E-5	2.0059E-5
13	1.2343	1.7868E-5	1.4476E-5	2.0191E-5
14	1.2300	1.7916E-5	1.4566E-5	2.0322E-5
15	1.2257	1.7965E-5	1.4657E-5	2.0454E-5
16	1.2215	1.8013E-5	1.4747E-5	2.0586E-5
17	1.2172	1.8061E-5	1.4838E-5	2.0718E-5
18	1.2130	1.8109E-5	1.4929E-5	2.0851E-5
19	1.2089	1.8157E-5	1.5020E-5	2.0984E-5
20	1.2047	1.8205E-5	1.5111E-5	2.1117E-5

Appendix H Maple™ script

```
> restart;
> with(LinearAlgebra):
Student(LinearAlgebra):
with(Student[NumericalAnalysis]):
with(ExcelTools):
Quasi-static approach
> Digits:=30:
Define workspace
> currentdir("D:\\SkyDrive\\Thesis\\Maple"):
> remove("D:\\SkyDrive\\Thesis\\Maple\\MCoR Upending.xlsx");
remove("D:\\SkyDrive\\Thesis\\Maple\\MCoR Upending-1.xlsx");
```

DEFINE EQUATIONS

```
> T := h0-z-l*sin(alpha):
Tb:= h0-z-(-S)*sin(alpha);
Tt:= h0-z-(LMP-S)*sin(alpha);
> A_d := Do^2/4*arccos((Do-2*d)/Do)-(Do/2-d)*sqrt((Do-d)*d):
A_Tt := subs(d=(TT/cos(alpha)),A_d):
A_Tb := subs(d=(TB/cos(alpha)),A_d):
A_D := Do^2/4*arccos((Do-2*T)/Do)-(Do/2-T)*sqrt((T*(Do-T))):
A_Do := Pi/4*Do^2:
dA := 2*sqrt(h*(Do-h)):
> Lim := TB/sin(alpha):
lim := (TB-Do*cos(alpha))/sin(alpha):
lim1 := (TB-Do*cos(alpha))/sin(alpha):
> Vsub := A_Tt*L+(A_Tb-A_Tt)*L/2:
Vsub1 := A_Tb*L/2:
Vsub2 := A_Do*(L+li)/2:
Vsub3 := A_Do*L:
> Dalpha:=(d_z/LMP):
Alpha := arcsin(z/S):
> Gx := -S+LMP/2: Gz := 0: > Cx := 0: Cz := 0:
> Bx := (A_Tt*L*(-S+L/2)+(A_Tb-A_Tt)*L/2*(-S+L/3))/(A_Tt*L+(A_Tb-A_Tt)*L/2):
Bx1 := (A_Tb*L/2*(-S+L/3))/(A_Tb*L/2):
Bx2 := (A_Do*li*(-S+li/2)+A_Do*(L-li)/2*(-S+li*2/3+L/3))/(A_Do*(L+li)/2):
Bx3 := (-S+L/2):
Bz := (A_Tt*L*(ro-TT/2)+(A_Tb-A_Tt)*L/2*(ro-(TT+(TB-TT)/3)))/(A_Tt*L+(A_Tb-A_Tt)*L/2):
Bz1 := (A_Tb*L/2*(ro-TB/3))/(A_Tb*L/2):
Bz2 := (A_Do*(L-li)/2*(ro-Do/3))/(A_Do*(L+li)/2):
Bz3 := 0:
> m := FB*(sin(alpha)*BX)+FG*(sin(alpha)*GX):
m1 := FB+FG+FC:
```

DEFINE VARIABLES

```
> g := 9.81: # gravitational constant
rho_sw:= 1025: # mass density seawater
rho_s := 7850: # mass density steel
LMP := 70: # length of the pile
> FMP := 1100000*g: # weight of the pile
XMP := -LMP/2+S: # X-coordinate CoG of the monopile
ZMP := 0: # Do/2: # Z-coordinate CoG of the monopile
Ftc := 9000*g: # weight of the top-cap
Xtc := LMP-S-0.5: # X-coordinate CoG of top-cap
Ztc := Do/2: # Z-coordinate CoG of top-cap
Fbc := 4500*g: # weight of the bottom-cap
Xbc := 0.5-S: # X-coordinate CoG of bottom-cap
Zbc := 0: # Do/2: # Z-coordinate CoG of bottom-cap
Frig := 6870*g: # weight of the rigging arrangement
Xrig := 0: # X-coordinate CoG of the rigging arrangement
Zrig := 0: # Do/2: # Z-coordinate CoG of the rigging arrangement
Fhook := 40000*g: # weight of the hook
FG := -FMP-Frig-Ftc-Fbc:# total weight
```



```

elif (TT<0 and (TB/cos(alpha))<Do and alpha<evalf(Pi/2)) then L:=evalf(Lim);
li:=evalf(lim)
elif (TT<0 and (TB/cos(alpha))>=Do and alpha<evalf(Pi/2)) then L:=evalf(Lim);
li:=evalf(lim1)
elif alpha>=evalf(Pi/2) then L:=evalf(Tb); li:=0 end if;
if L > LMP then L:=LMP end if;
if TT >= 0 then VSub := evalf(Vsub)
elif (TT<0 and (TB/cos(alpha))<Do and alpha<evalf(Pi/2)) then VSub := evalf(Vsub1)
elif (TT<0 and (TB/cos(alpha))>=Do and alpha<evalf(Pi/2)) then VSub:= evalf(Vsub2)
elif alpha>=evalf(Pi/2) then VSub:=evalf(Vsub3) end if;
FB := evalf(VSub*rho_sw*g);
if TT >= 0 then BX:=evalf(Bx)
elif (TT<0 and (TB/cos(alpha))<Do and alpha<evalf(Pi/2)) then BX:=evalf(Bx1)
elif (TT<0 and (TB/cos(alpha))>=Do and alpha<evalf(Pi/2)) then BX:=evalf(Bx2)
elif alpha>=evalf(Pi/2) then BX:=evalf(Bx3) end if;
if TT >= 0 then BZ:=evalf(Bz)
elif (TT<0 and (TB/cos(alpha))<Do and alpha<evalf(Pi/2)) then BZ:=evalf(Bz1)
elif (TT<0 and (TB/cos(alpha))>=Do and alpha<evalf(Pi/2)) then BZ:=evalf(Bz2)
elif alpha>=evalf(Pi/2) then BZ:=evalf(Bz3) end if;
if alpha<evalf(Pi/2) then MCOR := evalf(m)
else MCOR:=0 end if;
ALPHA(RowDimension(ALPHA)+1,..):=Matrix([[Re(BX),Re(BZ),Re(alpha),Re(MCOR)]]);
for t from 1 by 1 while check=1 do
TT := evalf(Tt);
TB := evalf(Tb);
if TT >= 0 then L:=LMP
elif (TT<0 and (TB/cos(alpha))<Do and alpha<evalf(Pi/2)) then L:=evalf(Lim);
li:=evalf(lim)
elif (TT<0 and (TB/cos(alpha))>=Do and alpha<=evalf(Pi/2)) then L:=evalf(Lim);
li:=evalf(lim1) end if;
if L > LMP then L:=LMP end if;
if TT >= 0 then VSub := evalf(Vsub)
elif (TT<0 and (TB/cos(alpha))<Do and alpha<evalf(Pi/2)) then VSub:= evalf(Vsub1)
elif (TT<0 and (TB/cos(alpha))>=Do and alpha<=evalf(Pi/2)) then VSub:=
evalf(Vsub2) end if;
if TT >= 0 then BX:=evalf(Bx)
elif (TT<0 and (TB/cos(alpha))<Do and alpha<evalf(Pi/2)) then BX:=evalf(Bx1)
elif (TT<0 and (TB/cos(alpha))>=Do and alpha<=evalf(Pi/2)) then BX:=evalf(Bx2)
end if;
if TT >= 0 then BZ:=evalf(Bz)
elif (TT<0 and (TB/cos(alpha))<Do and alpha<evalf(Pi/2)) then BZ:=evalf(Bz1)
elif (TT<0 and (TB/cos(alpha))>=Do and alpha<=evalf(Pi/2)) then BZ:=evalf(Bz2)
end if;
FB := evalf(VSub*rho_sw*g);
if alpha<evalf(Pi/2) then MCOR := evalf(m)
else MCOR:=evalf(m1) end if;
mcor := Matrix([[MCOR]]);
if MCOR > 0 then
alpha := alpha+dalpha;
elif MCOR < 0 then
alpha := alpha-dalpha;
end if;
if alpha>=evalf(Pi/2) then alpha:=evalf(Pi/2) end if;
salpha:= sin(alpha);
TT := evalf(Tt);
TB := evalf(Tb);
if TT >= 0 then L:=LMP
elif (TT<0 and (TB/cos(alpha))<Do and alpha<evalf(Pi/2)) then L:=evalf(Lim);
li:=evalf(lim)
elif (TT<0 and (TB/cos(alpha))>=Do and alpha<=evalf(Pi/2)) then L:=evalf(Lim);
li:=evalf(lim1) end if;
if L > LMP then L:=LMP end if;
if TT >= 0 then VSub := evalf(Vsub)
elif (TT<0 and (TB/cos(alpha))<Do and alpha<evalf(Pi/2)) then VSub:= evalf(Vsub1)
elif (TT<0 and (TB/cos(alpha))>=Do and alpha<=evalf(Pi/2)) then VSub:=
evalf(Vsub2) end if;
if TT >= 0 then BX:=evalf(Bx)

```

```

    elif (TT<0 and (TB/cos(alpha))<Do and alpha<evalf(Pi/2)) then BX:=evalf(Bx1)
    elif (TT<0 and (TB/cos(alpha))>=Do and alpha<=evalf(Pi/2)) then BX:=evalf(Bx2)
end if;
    if TT >= 0 then BZ:=evalf(Bz)
    elif (TT<0 and (TB/cos(alpha))<Do and alpha<evalf(Pi/2)) then BZ:=evalf(Bz1)
    elif (TT<0 and (TB/cos(alpha))>=Do and alpha<=evalf(Pi/2)) then BZ:=evalf(Bz2)
end if;
    FB := evalf(VSub*rho_sw*g);
    if alpha<evalf(Pi/2) then MCoR := evalf(m)
    else MCoR:=0 end if;
    mcor(RowDimension(mcor)+1,..):=MCoR;
    if (mcor(1)<0 and mcor(2)>0) then dalpha:=dalpha/2
    elif (mcor(1)>0 and mcor(2)<0) then dalpha:=dalpha/2 end if;
    if abs(MCoR) <= 1E-10 then check:=2 end if;
    MCoR(RowDimension(MCoR)+1,..):=Matrix([[BX,BZ,L,TT,TB,MCoR]]);
end do:
FC := evalf(-FG-FB+Fc);
FS := evalf(FG+FB+FC);
TT := evalf(Tt);
TB := evalf(Tb);
beta := alpha;
salpha:= sin(alpha);
ALPHA(RowDimension(ALPHA)+1,..):=Matrix([[Re(BX),Re(BZ),Re(alpha),Re(MCoR)]]);
ALPHA(RowDimension(ALPHA)+1,..):=Matrix([[z,alpha]]);
fprintf(fd,"\n%a %+06.10f %+06.10f %+06.10f %+06.10f %+06.10f %+06.10f %+06.10f %+
06.10f %+06.10f %+06.10f %a",z,FC,VSub,BX,BZ,TT,TB,alpha,L,li,MCoR,t);
if VSub <= 200 then phase:=2 end if;
end do:
fclose(fd);
n_steps := i;
> FC1:=readdata("Phases 2D Upending 0.01.txt",2):
> Export(ALPHA,"MCoR Upending.xlsx"):
> Export(MCoR,"MCoR Upending-1.xlsx"):
time[real]()/3600;

```

PLOT PHASES

```

> with(plots):
> Phase1 := FC1[1..242]: # Splitted with Phases 2D.txt for dz=0.01
[1..242],[242..1162],[1162..RowDimension(FC1)]
Phase2 := FC1[242..1162]:
Phase3 := FC1[1162..RowDimension(FC1)]:
#Phase4 := FC1[495..RowDimension(FC1)]:
> plot([Phase1,Phase2,Phase3],color=["Red","Blue","Green"],legend=["Phase 1","Phase
2","Phase 3"],title="Upending 1.100t monopile",titlefont=["Roman",20],labels=["dz
[m]","FC [N]"],labelfont=["Roman",20]); # x=49..50.5,y=5.8E6..6.5E6,
#plot([Phase1,Phase2],color=["Red","Blue"],legend=["Phase 1","Phase
2"],title="Upending 1.100t monopile",titlefont=["Roman",20],labels=["dz [m]","FC
[N]"],labelfont=["Roman",20]);
> plot([ALPHA],legend=["Alpha"],title="Upending 1.100t
monopile",titlefont=["Roman",20],labels=["dz [m]","alpha
[rad]"],labelfont=["Roman",20]);
> plot([Phase1],color=["Red"],legend=["Phase 1"],title="Upending 1.100t
monopile",titlefont=["Roman",20],labels=["dz [m]","FC
[N]"],labelfont=["Roman",20]);
> plot([Phase2],color=["Blue"],legend=["Phase 2"],title="Upending 1.100t
monopile",titlefont=["Roman",20],labels=["dz [m]","FC
[N]"],labelfont=["Roman",20]);
> plot([Phase3],color=["Green"],legend=["Phase 3"],title="Upending 1.100t
monopile",titlefont=["Roman",20],labels=["dz [m]","FC
[N]"],labelfont=["Roman",20]); # y=49.4..49.9,x=6E6..6.5E6,
> #plot([Phase4],color=["Black"],legend=["Phase 4"],title="Upending 1.100t
monopile",titlefont=["Roman",20],labels=["dz [m]","FC
[N]"],labelfont=["Roman",20]);

```

Appendix I Experimental results

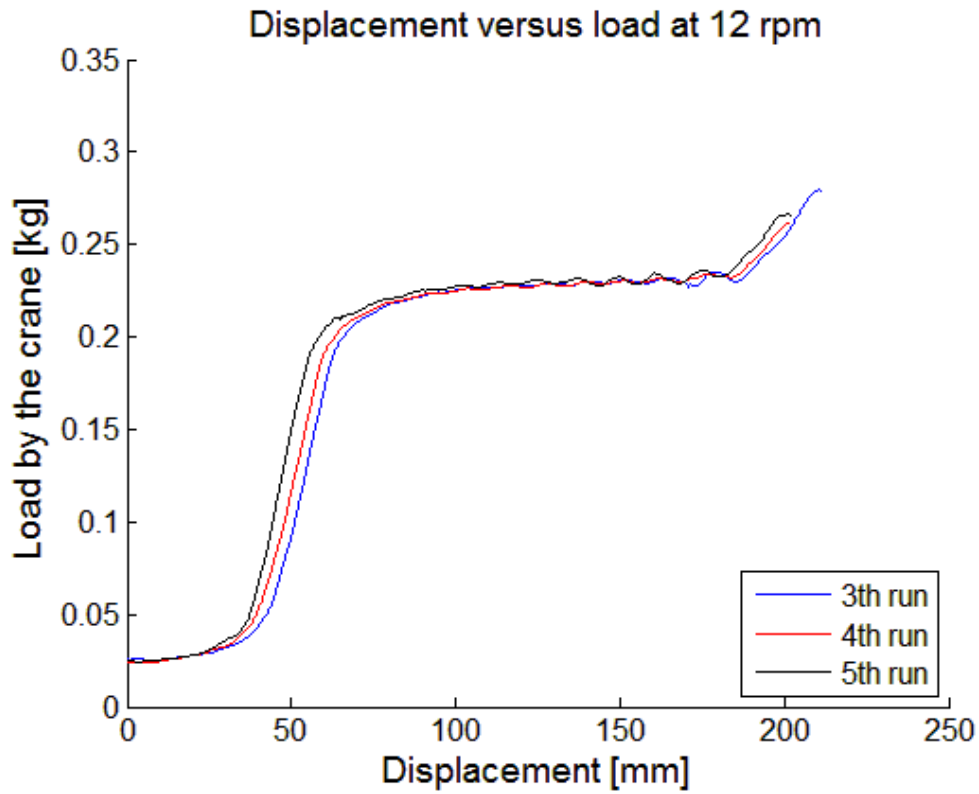


Figure 73: Run 3, 4 and 5

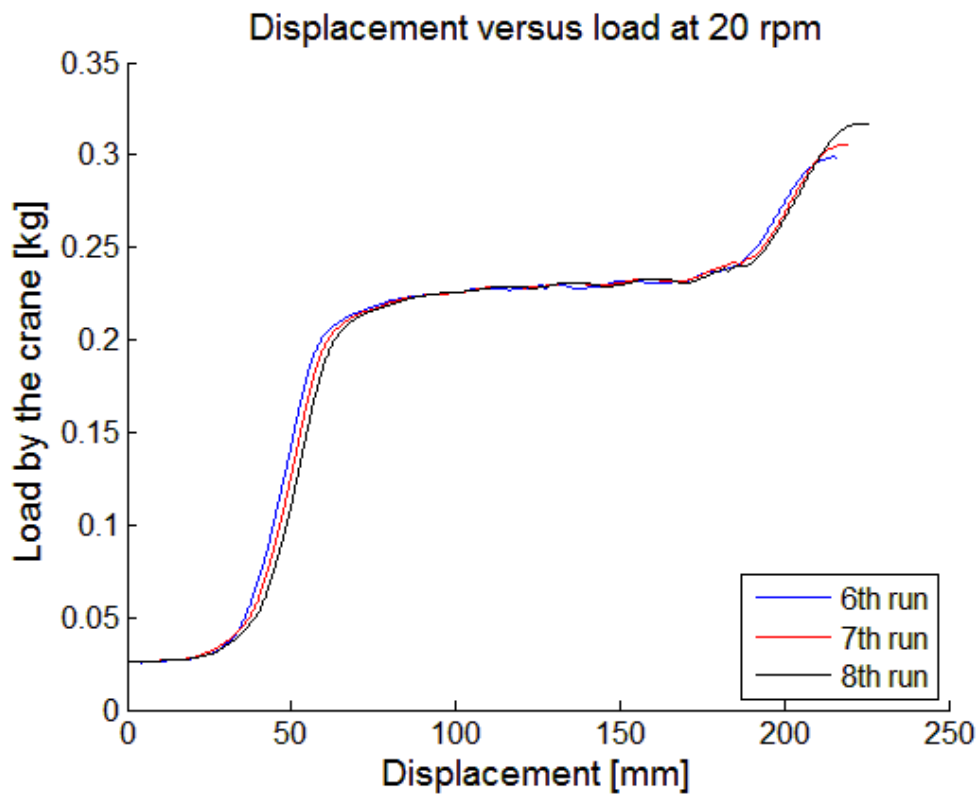


Figure 74: Runs 6, 7 and 8

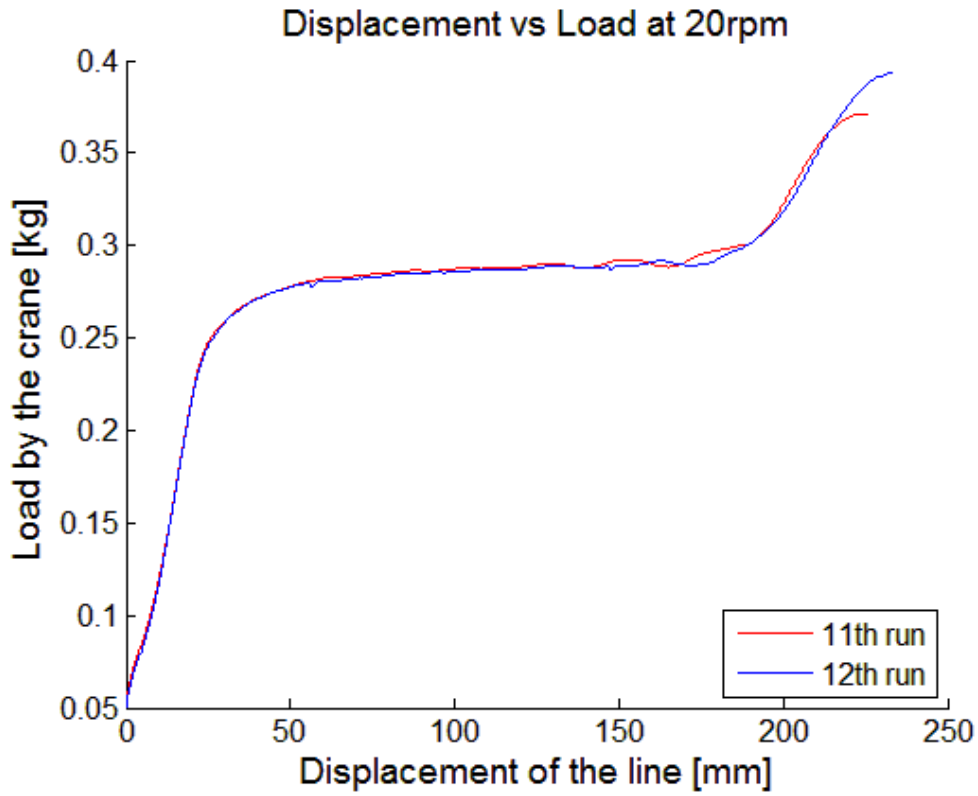


Figure 75: Run 11 and 12

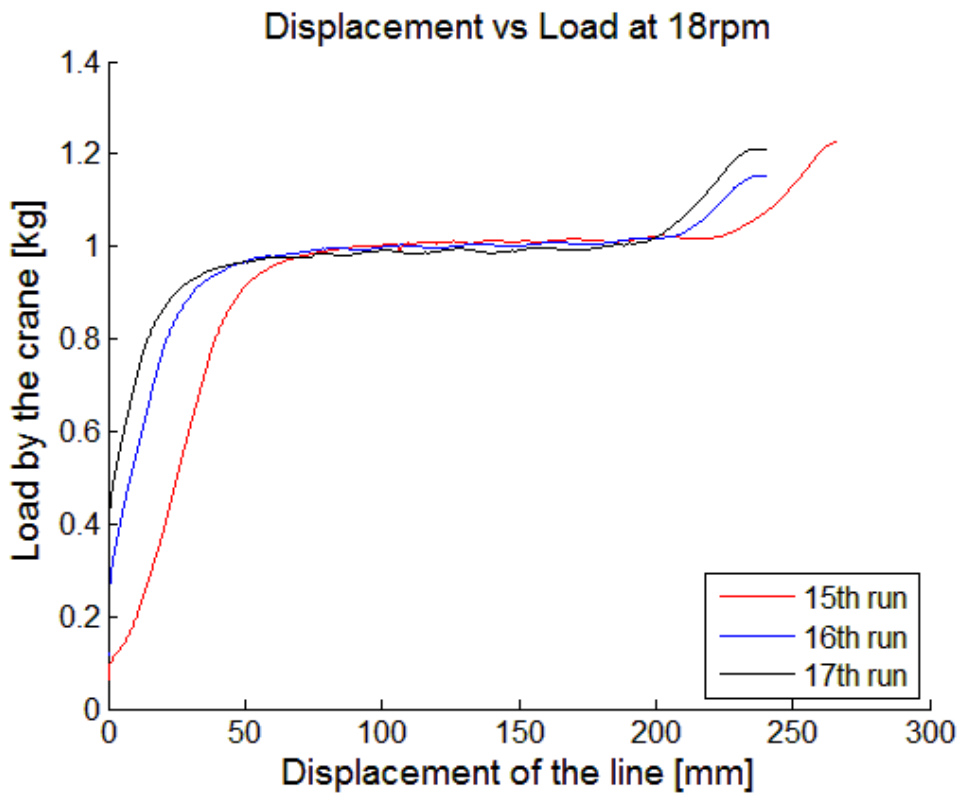


Figure 76: Run 15, 16 and 17

Appendix J Experiment



Figure 77: Initial conditions



Figure 78: Emerging of the top-cap



Figure 79: Submerging of the bottom-cap



Figure 80: Decreasing gradient of the crane load



Figure 81: Rotational acceleration of the pile



Figure 82: Static emerging



Figure 83: Final position

A List of symbols and abbreviations

Symbol	Description	§	Units
a	Amplitude of the surface elevation	2.2	m
a	Acceleration	3.2	m/s ²
A	Cross-sectional area	3.2	m ²
A_{ext}	External cross-sectional area	4.1	m ²
A_{int}	Internal cross-sectional area	4.1	m ²
A_{MP}	Cross-sectional area of the monopile	3.3	m ²
A_s	Submerged cross-sectional area	3.2	m ²
A_{Tb}	Submerged cross-sectional area at the bottom-cap, $A_{Tb} = A_s(-S)$	5.2	m ²
A_{Tt}	Submerged cross-sectional area at the top-cap, $A_{Tt} = A_s(L_{MP}-S)$	5.2	m ²
ν	Fluid viscosity	3.3	Pa s
CoB	Centre of buoyancy at Cartesian coordinates (x,y,z)	5.2	m
CoG	Centre of gravity at Cartesian coordinates (x,y,z)	3.2	m
CoR	Centre of rotation at Cartesian coordinates (x,y,z)	5.2	m
d	Water depth	2.2	m
D_i	Inner diameter of the monopile	6.3	m
D_m	Diameter of the model	6.1	m
D_{MP}	Diameter of the monopile (≈ 7000 mm)	6.1	m
D_o	Outer diameter of the monopile	5.2	m
E	Elasticity	3.2	N/m ²
F	Net force	3.2	N
F_c	Load lifted by the crane	3.2	N
F_E	Elasticity force	3.2	N
F_G	Gravity force	3.2	N
F_I	Inertia force	3.2	N
F_k	Spring force	3.3	N
F_{MP}	Weight of the monopile	3.3	N
F_P	Pressure force	3.2	N
F_{SWL}	Safe working load of the crane	3.2	N
F_T	Surface tension force	3.2	N
F_v	Viscous force	3.2	N
F_v	Buoyant force	3.2	N
g	Gravitational acceleration (≈ 9.81)	2.2	m/s ²
h	Distance below seawater level	3.2	m
h_0	Initial draft	5.2	m
H_{max}	Maximum wave height	2.2	m
H_s	Significant wave height	2.2	m
I	Mass moment of inertia	6.3	m ⁴
j	Rank number of the wave height, j=1 for highest etc.	2.2	-
k	Wave number ($= 2\pi / \lambda$)	2.2	1/m
k	Spring stiffness	3.3	N/m
l	Length	3.2	m
L	Submerged length of the monopile	5.2	m
L_{MP}	Length of the monopile (≈ 70)	3.2	m
m	Mass	3.2	kg
m'	Hydrodynamic mass	3.2	kg
m_m	Mass of the model	6.1	kg

m_{MP}	Mass of the monopile	6.1	kg
M_{CoR}	Moment at the centre of rotation	5.2	Nm
n	Amount of substance of air	3.3	mol
N	Number of waves in the wave record	2.2	-
p	Pressure	3.2	N/m ²
p_0	Atmospheric pressure (≈ 101325 N/m ²)	3.2	N/m ²
p_e	External pressure against the end-cap (hydrostatic pressure)	4.1	N/m ²
p_h	Hydrostatic pressure	3.2	N/m ²
p_i	Internal pressure	3.3	N/m ²
Q	Flow rate (≈ 5160 m ³ /h)	4.2	m ³ /s
r_o	Outer radius of the monopile	5.2	m
R	Gas constant (8.314472)	3.3	J/K mol
S	Distance between bottom-cap and trunnions (≈ 59.8)	5.2	m
t	time	2.2	s
T	Wave period	2.2	s
T_b	Draft of the bottom-cap	3.3	m
T_{mp}	Temperature inside the monopile	3.3	K
T_{MP}	Draft of the monopile	4.1	m
$T_{MP}(x)$	Draft of the monopile at coordinate x	5.2	m
$T_{MP,max}$	Maximum draft of the monopile	3.3	m
T_t	Draft of the top-cap, $T_t = T_{MP}(L_{MP}-S)$	5.2	m
u_0	Horizontal component of orbital velocity	2.2	m/s
u_b	Bottom orbital velocity	2.2	m/s
v_a	Flow velocity of air	4.1	m/s
v_m	Velocity of the model	6.1	m/s
v_{MP}	Velocity of the monopile	6.1	m/s
v_{sw}	Flow velocity of seawater	4.1	m/s
V	Velocity vector (u, v, w)	3.2	m/s
V_a	Volume of air	3.3	m ³
V_{ad}	Added volume of air	4.2	m ³
V_m	Volume of the model	6.1	m ³
V_{MP}	Volume of the monopile	6.1	m ³
$dV/d(x, y, z)$	Velocity gradient	3.2	s ⁻¹
x	Coordinate of Cartesian reference point horizontal		m
x_k	Displacement of the spring	3.3	m
$x_{k,0}$	Initial displacement of the spring	3.3	m
x_{MP}	Coordinate of centre of gravity along the x-axis (-24.8)	5.2	m
x_w	x in the direction of the wave	2.2	m
x_{∇}	Coordinate of centre of buoyancy along the monopile (CoB_x)	5.2	m
y	Coordinate of Cartesian reference point in depth		m
z	Coordinate of Cartesian reference point vertical		m
z	Vertical displacement by the crane	5.2	m

Greek symbols

Symbol	Description	§	Units
α	Angle of the monopile with the horizon	5.2	rad
Δ	Difference	3.3	-
δ	Scaling factor	6.1	-
δ_D	Diameter scale	6.1	-
δ_I	Inertia scale	6.1	-
δ_l	Length scale	6.1	-
δ_m	Mass scale	6.1	-
δ_p	Pressure scale	6.1	-
δ_v	Velocity scale	6.1	-
δ_V	Volume scale	6.1	-
δ_ρ	Density scale	6.1	-
ε	Eddy viscosity	3.2	N s/m ²
λ	Wave length	2.2	m
λ_i	Partially submerged length of the monopile, $0 < T(x) < D_o$	5.2	m
λ_s	Shallow water wave length	2.2	m
\mathcal{L}	Operator (of 3D Cartesian system)	3.3	m
μ	Dynamic viscosity	3.2	N s/m ²
μ_w	Dynamic viscosity of the wave	3.3	N s/m ²
ν	Kinematic viscosity	3.3	m ² /s
ρ	Volumetric mass density		kg/m ³
ρ_a	Volumetric mass density of air	3.3	kg/m ³
ρ_m	Volumetric mass density of the model	6.1	kg/m ³
ρ_{MP}	Volumetric mass density of monopile	6.1	kg/m ³
ρ_r	Relative density	3.3	-
ρ_s	Volumetric mass density of steel (≈ 7850)	3.3	kg/m ³
ρ_{sw}	Volumetric mass density of seawater (≈ 1025)	3.2	kg/m ³
σ	Surface tension	3.2	N/m
τ	Shear stress	3.2	N/m ²
Φ	Velocity potential	3.3	m/s
ϕ	Coordinate around the y-axis		rad
ω	Wave frequency	2.2	rad/s
ω_n	Natural frequency	6.3	rad/s
∇	Submerged volume	3.2	m ³
∇_1	Fully submerged volume	5.2	m ³
∇_2	Partially submerged volume	5.2	m ³

Subscript

Symbol	Description	Symbol	Description
θ	Atmospheric / initial	k	Kinematic / spring
a	Absolute / air	l	Lower half
ad	Added air	MP	Monopile
b	Bottom / bottom-cap / bottom half	o	Outer
bf	Ultimate base	p	Pressure
c	Constant	s	Shaft / significant / shallow / steel / submerged
e	Emerged	sf	Ultimate shaft
E	Elasticity	sw	Seawater
G	Gravity	t	Top / Top-cap / top half
h	Hydrostatic	tip	Skirt tip
i	Inner / internal / immersed	u	Undrained / upper half
I	Inertia	w	wall / water plane / wave
j	Rank number of wave height	∇	Buoyant / submerged

Top script

Symbol	Description
'	Effective
$\bar{}$	Average
\sim	Fluctuating
$\dot{}$	Derivative in time
$\ddot{}$	Second derivative in time

Unit factor

Symbol	Description
m	milli- (1E-3)
c	centi- (1E-2)
d	deci- (1E-1)
h	hecto- (1E2)
k	kilo- (1E3)
M	mega- (1E6)
G	giga- (1E9)

Enclosing symbol

()	Parentheses for clarification or personal comment
[]	Brackets to define the unit of the variable
{ }	Braces for the boundaries of the equation with additional subscript
	Braces to define the absolute value of that result

Abbreviations

BS	British Standard
CoB	Centre of Buoyancy
CoC	Centre of the Crane
CoG	Centre of Gravity
CoR	Centre of Rotation
EN	European Standard
EWEA	European Wind Energy Association
FAD	Free Air Delivery
FLS	Fatigue Limit State
ISO	International Organisation for Standardization
MP	Monopile
NMF	Neuenfelder Maschinenfabrik GmbH ^{xxiii}
OHVS	Offshore High Voltage Station
OWTF	Offshore Wind Turbine Foundation
PTFE	Polytetrafluoroethylene
RPM	Rotation per minute
SLS	Serviceability Limit State
SWL	Safe Working Load / Seawater Level
ULS	Ultimate Limit State

B List of Figures

No.	Description	Page
1	Experimental set-up	V
2	Result experiment and Maple™	V
3	Conceptual design	V
4	Transport of a monopile	1
5	Arrival of the monopile at the installation site	2
6	Removal of the bottom-cap	2
7	Flowchart of the Installation of a monopile of an OWTF	3
8	Installed offshore monopile wind turbine foundations with transition piece	3
9	Wind turbine	5
10	Used foundations of wind farms, end 2012	5
11	Orbital motion in deep, intermediate-depth and very shallow water	6
12	Design process for Offshore wind turbine	9
13	Foundation and substructure of a wind turbine	9
14	Loads on the wind turbine	9
15	Various components of a monopile foundation (Iuga)	10
16	Salvage monopile A04	11
17	monopile C05	11
18	Downtime Analysis monopile Installation	12
19	Towing monopile on the monopile and not the end-cap	13
20	Towage of a monopile	17
21	The Aeolus	17
22	Connection to local tug close to the installation vessel	18
23	Handover from tug to jack-up	18
24	Initial forces on the monopile	19
25	Initial pressure on the bottom-cap	23
26	Pressure on the bottom-cap	23
27	Spring controlled pressure valve	25
28	Some common shapes and their drag coefficient	29
29	Conceptual design 1, bottom-cap	32
30	Conceptual design 1, top-cap	32
31	Conceptual design 2, bottom-cap	33
32	Conceptual design 2, top-cap	33
33	Conceptual design 1, top-cap with spherical protection plate	33
34	Dimensions monopile and end-cap	34
35	Dimensions sealed (yellow) end-cap	34
36	Conceptual design 1	34
37	Conceptual design 2, sealed and unsealed	36
38	Initial conditions of the monopile	39
39	End of phase 1	39
40	End of phase 2	41
41	Position of the monopile during phase 3	42
42	End of phase 3	43
43	End of phase 4	43
44	Upending according Maple™	44
45	Upending monopile phase 1 according Maple™	44
46	Upending monopile phase 2 according Maple™	44

47	Upending monopile phase 3 according Maple™	45
48	Angle α during upending according Maple™	45
49	Overview experimental setup	49
50	Experimental setup	49
51	Displacement versus load, quasi-static runs	51
52	Run 1, 3, 6	52
53	Run 1, 4, 7	52
54	Run 1, 5, 8	52
55	Run 2, 3, 6	52
56	Run 2, 4, 7	52
57	Run 2, 5, 8	52
58	3 runs at different hoisting speed	53
59	3 runs at different hoisting speed	53
60	Displacement versus load of long pile at 20rpm	53
61	Displacement versus load of steel pile at 18rpm	53
62	Initial conditions	54
63	End of phase 1	54
64	End of phase 2	54
65	Final position	54
66	Aluminium pile of 366mm	55
67	Aluminium pile of 467mm	55
68	FLOW Upending monopile	65
69	FLOW Controlled pressurized and release bottom-cap	65
70	Run 3, 4 and 5	73
71	Run 6, 7 and 8	73
72	Run 11 and 12	74
73	Run 15, 16 and 17	74
74	Initial conditions	75
75	Emerging of the top-cap	75
76	Submerging of the bottom-cap	75
77	Decreasing gradient of the crane load	75
78	Rotation acceleration of the pile	75
79	Static emerging	75
80	Final position	75

C List of Tables

No.	Description	Page
1	Soil classification after BS EN ISO 14688-1:2002	8
2	Workable days for the Aeolus in 2012 and 2013	14
3	Properties of monopiles of projects of Van Oord	28
4	Phase change from phase 1 to 2	44
5	Scale factors and calculated length of the models	48
6	List of all experimental runs	50

D References

-
- ⁱ Key trends and statistics 1st half 2014 by the European Wind Energy Association in July 2014
- ⁱⁱ Belwind monopiles installed by Roger Lindley for VVV Limited
- ⁱⁱⁱ Waves in Oceanic and Coastal Waters by L.H. Holthuijsen for TU Delft and UNESCO-IHE in 2007.
- ^{iv} Calculating wave-generated bottom orbital velocities from surface-wave parameters by P.L. Wiberg and C.R. Sherwood in *Computer and Geosciences* 34 in 2008.
- ^v Freak waves by D. Faulkner in *Navigation News* in July 2003.
- ^{vi} www.britannica.com, Shelf break (geology) in October 2013.
- ^{vii} BSI British Standards, Code of practice for earthworks by BSI in December 2009.
- ^{viii} Introduction to the Physics of Landslides by F.V. De Blasio in 2011.
- ^{ix} Selection, Design and Construction Guidelines for Offshore Wind Turbine Foundations by S. Malhotra for PB Research & Innovation Report in October 2007.
- ^x Alternatives and modification of Monopile foundation or its installation technique for noise mitigation by Z. Salee for North Sea Foundation in April 2011.
- ^{xi} Lessons Learned, transport, operations and installation of foundations about Belwind Offshore Wind Farm by M. Bot ea. for Van Oord on 8th August 2011.
- ^{xii} MINIMESS is a brand at Hydrotechnik with ball sealing threaded test point and plug-in coupling and proved to be a major advance for pressure measurement on hydraulic systems.
- ^{xiii} Offshore Hydromechanics at Delft University of Technology by J.M.J. Journée and W.W. Massie in January 2001.
- ^{xiv} Viscous Flow Along a Wall at Stanford by Prof. B.J. Cantwell in April 2014.
- ^{xv} Surface tension of Seawater at Massachusetts Institute of Technology by K.G. Nayar ea. in October 2014.
- ^{xvi} Elementary fluid mechanics 7th ed. by R.L. Street, G.Z. Watters and J.K. Vennard in 1996.
- ^{xvii} Hydrodynamics of Offshore Structures by S.K. Chakrabarti of CBI Industries, Inc. on 24th of June 1985.
- ^{xviii} www.kaeser.com, Rotary Screw Compressors HSD/HSD SFC Series P-651/27ED/09.
- ^{xix} www.kaeser.com, Screw Blowers by Kaeser Kompressoren SE.
- ^{xx} Maplesoft™ on www.maplesoft.com
- ^{xxi} ITTC – Recommended Procedures ‘Fresh Water and Seawater Properties’ at 26th ITTC by 26th ITTC Specialist Committee on Uncertainty Analysis in September 2011.
- ^{xxii} Fluid Properties Calculator at www.mhtl.uwaterloo.ca.
- ^{xxiii} NMF, Neuenfelder Maschinenfabrik on www.nmf-crane.com in March 2014.